CONSECUTIVE SOLVENT – C_{60} EXCHANGE ON (η^2 – C_{60}) $Ir(CO)Cl(PPh_3)_2$ AND CATALYTICALLY SIGNIFICANT ORGANOMETALLIC REACTIONS ON $Ir(CO)(PPh_3)_2Cl(SOLVENT)$

by

Tamara Félix Massa

A thesis submitted in partial fulfillment of the requirements for the degree of

MASTER OF SCIENCE
in
Chemistry

UNIVERSITY OF PUERTO RICO
MAYAGÜEZ CAMPUS
2010

Approved by:

_____	_____
José E. Cortés Figueroa, PhD President, Graduate Committee	Date
_____	_____
Mayra E. Cádiz, PhD Member, Graduate Committee	Date
_____	_____
Enrique Meléndez, PhD Member, Graduate Committee	Date
_____	_____
Aldo Acevedo, PhD Representative of Graduate Studies	Date
_____	_____
Francis Patron, PhD Chairperson of the Department	Date

Abstract

The solvent/C_{60} exchange reactions on (η^2 – C_{60})Ir(CO)(PPh_3)$_2$Cl (solvent = benzene and cyclohexane) are biphasic. Plots of absorbance values at 550 nm vs. time are biexponential. Experiments where the reactions were monitored by infrared spectroscopy and ^{1}HNMR spectrometry permitted identification of the consecutive processes suggested by absorbance (550 nm) vs. time plots. The first segment of absorbance vs. time plots was assigned to C_{60}/benzene exchange producing (benzene)Ir(CO)(PPh_3)$_2$Cl, whereas the corresponding second segment was attributed to a series of reactions involving C-H bond oxidative cleavage of η^2-coordinated benzene followed by a series of catalytically-relevant reactions. Activation parameters for benzene/C_{60} exchange reactions on (η^2 – C_{60})Ir(CO)(PPh_3)$_2$Cl suggested an interchange associative mechanism. This interpretation prompted kinetics studies of the reactions in benzene/cyclohexane mixtures to determine rate constant values without unresolved solvent concentration dependences. Interestingly, rate constant values obtained from the second segment of the plot were [solvent]-dependent, suggesting the existence of benzene-cyclohexane exchange on the solvated (benzene)Ir(CO)(PPh_3)$_2$Cl and (cyclohexane)Ir(CO)(PPh_3)$_2$Cl intermediates. The proposed mechanism was tested by monitoring the reactions by infrared spectroscopy and ^{1}HNMR spectrometry of actual samples of commercially available Vaska's compound. These experiments confirmed that once the solvated intermediates are produce they undergo C-H bond oxidative cleavage followed by a series of parallel PPh_3 dissociation and σ-complexes formation.

Resumen

Las reacciones de intercambio C_{60}/disolvente en $(\eta^2\text{-}C_{60})Ir(CO)(PPh_3)_2Cl$ (disolvente = benceno/ciclohexano) son bifásicas. Las gráficas de absorbancia a 550 nm vs tiempo son biexponencial. Experimentos donde las reacciones eran monitoreadas por espectroscopia infrarroja y espectrometría ^{1}HNMR permitieron identificar las reacciones consecutivas sugeridas por las gráficas de absorbancia vs tiempo. El primer segmento de las gráficas de absorbancia vs tiempo fue asignado al intercambio entre C_{60}/benceno produciendo (benceno)$Ir(CO)(PPh_3)_2Cl$, mientras que el segundo segmento fue atribuido a una serie de reacciones que envuelven el rompimiento oxidativo del enlace C-H del (η^2) benceno, seguido por una serie de reacciones de relevancia catalítica. Los parámetros de activación para la reacción de intercambio C_{60}/benceno en $(\eta^2\text{-}C_{60})$ $Ir(CO)(PPh_3)_2Cl$ sugirieron un mecanismo de intercambio asociativo. Esta interpretación propició estudios cinéticos de la reacción en mezclas benceno/ciclohexano para determinar los valores de las constantes cinéticas, sin factor concentración del disolvente. Interesantemente, los valores de las constante de rapidez obtenidos del segundo segmento de la gráfica son dependientes de la concentración del disolvente sugiriendo la existencia de un intercambio benceno/ciclohexano en los intermediarios solvatados (benceno)$Ir(CO)(PPh_3)_2Cl$ y (ciclohexano)$Ir(CO)(PPh_3)_2Cl$. El mecanismo propuesto fue corroborado monitoreando la reacción por espectroscopia IR y espectrometría ^{1}HNMR de la muestras del compuesto de Vaska, disponible comercialmente. Estos experimentos confirmaron que una vez se produce el intermediario solvatado se produce rompimiento oxidativo del enlace C-H seguido por una serie paralela de disociación de PPh_3 y formación de complejos σ.

To God, my mom (Tomasa Massa) and my family.

Cuando la sabiduría entrare en tu corazón,
Y la ciencia fuere dulce a tu alma,
El consejo te guardará;
te preservará la inteligencia
Proverbio 2:10 – 11

For wisdom will enter your heart,
and moral knowledge will be attractive to you.
Discretion will protect you,
understanding will guard you,
Proverbs 2: 10 – 11

Acknowledgments

First, I would like to thank God for being my guide and support through my career. I would like to thank Dr. José E. Cortés-Figueroa for guiding me through my graduate education. Additional thanks to Elvin Igartúa –Nieves, Cynthia Capella-Capella for assistance on my scientific training and experimental assistance, and to Ms. Aracelis Cardona-Mejías for her assistance on NMR spectroscopy experiments. I would also like to thank my laboratory partners, Wanda I. Perez, José Lopez, Antonio Rivera, and the participants of the UPRM Undergraduate Research Program for their assistances and support.

I would also like to thank my family, specially my parents Tomasa Massa and Rafael Félix, my brother Rafael J. Félix, my grandparents Tomasa González and Rosa González, my cousin Antonio Roldán and my aunt Alma Félix for the unconditional support and love they gave me throughout my live. I would like to express my gratitude to my friends, especially Marisa E. Martínez, Maribel García, Abigail Padilla, Misael Viruet, Iris Suero, Nicole Moreno and José A. Carmona.

Table of Contents

List of table

List of Figures

Chapter I

Introduction

In the last three decades the field of hydrocarbon C–H bonds activation and functionalization has become a rapidly evolving area of study[1-2,37-40]. Functionalization and selective activation of C–H bonds can be achieved by oxidative addition of hydrocarbons to unsaturated organometallic complexes[1-2,37-40]. Iridium-based complexes have received considerable attention because this metal readily undergoes oxidative addition of a large variety of substances[1]. Iridium (+1) complexes acquired significance because formation of stable Iridium (+3) species promotes oxidative addition reactions[1-3]. In the decade of the 80's, Senoff and her collaborators reported an iridium complex used to activate S-H bonds by oxidative addition of benzenethiols to Vaska's complex producing $IrHCI(SC_6H_4Y)(CO)(PPh_3)_2$ where Y = NO_2, Br, C1, F, H, CH_3 and CH_3O[3]. Oxidative addition of alkane and arenes to photochemically-produced $(\eta^5\text{-}C_5(CH_3)_5)Ir(PPh_3)_2$ resulting on S–H and C–H bond activation were also reported 1982[3].

Simultaneously, the chemical interactions of unsaturated organometallic complexes with weakly-coordinating molecules such as hydrocarbon molecules have been investigated to understand the role of solvent in transition metal mediated C–H bonds activation[1,39]. The mechanism of C_{60}/solvent exchange on $(\eta^2 - C_{60})Ir(CO)(PPh_3)_2Cl$ and subsequent reactions will be described here. This mechanism includes key mechanistic steps of iridium–based homogeneous catalysis.

Vaska's complex $IrCl(CO)(PPh_3)_2$ is a square planar organometallic complex that consists of a central iridium atom bound to two mutually *trans* triphenyl phosphine ligands, carbon monoxide and a chloride ion[4]. The complex was first reported by J. W. DiLuzio and L.

Vaska in 1961[24]. It is a bright yellow crystalline solid[4]. Vaska's complex has sixteen (16) valence electrons, and as such it is considered coordinative unsaturated[5].

Vaska's complex is an excellent candidate for chemical modification by C_{60}[4]. The synthesis of fullerene (C_{60}) coordinated Vaska's complex $(\eta^2\text{-}C_{60})Ir(CO)(PPh_3)_2(Cl)$ is reported in the literature[4]. Its chemical characterization was based on crystallographic data, elemental analysis, and solid phase IR spectroscopy[4].

[60]Fullerene is similar in structure to graphite, which is composed of stacked sheets of linked hexagonal rings, that also contains pentagonal rings that prevent a planar structure[6]. [60] fullerene's structure is a truncated icosahedron, which resembles a soccer ball formed of 60 identical carbon atoms containing two distinct types of C–C bonds[6]. According with molecular orbital theory the topological character of C_{60} suggests that the molecule will undergo facile one-electron reductions; however comparison with planar conjugated hydrocarbons shows that this feature alone cannot account for the observed low half – wave reduction potentials of [60]fullerene[7]. Because of the carbon atoms spatial arrangement [60]fullerene hybridization falls between graphite (sp^2) and diamond (sp^3)[7]. According to π – orbital axis vector (POAV) theory[8], the carbon atoms' hybridization in [60] fullerene is $sp^{(2.28)}$[7].

For an undoped C_{60} solid, the 5-fold h_u band is the HOMO level and the 3-fold t_{1u} band is the empty LUMO level, this system is a band insulator[9]. However when the C_{60} solid is doped with metal atoms, the metal atoms give electrons to the t_{1u} band or the upper 3-fold t_{1g} band[9]. This partial electron occupation of the band leads to sometimes metallic behavior, although the t_{1u} band is only partially filled and it should be a metal according to band theory[9]. This unpredicted behavior may be explained by the Jahn-Teller effect, where spontaneous

deformations of high-symmetry molecules induce the splitting of degenerate levels to gain the electronic energy stabilization[6].

Owing to the chemical properties of C_{60} discussed above, it has the ability to coordinate transition metals in a dihapto (η^2) mode with the potential of forming organometallic complexes[4]. The fact that C_{60}-metal bond resembles an olefin-metal bond is a consequence of C_{60} capacity to participate in π-back bonding with transition metals and to its radially-oriented **p** molecular orbital's, preventing higher hapticities[4,10-19]. Moreover, [60] fullerene's high electron affinity facilitates its organometallic functionalization[20-26]. Fullerene (C_{60}) has the potential to modify and improve the efficiency of existing organometallic catalysts by altering their chemical reactivity[4]. Fullerene (C_{60}) can labialize bonds of co-coordinated ligand, and it has the potential to stabilize electron rich transition states or intermediates species involved in the catalysts ligand exchange reactions[13].

1.1 Objectives

The goal of this research is to undertake a systematic mechanistic investigation of C_{60}/solvent exchange reactions on $(\eta^2\text{-}C_{60})Ir(CO)(PPh_3)_2(Cl)$ complex and to characterize the mechanistic nature of subsequent reactions of solvated Vaska's complex. Specific goals are:

- To synthesize and characterize $(\eta^2\text{-}C_{60})Ir(CO)(PPh_3)_2(Cl)$ complex
- To study the ligand and solvent ligand exchange reactions on $(\eta^2\text{-}C_{60})Ir(CO)(PPh_3)_2(Cl)$ complex.
- To propose a plausible mechanism for the reactions.
- To use activation parameters to propose or assess mechanisms.

Chapter II
Previous Work

The structure of fullerene is a truncated icosahedron, which resembles a soccer ball of the type containing twenty hexagons and twelve pentagons[4]. Fullerenes have the ability to react with transition metal carbonyl complexes and with amines[11]. [60] Fullerene's ability to simultaneously act as a good π-acceptor and a good σ-Lewis base[11] can be explained by its tendency to accept electron via π-backbonding[15,22]. As a result of fullerene's high electron affinity, its chemical and physical properties are similar to those of electron deficient olefins[29]. There are 30 filled π-type orbital with 5-fold degenerate orbital which constitutes C_{60}'s HOMOs[27,29]. The LUMOs are triply degenerate t_{lu} orbitals, and a second set of triply degenerate orbitals of t_{1g} symmetry are the LUMOs+ 1's [27-29]. Fullerene has six reversible reduction waves at potentials ranging from -0.50V to -3.26V, versus ferrocene/ferrocenium (Fc/Fc^{+}) [15,22,29]. Fullerene's π-back bonding can be assessed by infrared spectroscopy because its interaction with transition metals induces a shift in the CO stretching on metal-coordinated carbon monoxide.[5]

One metal that is a candidate to be fullerene-coordinate is iridium, as in the Vaska's complex. The Vaska's complex has a characteristic CO-stretching band at 1965 cm^{-1} [5,28]. The corresponding υco in C_{60}-Vaska's complex appears at 2015 cm^{-1} due to C_{60}-Ir π-back bonding[5,28]. The infrared spectra in Figure 2.1 show the described υ(co) shift a consequence of C_{60} coordination.

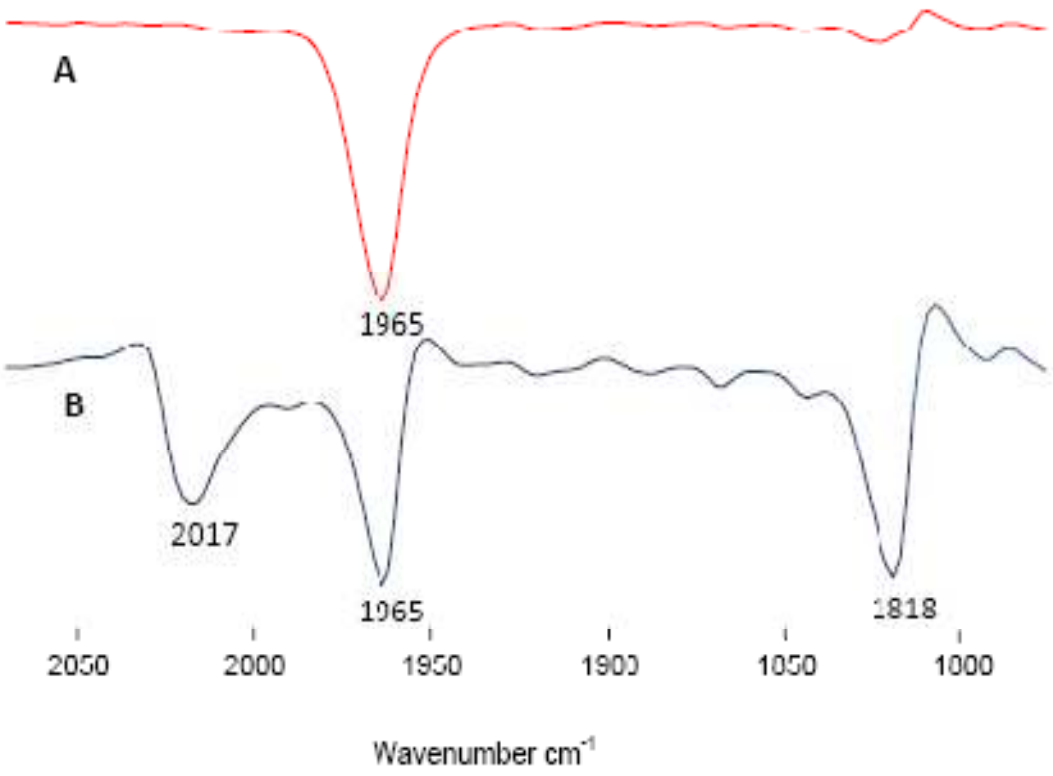

Figure 2.1 Infrared spectrum in the υ(CO) region of: A)Vaska's complex in benzene; B)η^2-C_{60})Ir(CO)$(PPh_3)_2$Cl in benzene[28].

The reaction between Vaska's complex and C_{60} produces (η^2-C_{60})Ir(CO)$(PPh_3)_2$Cl) as deduced from X – ray diffraction data[5]. The product of this reaction suggests that fullerene is attached to iridium in a dihapto mode (η^2) through a 6 – 6 ring fusion with bond lengths of 2.19 Å for iridium – C_{60} bonds[5]. In the structure shown in Figure 2 the two triphenylphosphine fold back into a nearly *cis* geometry in contrast to their original *trans* position in Vaska's Complex, while the carbonyl and chloride ligands retain their original *trans* positions[5].

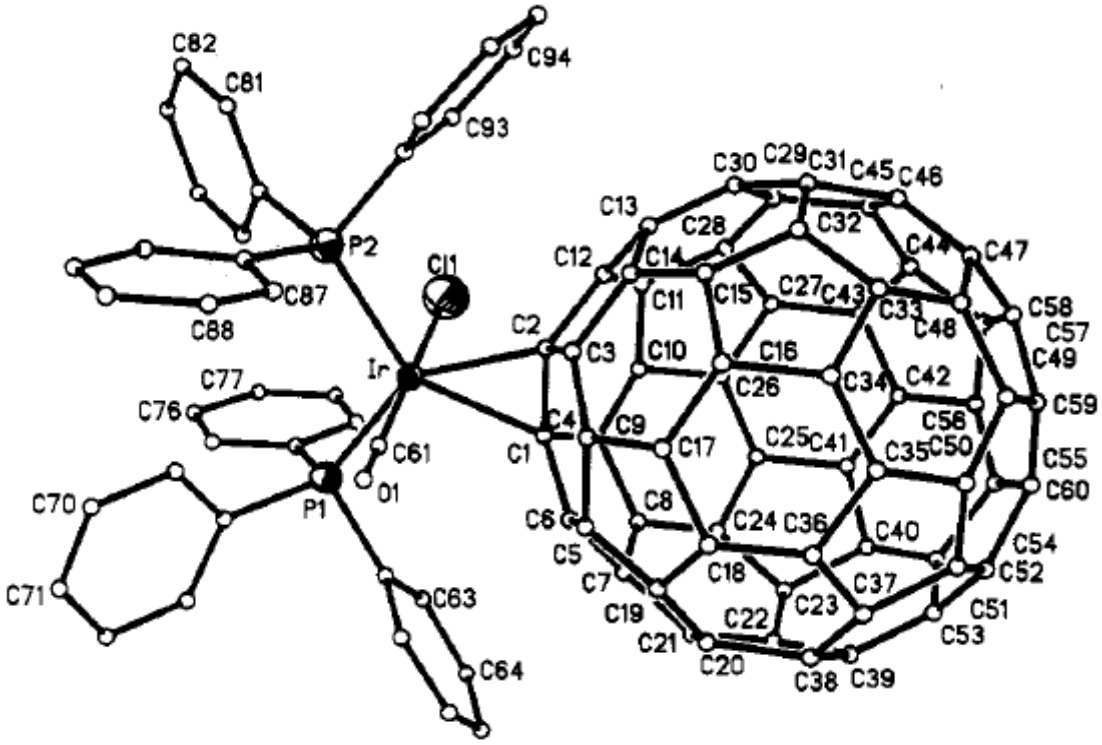

Figure 2.2 Structure of $(\eta^2\text{-}C_{60})Ir(CO)(PPh_3)_2Cl$ based on X-ray diffraction[4].

Organometallic complexes such as $(\eta^2\text{-}C_{60})W(CO)_5$ have been reported where Lewis bases like triphenyl phosphine(PPh_3) displace C_{60} from the metal coordination sphere to produce $(\eta^1\text{-}P(C_6H_5)_3W(CO)_5$, show in figure 3.3.[12]

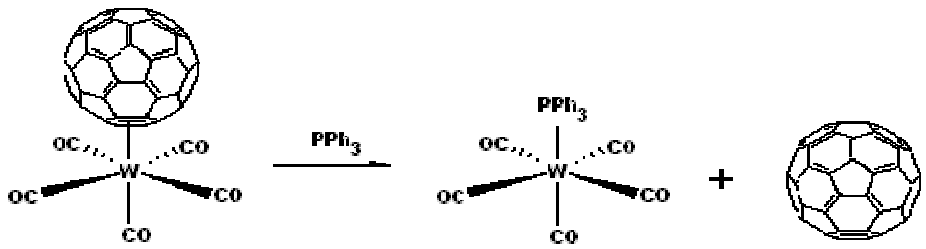

Figure 2.3 Proposed reaction for fullerene displacement by PPh_3 from $(\eta^2\text{-}C_{60})W(CO)_5$, producing $(\eta^1\text{-}P(C_6H_5)_3W(CO)_5$.[12]

For this reason as part of this project to study fundamental reactions of C_{60}-coordinated organometallic catalysts we reported a mechanistic investigation of C_{60} dissociation from (η^2-C_{60})Ir(CO)(PPh_3)$_2$(Cl) in various solvents and in binary solvent mixtures.

Chapter III

Solvent – assisted C_{60} dissociation from (η^2 – C_{60})Ir(CO)(Cl)(PPh_3)$_2$ in solvent mixtures and solvent$_1$/solvent$_2$ exchange on Ir(CO)(Cl)(PPh_3)$_2$(solvent).

3.1 Materials and methodology.

3.1.1 General

The synthesis of (η^2-C_{60})Ir(CO)(PPh_3)$_2$Cl used commercially available Vaska's complex Ir(CO)(PPh_3)$_2$Cl (Aldrich) and Fullerene (C_{60}) (Aldrich). The solvents benzene (Bz), tetrahydrofuran (THF) and cyclohexane (Cy) were fractionally-distilled under N_2 over phosphorous pentoxide or sodium to remove moisture and other impurities.

The complexes' υ(CO) active bands were predicted using group theory concepts[30]. Infrared spectra were obtained on a Bruker Vector 22 Fourier transform infrared spectrophotometer using a 0.10 mm KBr cell. All reactions were carried out under a nitrogen atmosphere or under ultra high vacuum.

3.1.2 Preparation and characterizations of (η^2-C_{60})Ir(CO)(PPh_3)$_2$(Cl)

This complex was prepared from (Ir(CO)(PPh_3)$_2$Cl (Aldrich) and C_{60} (Aldrich) following a reported method[2]. Approximately equimolar amounts of Vaska's complex and C_{60} were used. For example, 0.04053 (± 0.00001) g (5.6239 x 10^{-5} mol) of fullerene and 0.04055 (±0.00001) g (5.1971 x 10^{-5}mol) of Vaska's complex were dissolved in 10.0 mL of benzene in a 15.0 mL round bottom flask equipped with a magnetic stirrer and under nitrogen (Figure 3.1). Alternatively, the synthesis was performed under vacuum using a high vacuum line to prevent oxygen at any trace concentration. The original Vaska's complex is yellow and fullerene is violet, when both reagents were mixed the solution became dark green. The production of (η^2-C_{60})Ir(CO)(PPh_3)$_2$(Cl) was effected after about eighteen minutes of constant stirring judged by the reaction solution's υ(CO) infrared spectrum as shown in Figure 3.2.

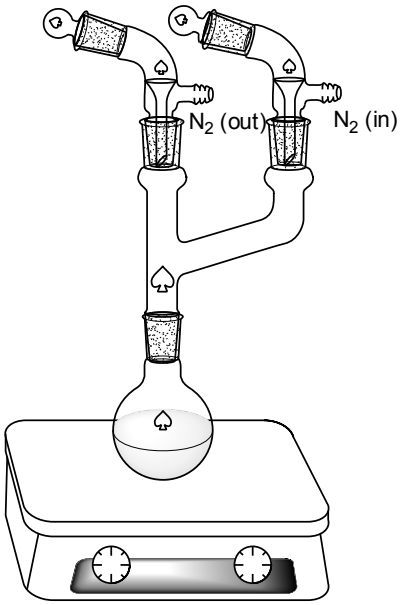

Figure 3.1 Schematic representation of the equipment used for the preparation of (η^2-C_{60})Ir(CO)(PPh_3)$_2$Cl

Once the preparation was completed, benzene was evaporated from the mixture using a gentle nitrogen flow. The complex ($\eta^2 - C_{60}$) Ir (CO)(PPh_3)$_2$Cl showed its characteristic υ(CO) band at approximately 2015 cm^{-1}.[4]

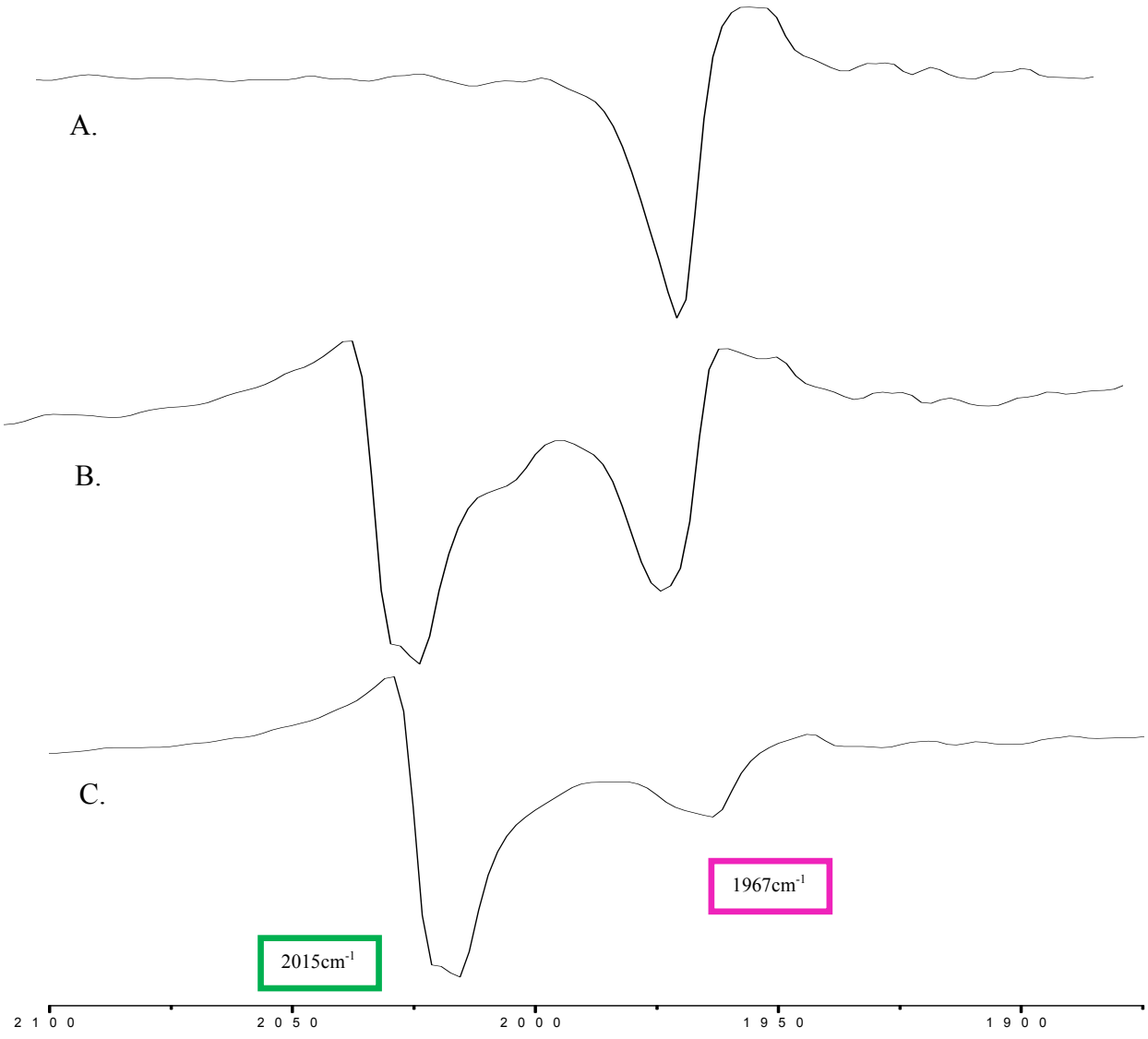

Figure 3.2 Infrared spectra in the ν(CO) ***of C_{60}/Vaska's complex mixture (ca. 1/1 molar ratio) under continuous stirring under nitrogen. Spectrum A, corresponding to 0.0 s of reaction time, Spectrum B, corresponding to 450 s of reaction time, and Spectrum C, to 1050s of reaction time.***

3.1.2.1 Distillation of solvents

Benzene (C_6H_6), tetrahydrofurene (THF) and cyclohexane(C_6H_{12}) were dried and fractionally-distilled under nitrogen. Benzene and cyclohexane were dried over phosphorous pentoxide and THF over sodium.

3.2 Kinetics studies of the solvent exchange reactions on ($\eta^2 - C_{60}$) Ir (CO)(PPh_3)$_2$Cl

3.2.1 General

Kinetics experiments were performed using a Perkin Elmer Lambda 25 UV–Vis Spectrometer to monitor the progress of reactions. The reactions were conducted under a nitrogen atmosphere. A 10 mm jacketed quartz cell was used to ensure that the temperature was constant during each kinetic run. The temperature was controlled with a Julabo F–12 constant temperature water circulator and monitored with a K/J Fluke digital thermometer equipped with a bead thermocouple.

For determination of the monitoring wavelength UV – Vis, scans were performed to solutions of reacting mixtures. The resulting spectra are shown in figure 3.2. Rate constant values were determined using a non-linear regression analysis computer program (Origin Pro 8.0^{TM}) by plotting absorbance values versus time.

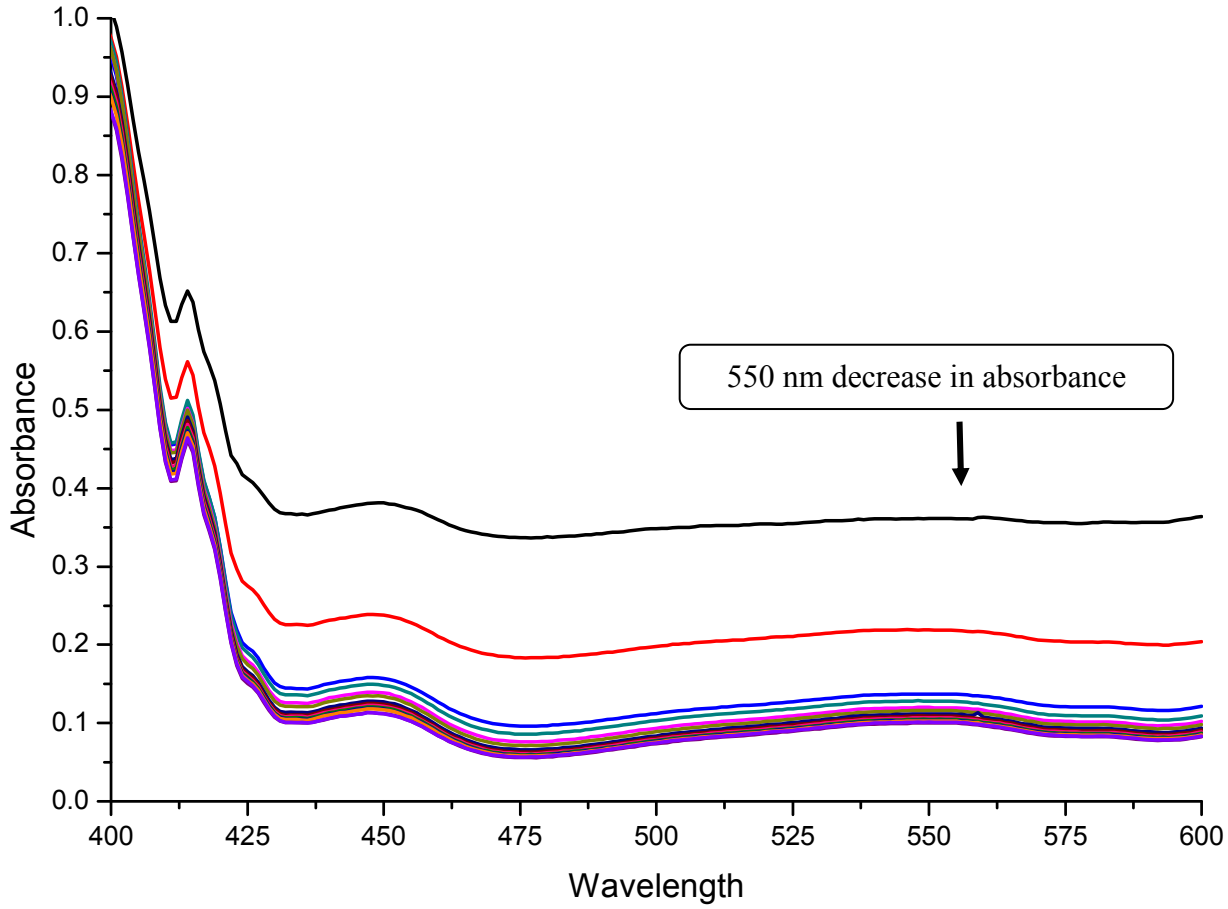

Figure 3.3 Plots of absorbance vs. wavelength at various stages of the reaction progress of $(\eta^2\text{–}C_{60})Ir(CO)(PPh_3)_2Cl$ in benzene at 295K.

3.2.2 Kinetics experiments for (η^2–C_{60}) Ir (CO)(PPh_3)$_2$Cl

The dissociation of C_{60} from the complex (η^2–C_{60})Ir(CO)(PPh_3)$_2$Cl and subsequent reactions in benzene and in solvent mixtures were monitored by observing and recording the absorbance values at 550 nm. Rate constant values were determined for reactions in benzene and benzene/cyclohexane mixtures at various temperatures. Solvent mixtures prepared at various compositions ranging from 0 to 10 M, where one of the components is actually a solvent, while the other component is considered as solute.

3.2.3 Data Analysis

Rate constant values were determined using a non-linear least squares computer program. Plots of absorbance vs. time consist of two consecutive decreasing segments. The functions that best describe the relation between absorbance values and time were bi-exponential. The general form of the functions is given by equation 3.1.

$$\text{Absorbance} = \alpha e^{-kt} + \beta e^{-k't} + \gamma \qquad 3.1$$

In equation 3.1 the pre-exponential coefficients α and β are constants which values depend on k_{obs}, k'_{obs}, and the extinction coefficients of the chemical species involved in the consecutive reactions, while γ represents the absorbance at time infinity or considered as more than $10t_{1/2}$.[31-33]

3.2.4 Result

3.2.4.1 Reactions in benzene (one-solvent system)

The reaction of C_{60} with $Ir(CO)(PPh_3)_2Cl$ in benzene produced $(\eta^2\text{-}C_{60})Ir(CO)(PPh_3)_2Cl$. The $\upsilon(CO)$ spectrum of $(\eta^2\text{-}C_{60})Ir(CO)(PPh_3)_2Cl$ shows two bands at 1967cm^{-1} and at 2015cm^{-1}; this spectrum is shown in (Figure 3.2). The band at 1967 cm^{-1} was attributed to Vaska's complex whereas the band at 2015 cm^{-1} was assigned to $(\eta^2\text{-}C_{60})Ir(CO)(PPh_3)_2Cl$[4,28]. These results suggest an equilibrium that favors the dissociated species, equation (3.2).

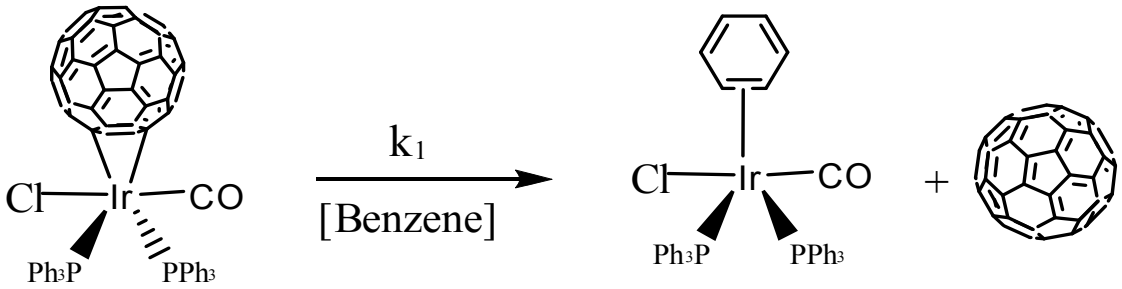

3.2

The reactions of $(\eta^2\text{-}C_{60})Ir(CO)(PPh_3)_2Cl$ producing [(solvent)$Ir(CO)(PPh_3)_2Cl$] and other species in various one-solvent systems and in solvent mixtures were mechanistically-investigated. The reactions were first order with respect to the molar concentrations of $(\eta^2\text{-}C_{60})Ir(CO)(PPh_3)_2Cl$. Attempts to study the reaction in THF and in cyclohexanene were unsuccessful due to the low solubility of $(\eta^2\text{-}C_{60})Ir(CO)(PPh_3)_2Cl$ in these solvents. The solubility of $(\eta^2\text{-}C_{60})Ir(CO)(PPh_3)_2Cl$ in benzene is high enough and the reaction's rates are sufficiently slow in this solvent to be monitored by following the decrease of absorbance at 550 nm (Figure 3.3). The reactions were studied at various temperatures under what can be

considered flooding conditions since [solvent] >> [(η^2-C_{60})Ir(CO)(PPh_3)$_2$Cl]. Pseudo-first order rates constants values (k_{obs}) were determined using a non-linear curve fitting of the absorbance versus time plots.

Solvent displacement of C_{60} from (η^2-C_{60})Ir(CO)(PPh_3)$_2$Cl and subsequent reactions are biphasic. Plots of absorbance vs. time (Figure 3.4) consist of two decreasing segments. The fast segment of the plots was ascribed to C_{60}/solvent exchange on (η^2-C_{60})Ir(CO)(PPh_3)$_2$Cl , while the slow segment was attributed to parallel triphenyl phosphine dissociation and to other reactions that will be described later.

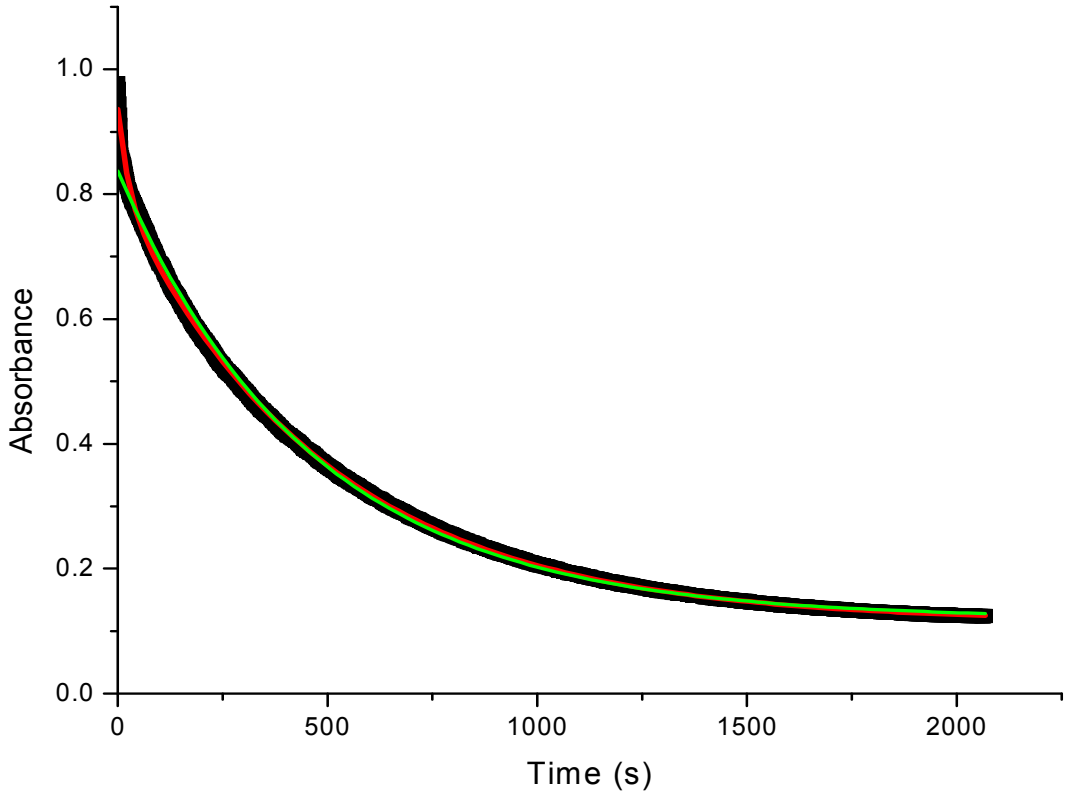

Figure 3.4 Plot of absorbance vs. time(s) obtained by monitoring absorbance at 550nm of a solution containing (η^2-C_{60})Ir(CO)(PPh_3)$_2$Cl in benzene at 295K. The continuous red trace are absorbance values obtained from the function Absorbance = $0.6500(6)e^{-(0.010\pm1)t1} + 0.0321(7)e^{-(0.081\pm3)t2} + 0.09901(7)$. The continuous green trace are absorbance values obtained from the function Absorbance = $0.717(8)\, e^{-(0.00216\pm5)t1} + 0.120(4)$[37]

3.2.4.2 Monitoring progress of reaction of ($\eta^2 - C_{60}$) Ir (CO)(PPh_3)$_2$Cl in benzene and products characterization

Infrared spectra were obtained on a Bruker Vector 22 Fourier transform infrared spectrophotometer using a 0.10 mm light path KBr cell. All reactions were carried out under a nitrogen atmosphere to prevent oxidation by O_2. The reactions of (η^2–C_{60})Ir(CO)(PPh_3)$_2$Cl in benzene were monitored by observing the ν(CO) region of the IR spectrum from 2100 to 1700 cm^{-1}.

3.2.4.3 C_{60} /benzene exchange on (η^2 – C_{60}) Ir (CO)(PPh_3)$_2$Cl

The IR spectrum of a fresh solution of (η^2 – C_{60})Ir(CO)(PPh_3)$_2$Cl in benzene shows three IR bands at 2021cm^{-1}, 1965 cm^{-1} and 1818 cm^{-1} (figure 3.5).

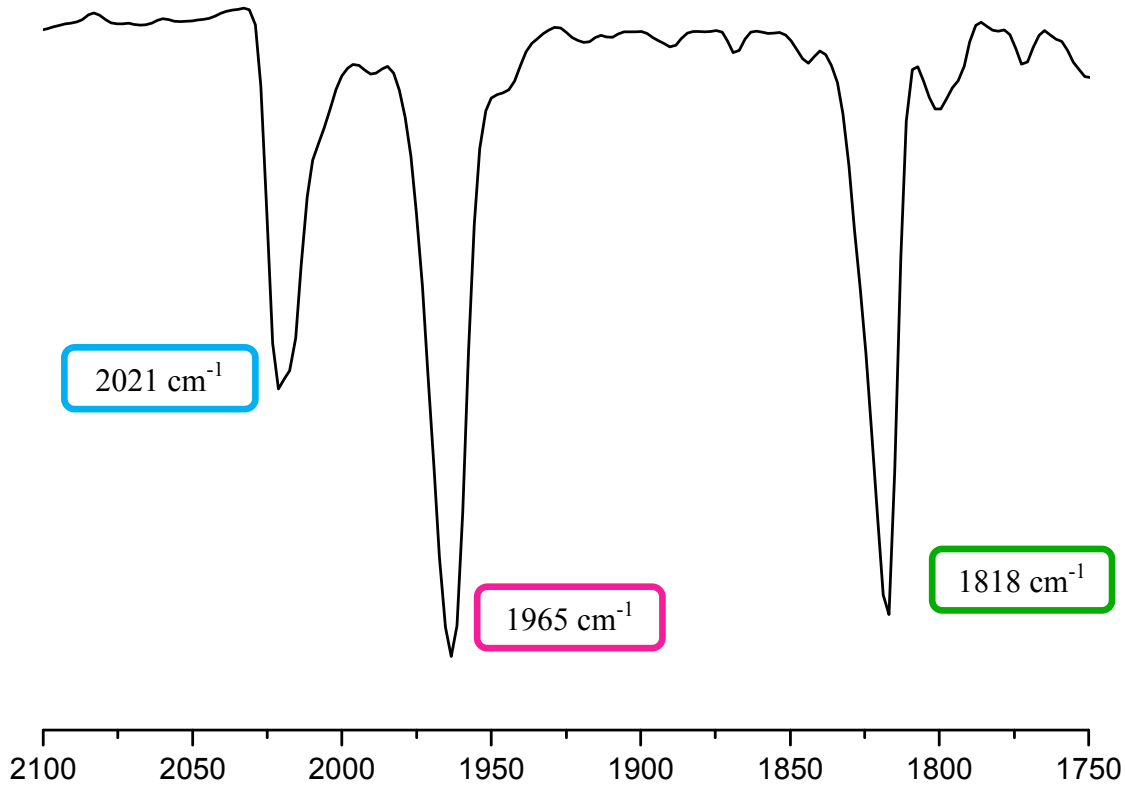

Figure 3.5 Infrared spectrum of a fresh solution of (η^2–C_{60}) Ir (CO)(PPh_3)$_2$Cl in benzene showing three IR bands at 2021 cm^{-1}, 1965 cm^{-1} and 1818 cm^{-1}

A new IR band at 1822 cm^{-1} appears in the spectrum 240 seconds after mixing, while the band at 1818 cm^{-1} disappears. Also a negative absorbance at 1816 cm^{-1} is observed 240 seconds after mixing (figure 3.6).

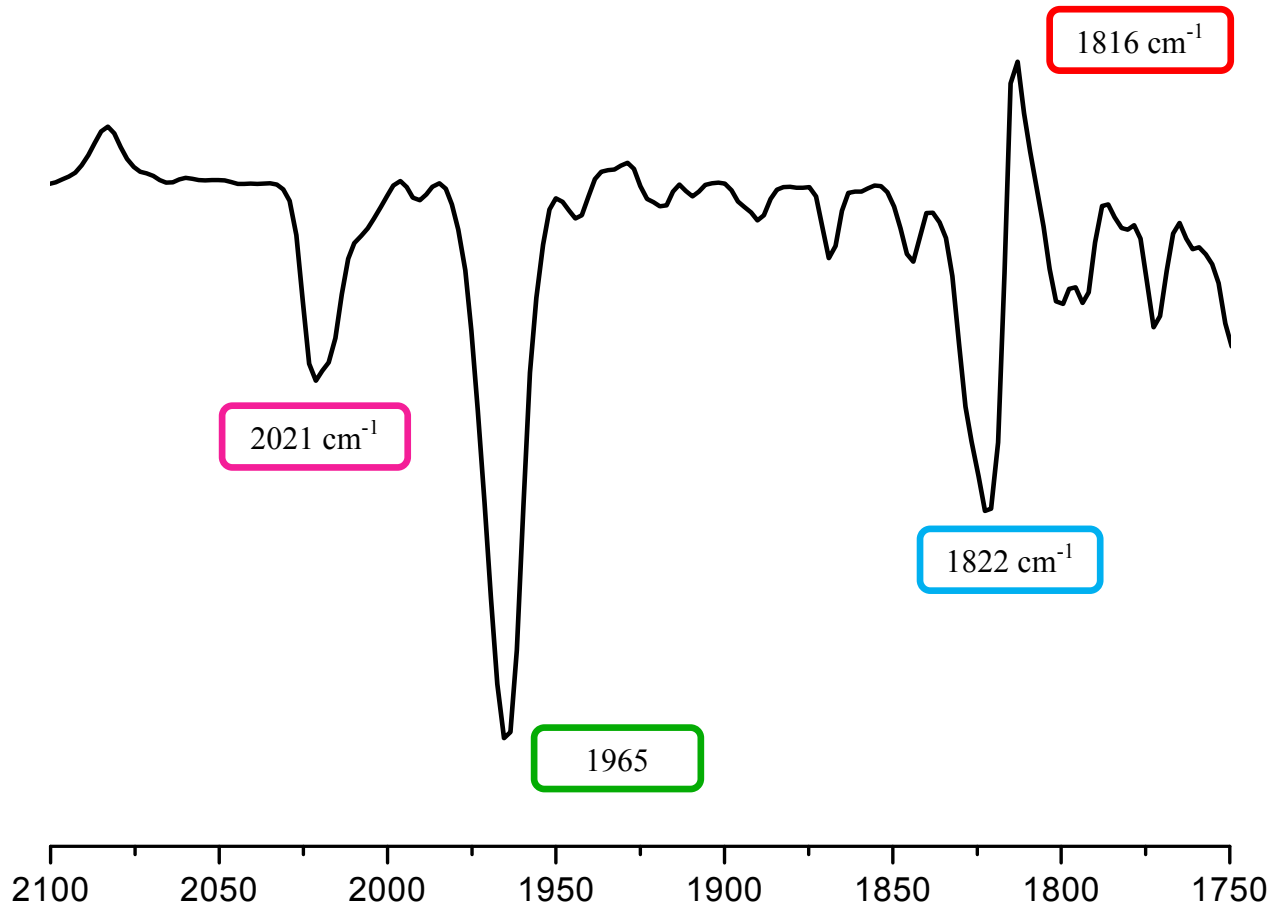

Figure 3.6 Infrared spectrum of (η^2-C_{60}) Ir (CO)$(PPh_3)_2$Cl in benzene obtained 240 seconds after mixing showing a new band at 1822 cm^{-1} and a negative band at 1816 cm^{-1}

At 420 s after mixing the band at 1818 cm^{-1} that had a negative absorbance grew and became a new band in the spectrum. Two shoulders were also observed in the spectrum at 1801 cm^{-1} and 1950 cm^{-1} (Figure 3.7).

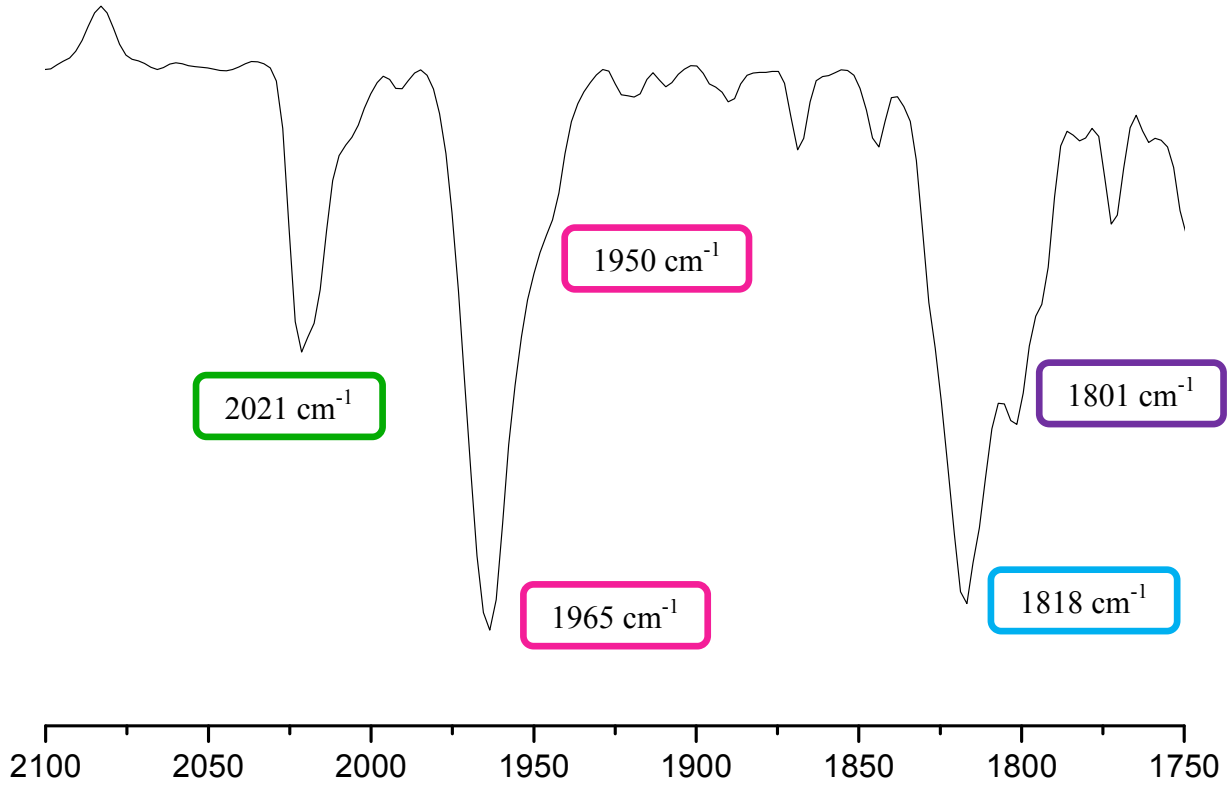

Figure 3.7 Infrared spectrum of (η^2–C_{60})Ir(CO)(PPh_3)$_2$Cl in benzene after 420 seconds of reaction, the band at 1818 cm^{-1} and two shoulder at 1950 cm^{-1} and 180 cm^{-1} are observed

In order to identify the reaction products, infrared spectra of pure samples of triphenyl phosphine and benzene were obtained. Benzene's IR spectrum is presented in Figure 3.8 showing two overtones at 1952 cm^{-1} and 1807 cm^{-1}. The triphenylphosphine IR spectrum in benzene is presented in figure 3.9 and shows four absorption bands: two positive ν(C=C) bands located at 1952 cm^{-1} and 1804 cm^{-1}, and two negative absorption bands located at 1962 cm^{-1} and 1817 cm^{-1}.

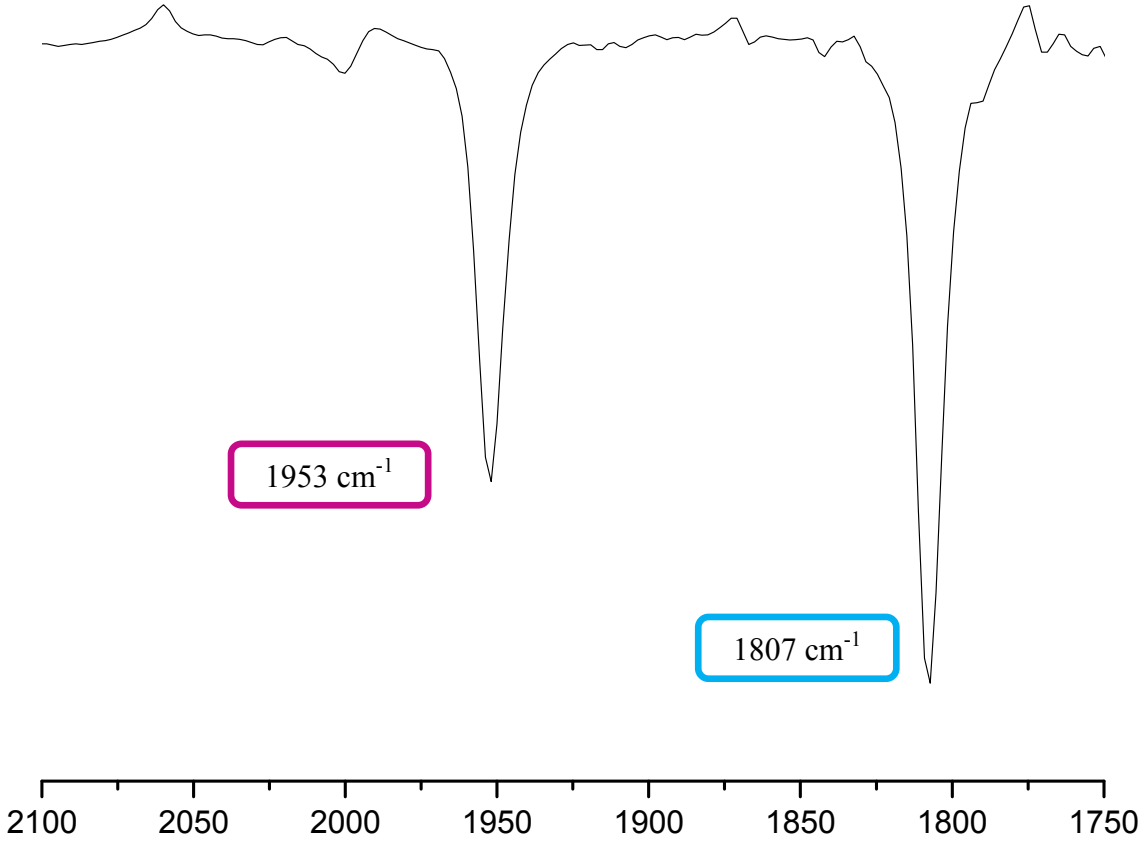

Figure 3.8 Infrared spectrum of benzene in cyclohexane measured to identify benzene's IR bands.

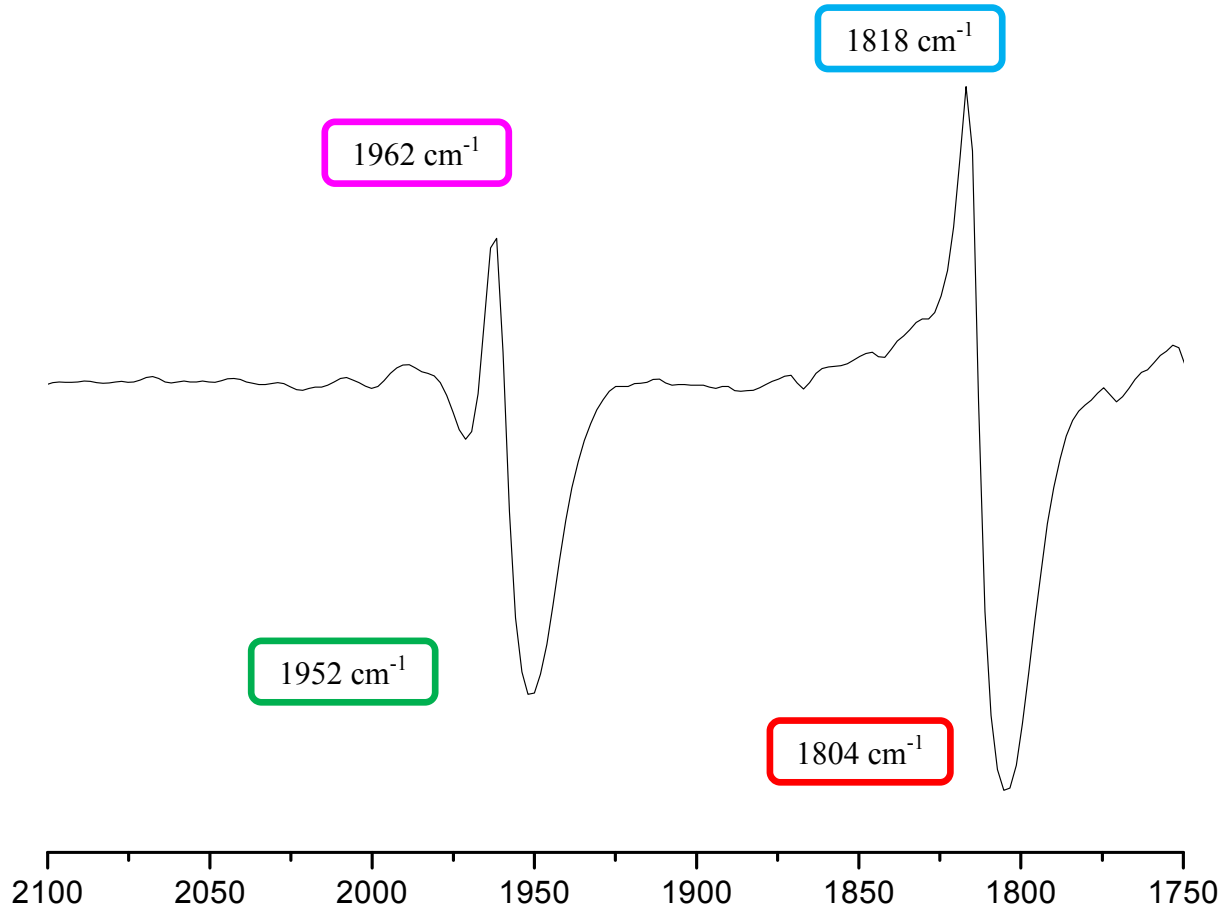

Figure 3.9 Infrared spectrum of a triphenylphosphine-saturated solution in benzene, showing four bands; two with positive absorbances at 1951 cm^{-1} and 1804 cm^{-1} assigned to triphenyl phosphine and two bands with negative absorbance at 1962 cm^{-1} and 1817cm^{-1} assigned to benzene

Due to the possibility that the fast segment can be assigned to C_{60}/solvent exchange on (η^2-C_{60})Ir(CO)(PPh_3)$_2$Cl, the reaction progress of Ir(CO)(PPh_3)$_2$Cl in benzene was monitored in absence of C_{60}. The purpose of this experiment was to identify the nature of subsequent reactions, including triphenyl phosphine dissociation and other reactions that will be described later.

3.2.4.4 Product(s) characterization of the reactions of Vaska's complex in benzene

The reagents that were used for the preparation of the complex are $Ir(CO)(PPh_3)_2Cl$ (Aldrich) and Benzene (Aldrich). The synthesis was performed under vacuum using a high vacuum line to prevent oxygen at any trace concentration; using a 15.0 mL round bottom flask approximately 6.0 mg of Vaska's complex were dissolved in 5.0 mL of benzene. Vaska's complex is a mustard yellow solid and benzene is a colorless liquid, (figure 3.10). When both reagents were mixed after 24 hours, the solution becomes light yellow, (figure 3.11). After approximately 24 hours of constant stirring under nitrogen the synthesis was considered complete,

Figure 3.10 A photograph of a fresh Vaska's complex/ benzene solution showing a bright yellow color

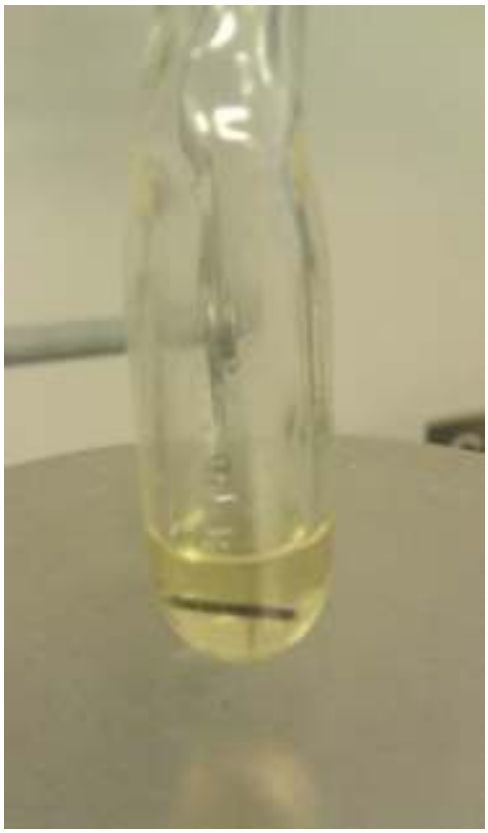

Figure 3.11 A photograph of a Vaska's complex/ benzene solution after 24 h of constant stiring under nitrogen showing a pale yellow color .

The reaction was monitored by observing the ν(CO) region of the IR spectrum from 2100 cm^{-1} to 1700 cm^{-1}. Before mixing, Vaska's complex shows a band at 1953 cm^{-1} in a KBr pellet (Figure 3.12). After 24 hours of mixing, the solvent was evaporated with a slow flow of nitrogen. The product's IR shows two bands at 2001 cm^{-1} and 1952 cm^{-1} (Figure 3.13). These results confirm the existence of subsequent reactions after C_{60} dissociation from (η^2-C_{60})Ir(CO)(PPh_3)$_2$Cl .

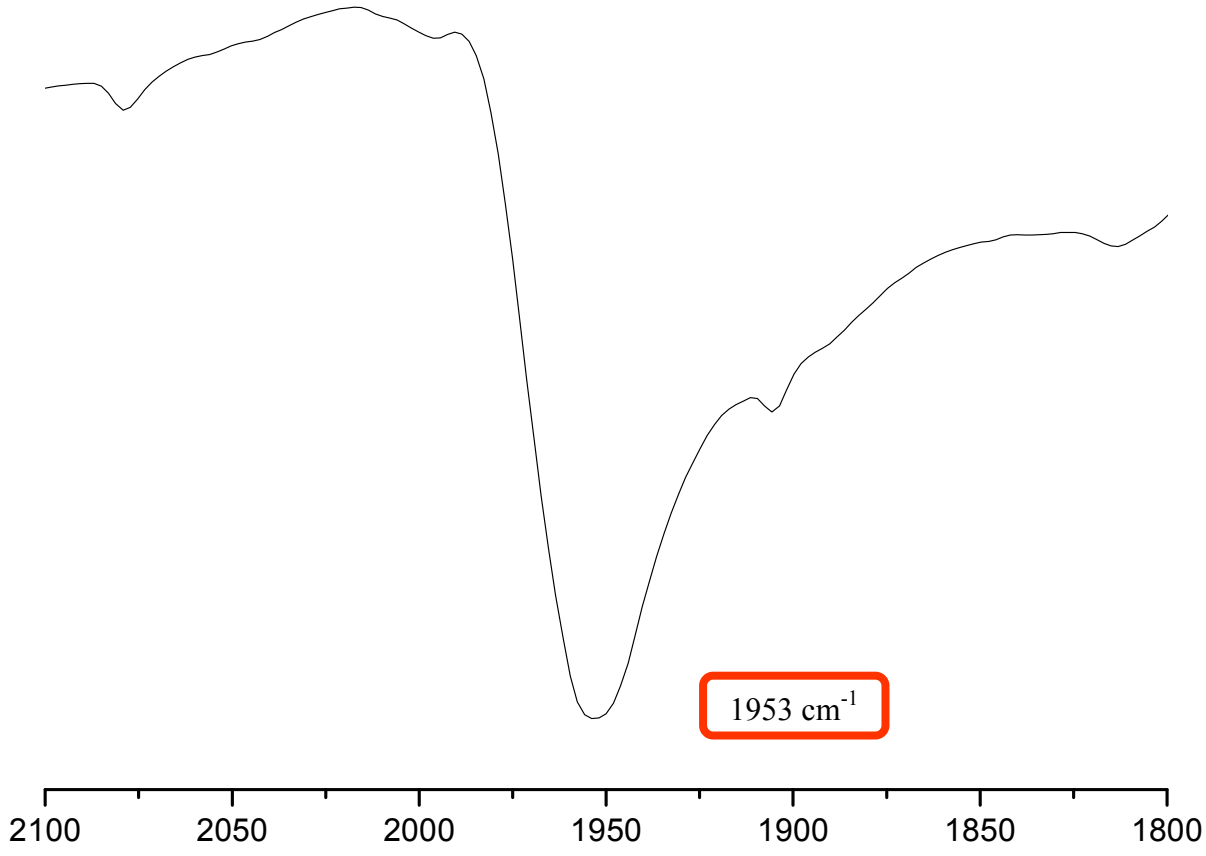

Figure 3.12 ν(CO) region (KBr pellet) of Vaska's complex showing one band at 1953cm^{-1}.

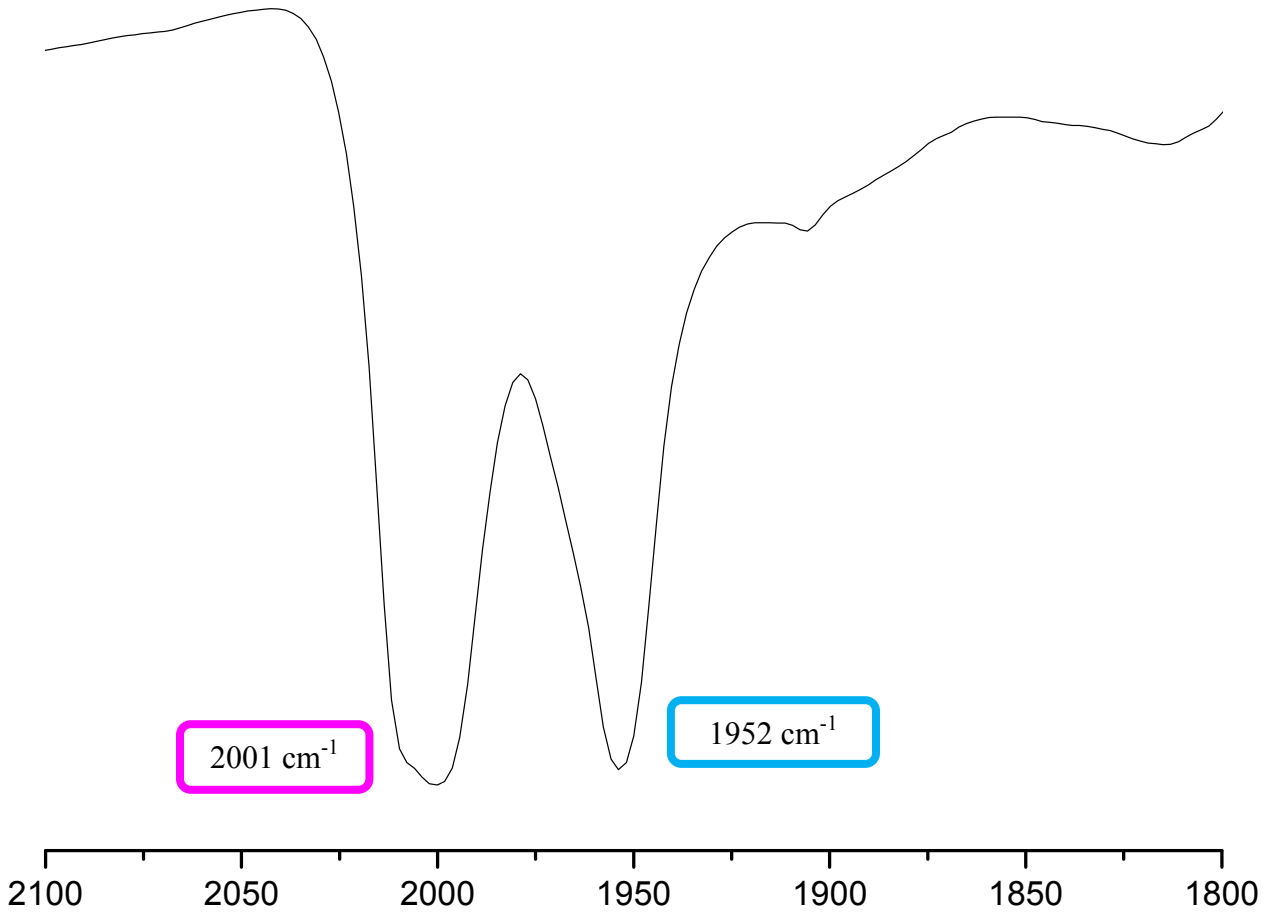

Figure 3.13 υ(CO) (KBr pellet) of Vaska's complex after 24 hours of constant stirring showing two bands at 2001 cm^{-1} and 1952 cm^{-1}

3.2.4.5 Monitoring Ir (CO)(PPh$_3$)$_2$Cl reaction's progresses using IR spectroscopy.

An IR spectrum of a fresh solution of Ir(CO)(PPh$_3$)$_2$Cl in benzene shows three IR bands at 1967 cm^{-1}, 1953 cm^{-1} and 1810 cm^{-1}, also shows two shoulders at 1821 cm^{-1} and 1802 cm^{-1} (figure 3.14).

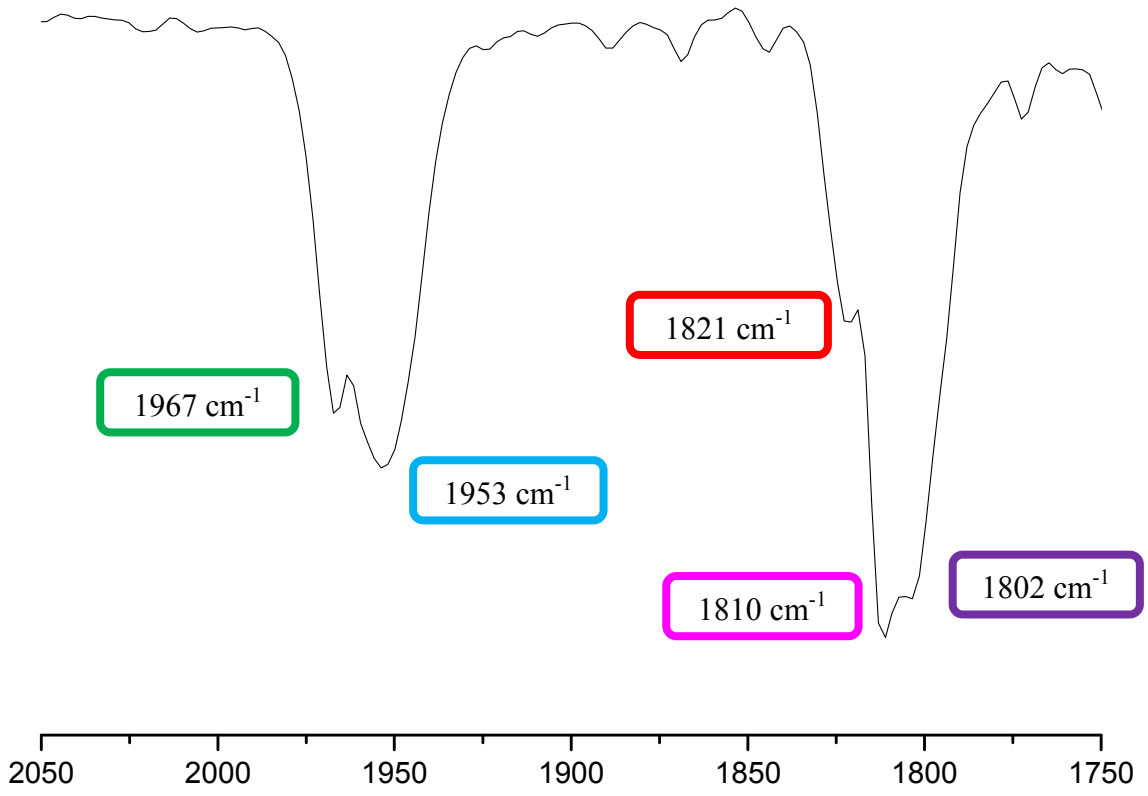

Figure 3.14 Infrared spectrum of a fresh solution of Ir (CO)(PPh$_3$)$_2$Cl in benzene showing three IR bands at 1967 cm^{-1}, 1953 cm^{-1} and 1810 cm^{-1}, also showing two shoulders at 1821 cm^{-1} and 1802 cm^{-1}

Thirty seconds after mixing, the IR spectrum shows that the intensity of the band at 1953 cm^{-1} increases (Figure 3.15). A comparison of the spectra in figures 3.11, 3.14 and 3.15 suggest that triphenyl phosphine dissociates from the parent complex.

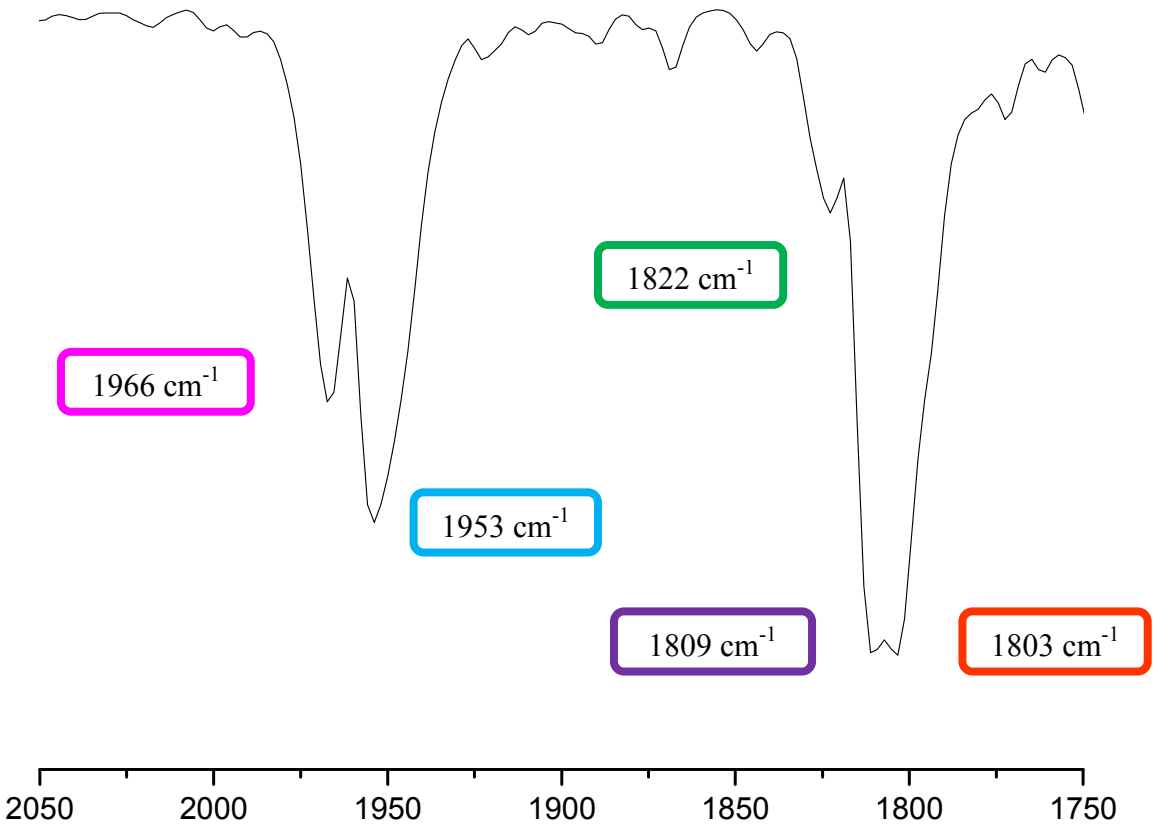

Figure 3.15 Infrared spectrum of Ir (CO)(PPh$_3$)$_2$Cl in benzene obtained 30 seconds after mixing showing that the band intensity at 1966 cm^{-1} increases. The band at 1953 cm^{-1} and 1803 cm^{-1} suggest triphenyl phosphine dissociation.

After 320 seconds of mixing the bands at 1953 cm^{-1} and 1804 cm^{-1} disappear. In addition, two bands appear at 1944 cm^{-1} and 1802 cm^{-1}, (figure 3.16).

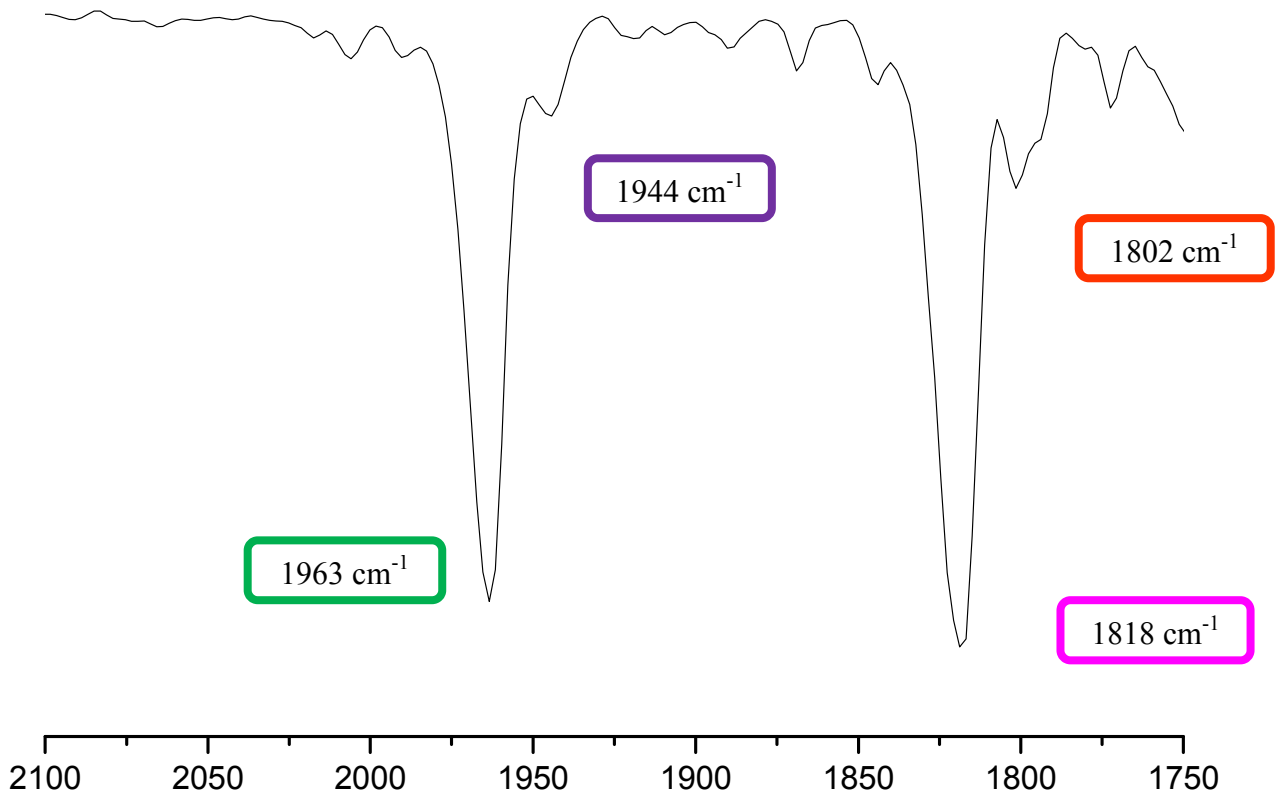

Figure 3.16 Infrared spectrum of $Ir(CO)(PPh_3)_2Cl$ in benzene obtained after 320 seconds of mixing, showing two bands at 1944 cm^{-1} and 1802 cm^{-1}.

After mixing for 1380 seconds, two small bands are observed at 1802 cm^{-1} and 1800 cm^{-1} (Figure 3.17).

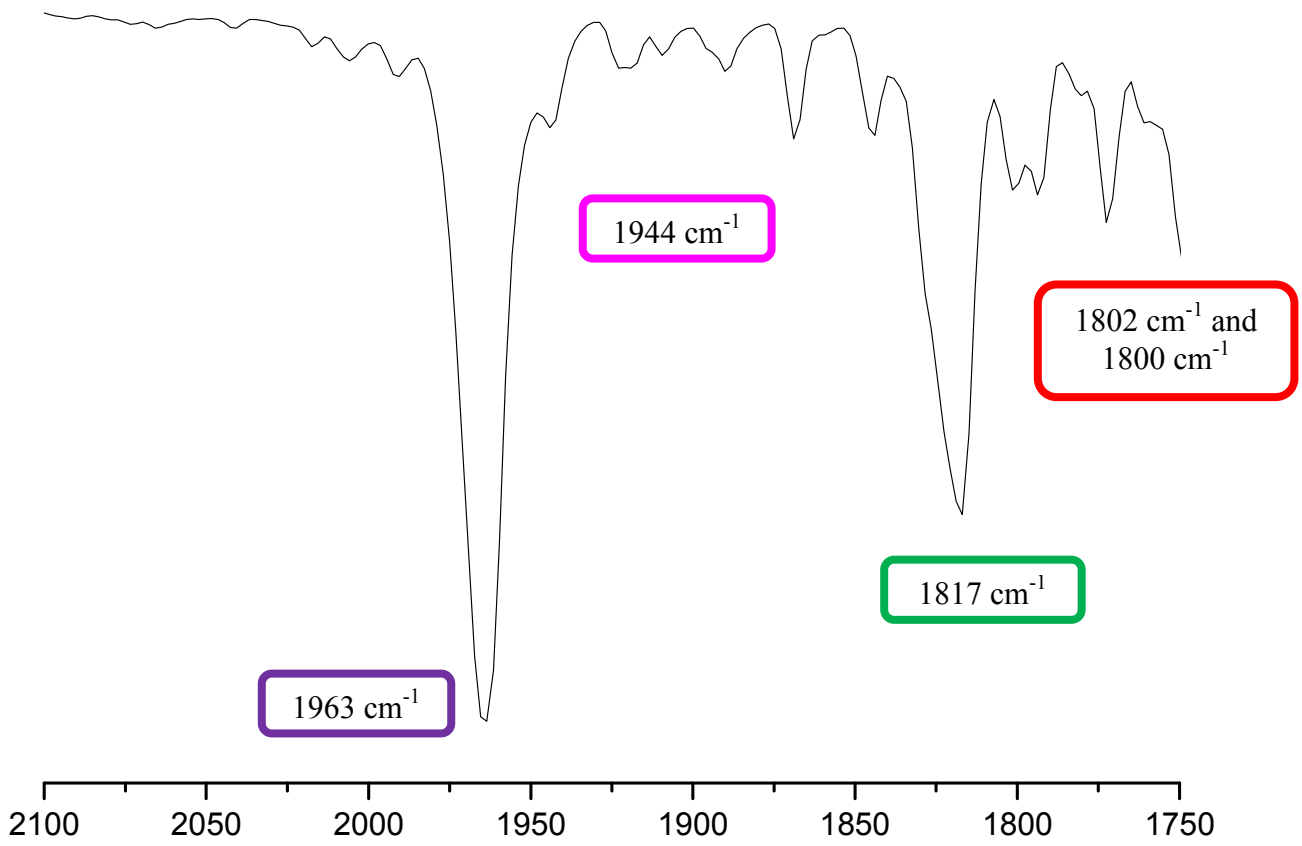

Figure 3.17 Infrared spectrum of $Ir(CO)(PPh_3)_2Cl$ in benzene obtained 1380 seconds after mixing showing two small bands at 1802 cm^{-1} and 1800 cm^{-1}.

After 1710 seconds of mixing, a band at 2005 cm^{-1} and a shoulder at 1807 cm^{-1} are observed, (figure 3.18).

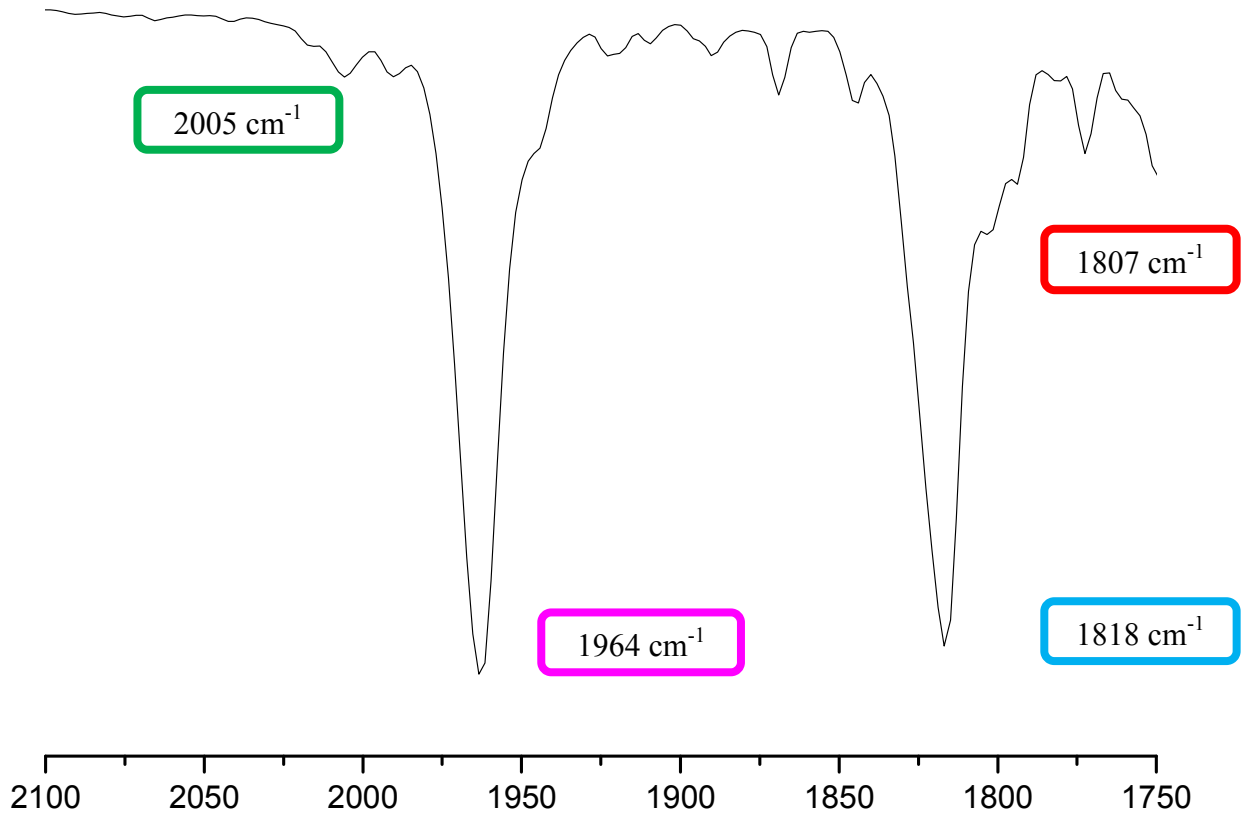

Figure 3.18 Infrared spectrum of $Ir(CO)(PPh_3)_2Cl$ in benzene obtained 1710 seconds after mixing showing a band at 2005 cm^{-1} and shoulder at 1807 cm^{-1}.

After 2190 seconds of mixing, the band at 1802 reapperared (Figure 3.19).

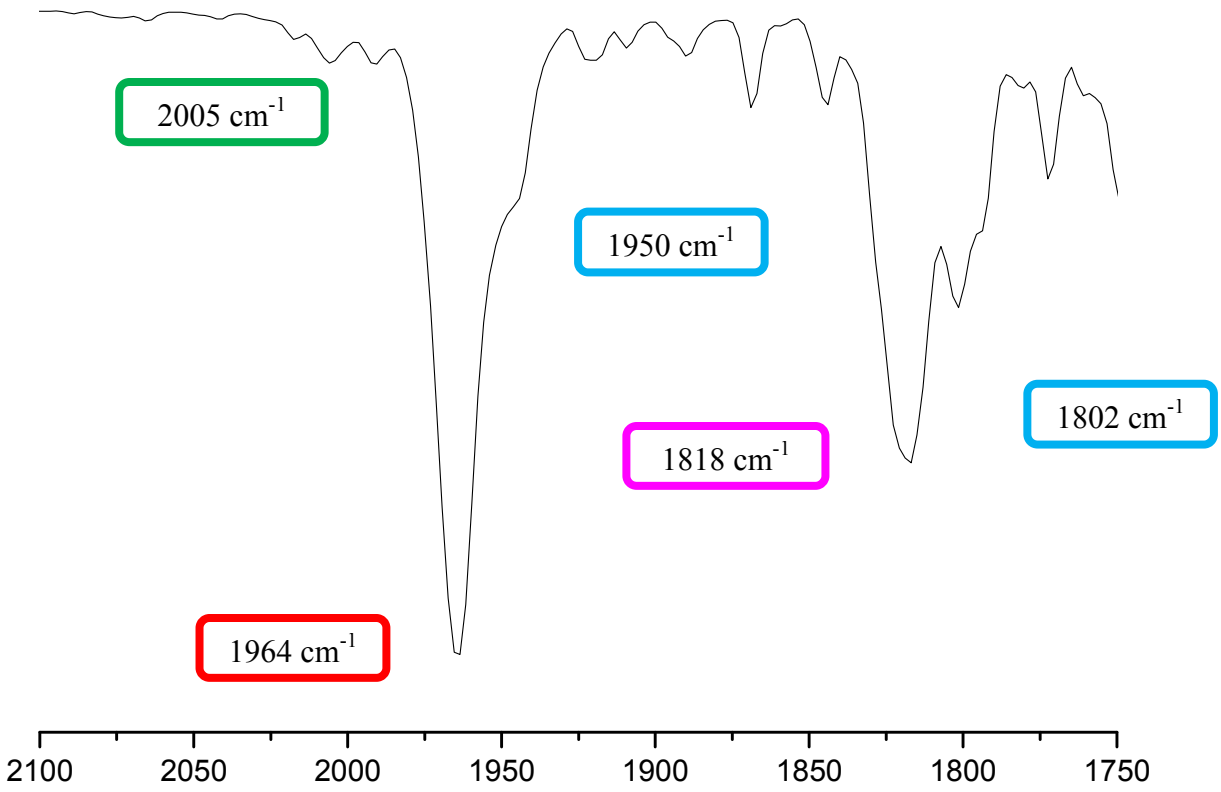

Figure 3.19 Infrared spectrum of $Ir(CO)(PPh_3)_2Cl$ in benzene obtained 2190 seconds after mixing showing a re-growth of the band at 1802 cm^{-1} and the emergence of a shoulder at 1945 cm^{-1}

Next, at 2765 second after mixing, two shoulders at 1805 cm^{-1} and 1802 cm^{-1} were observed (figure 3.20). The shoulders at 1950 cm^{-1} and the band at 1802 cm^{-1} disappeared (figure 3.21). This evidence suggest that triphenyl phosphine dissociation $Ir(CO)(PPh_3)_2Cl$ may be reversible.

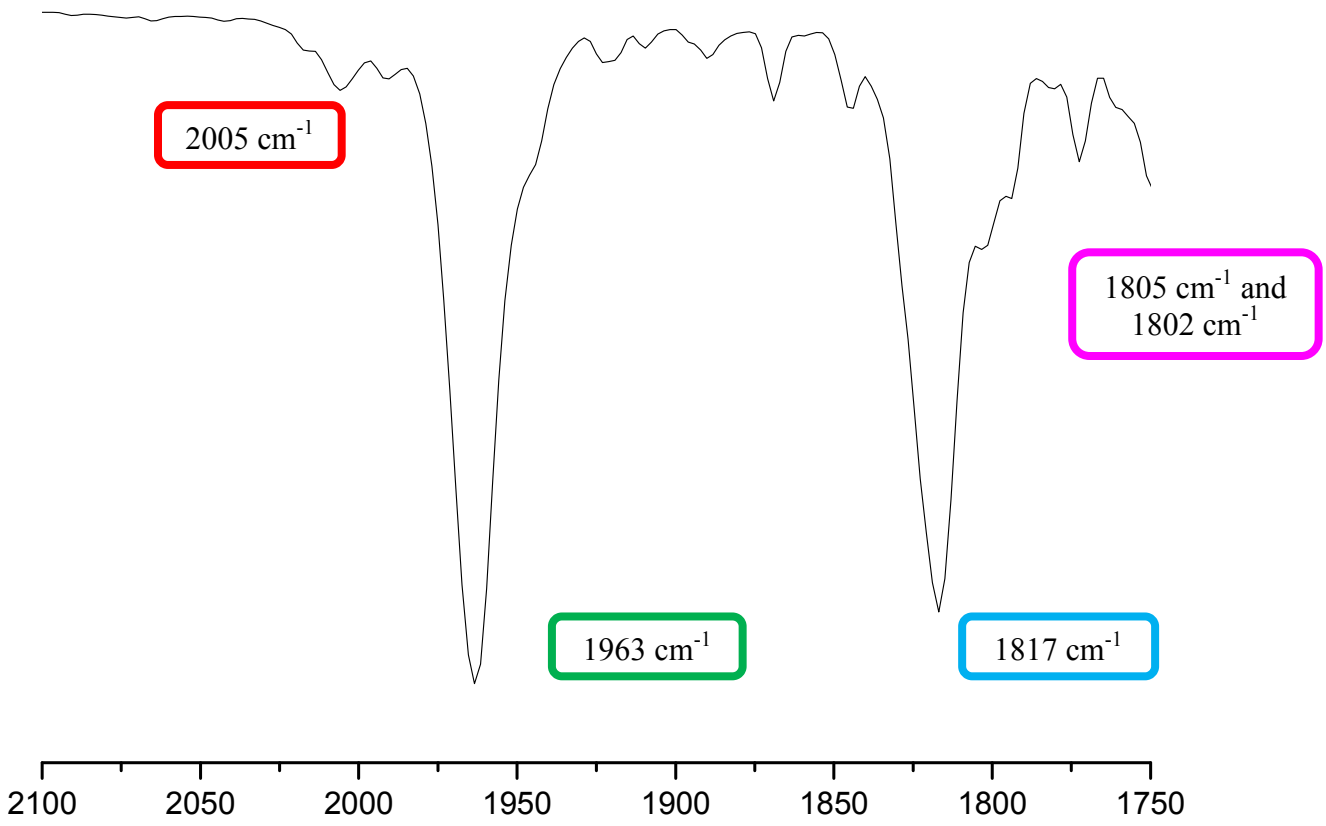

Figure 3.20 Infrared spectrum of $Ir(CO)(PPh_3)_2Cl$ in benzene obtained 2765 seconds after mixing showing two shoulders at 1805 cm^{-1} and 1802 cm^{-1}

Finally, after 24 hours of mixing, the shoulder at 1805 cm^{-1} and 1802 cm^{-1} disappear, (figure 3.21).

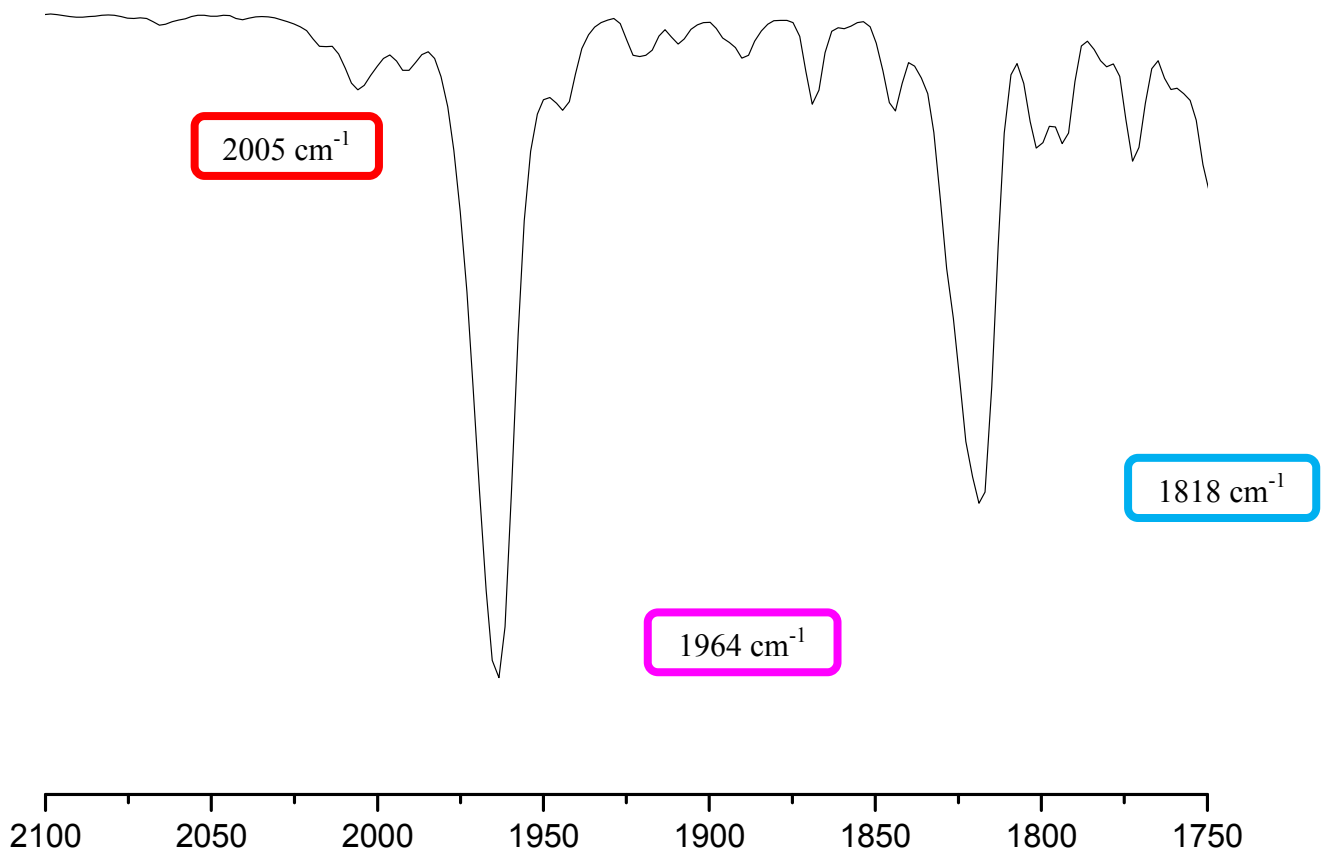

Figure 3.21 Infrared spectrum of $Ir(CO)(PPh_3)_2Cl$ in benzene obtained 24 hours after mixing the two shoulder at 1805 cm^{-1} and 1802 cm^{-1} disappears.

The presence of a band at 2005 cm^{-1} suggests that after mixing; i) triphenyl phosphine dissociates and ii) it could be possible that other parallel reactions are occurring. A saturated solution of triphenyl phosphine in benzene was prepared, which was further mixed with Vaska's

complex. The purpose of adding triphenyl phosphine is to try to inhibit the triphenyl phosphine dissociation with the expectation that the parallel reactions that may be occurring will be observed. The IR spectrum of a fresh solution of $Ir(CO)(PPh_3)_2Cl$ in a saturated solution of triphenyl phosphine in benzene shows a positive absorbance band located at 1964 cm^{-1} and other at negative absorbance band located at 1816cm^{-1}, (figure 3.22).

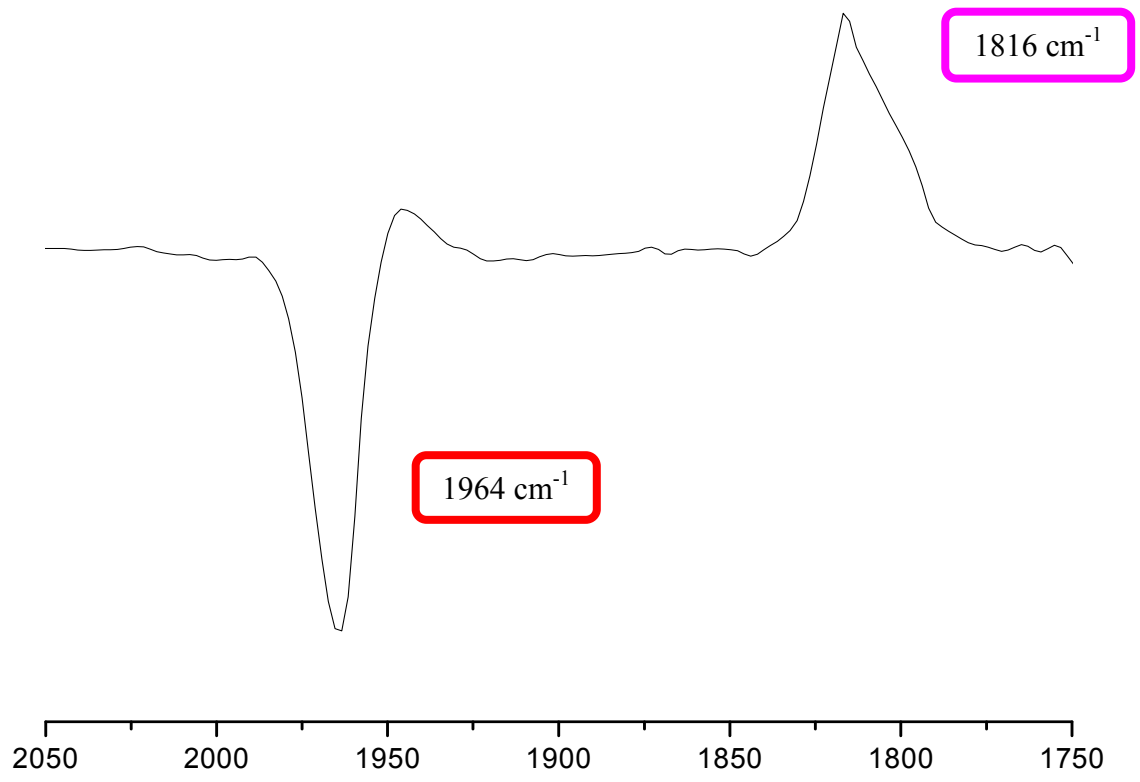

Figure 3.22 IR spectrum of a fresh solution of Ir (CO)(PPh$_3$)$_2$Cl in a triphenyl phosphine saturated solution in benzene. Two bands are observed: a positive absorbance at 1964 cm^{-1} and a negative absorbance at 1816 cm^{-1}.

After 24hours of mixing, a growth of a band at 2005 cm^{-1} is observed (figure 3.23). The band at negative absorbance is assigned to benzene (figure 3.11), these results suggest the possibility that another reaction which involves benzene depleting may be occurring. In an attempt to analyze this suspected reaction, the reaction progress was monitored using ^{1}H NMR spectroscopy.

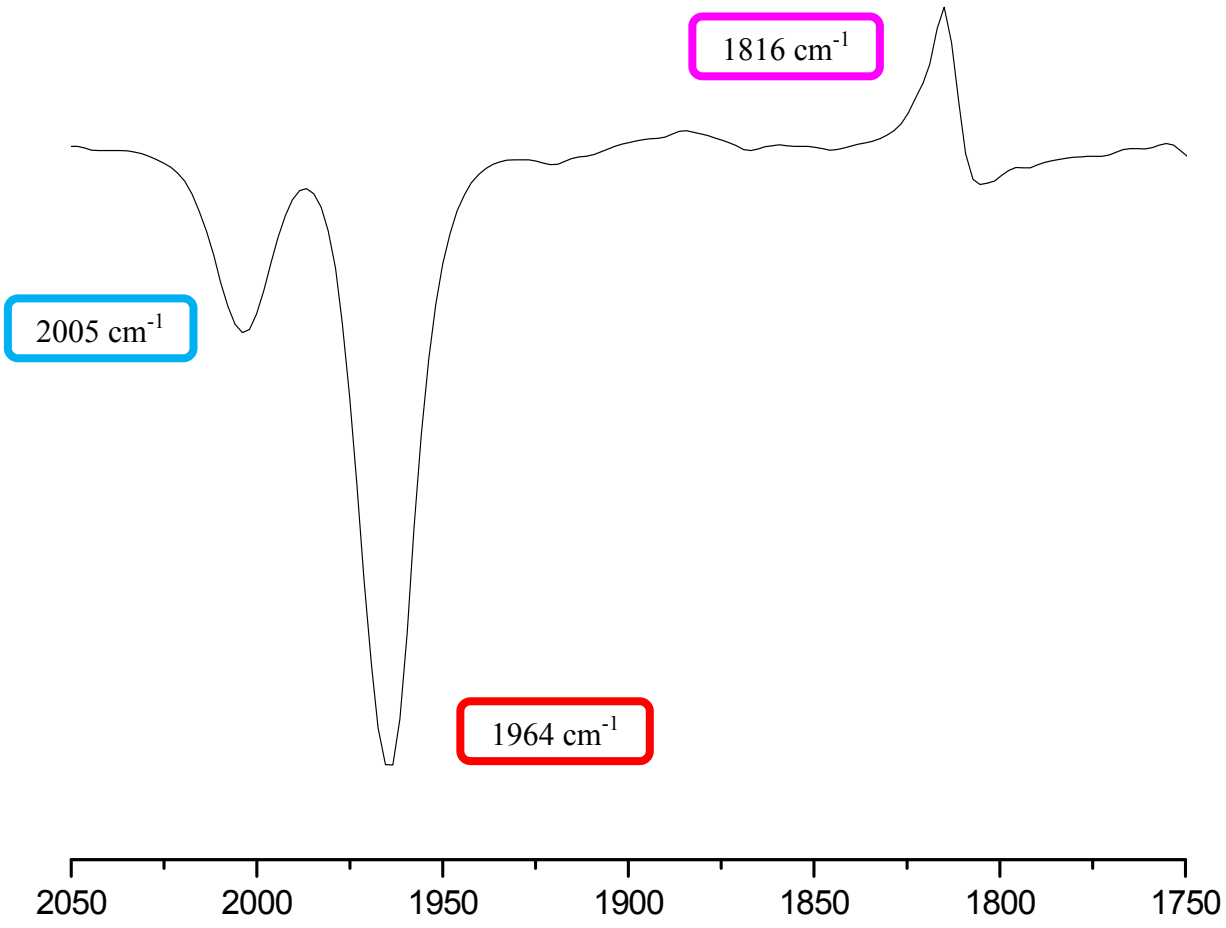

Figure 3.23 IR spectrum obtained 24 hours after mixing Ir (CO)(PPh$_3$)$_2$Cl in a saturated solution of triphenyl phosphine in benzene a growing band at 2005 cm^{-1} is observed.

3.2.4.6 NMR spectroscopy of the solvent exchange reactions on ($\eta^2 - C_{60}$) Ir (CO)(PPh_3)$_2$Cl and subserquent reactions

^{1}H NMR spectra were obtained on a A 500 MHz (11.74 Tesla magnetic field), Bruker Advance 500 instrument, equipped with a Linux computer, special legs to absorb vibrations, three channels of detection and two probes (a broadband detection and a QXI-4 inverse detection) was used for NMR analyses. The equipment has a VT unit controller for temperature control. The acquisition parameters for 1D experiments used were 1200-1400 transients and a zgpr pulse program, for water suppression.

3.2.4.7 ^{1}HNMR of (η^2 – C_{60}) Ir (CO)(PPh_3)$_2$Cl in benzene

The reactions of (η^2 – C_{60})Ir(CO)(PPh_3)$_2$Cl in benzene were monitored using NMR spectroscopy. In the ^{1}HNMR spectrum it was observed one signal at 0.55 ppm. In order to identify and assign the signals that belong to benzene and to triphenyl phosphine, a ^{1}H NMR spectrum of deuterated benzene (C_6D_6) and of triphenylphosphine (PPh_3) in C_6H_6 were obtained (Figure 3.24).

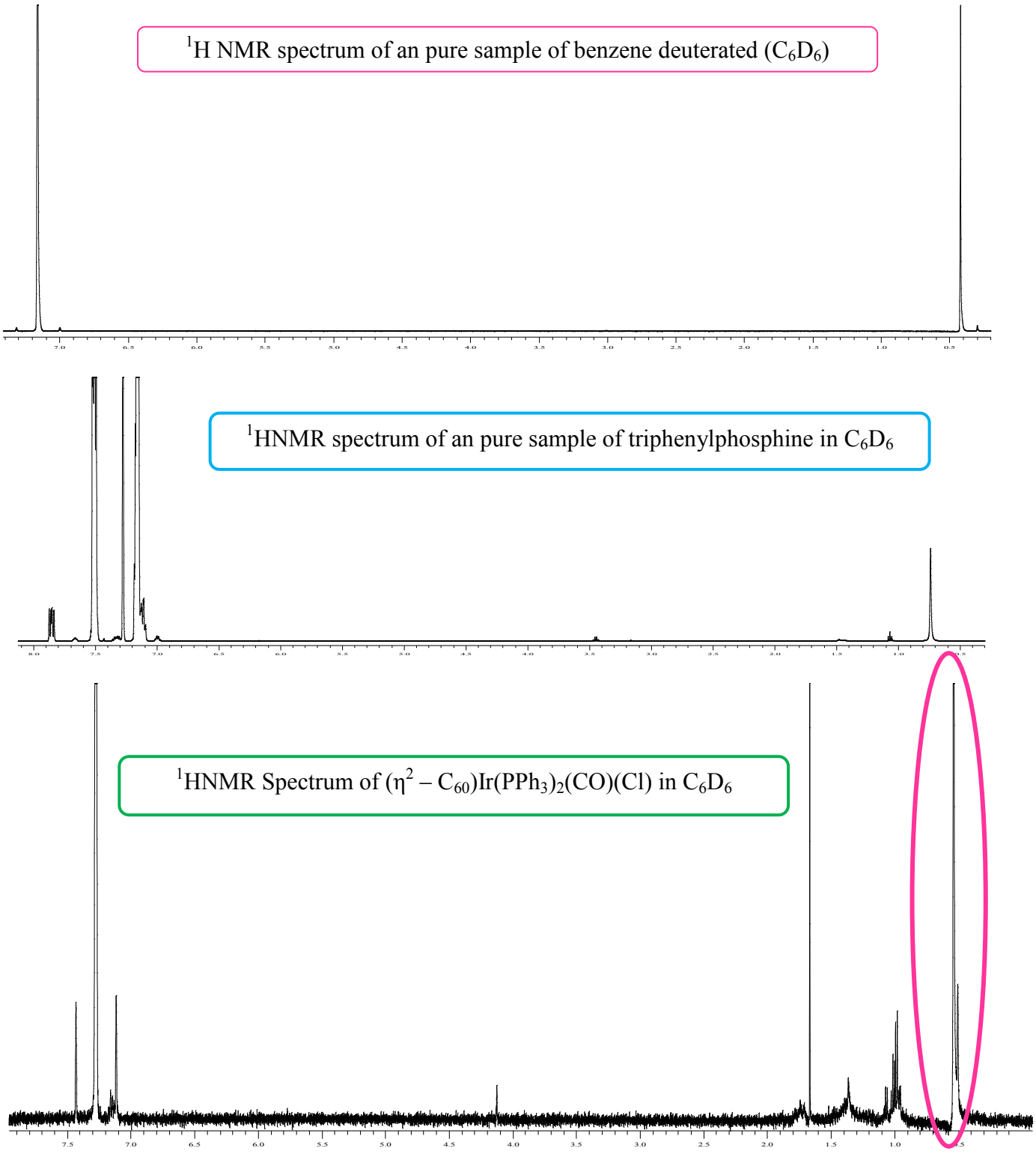

Figure 3.24 ^{1}H NMR Spectrum of: A. deutered benzene (C_6D_6), B. Standard of triphenyl phosphine in C_6D_6 and C. ($\eta^2 - C_{60}$)Ir(PPh_3)$_2$(CO)(Cl) complex in C_6D_6 showing a signal at 0.55 ppm. The circulated area is the signal of interest.

In a attempt to identify the reactions products, the complex (η^2 – C_{60})Ir(PPh_3)$_2$(CO)(Cl) was mixed in benzene under an inert nitrogen atmosphere and it was left under constant stirring during 24 hours. After 24 hours the solvent was evaporated and the resulting solid was redissolved in C_6D_6. Two different signals were observed in the ^{1}HNMR spectrum; one signal at 0.55 ppm and the other at 8.10 ppm (figure 3.25). In the spectrum of (η^2-C_{60})Ir(PPh_3)$_2$(CO)(H)(Cl), (Figure 3.24), observed a signal at 0.55 ppm, and could be attributed to a remnant that would be reacting in the synthesis of the complex, because the synthesis was carried out in benzene, (Figure 3.26).

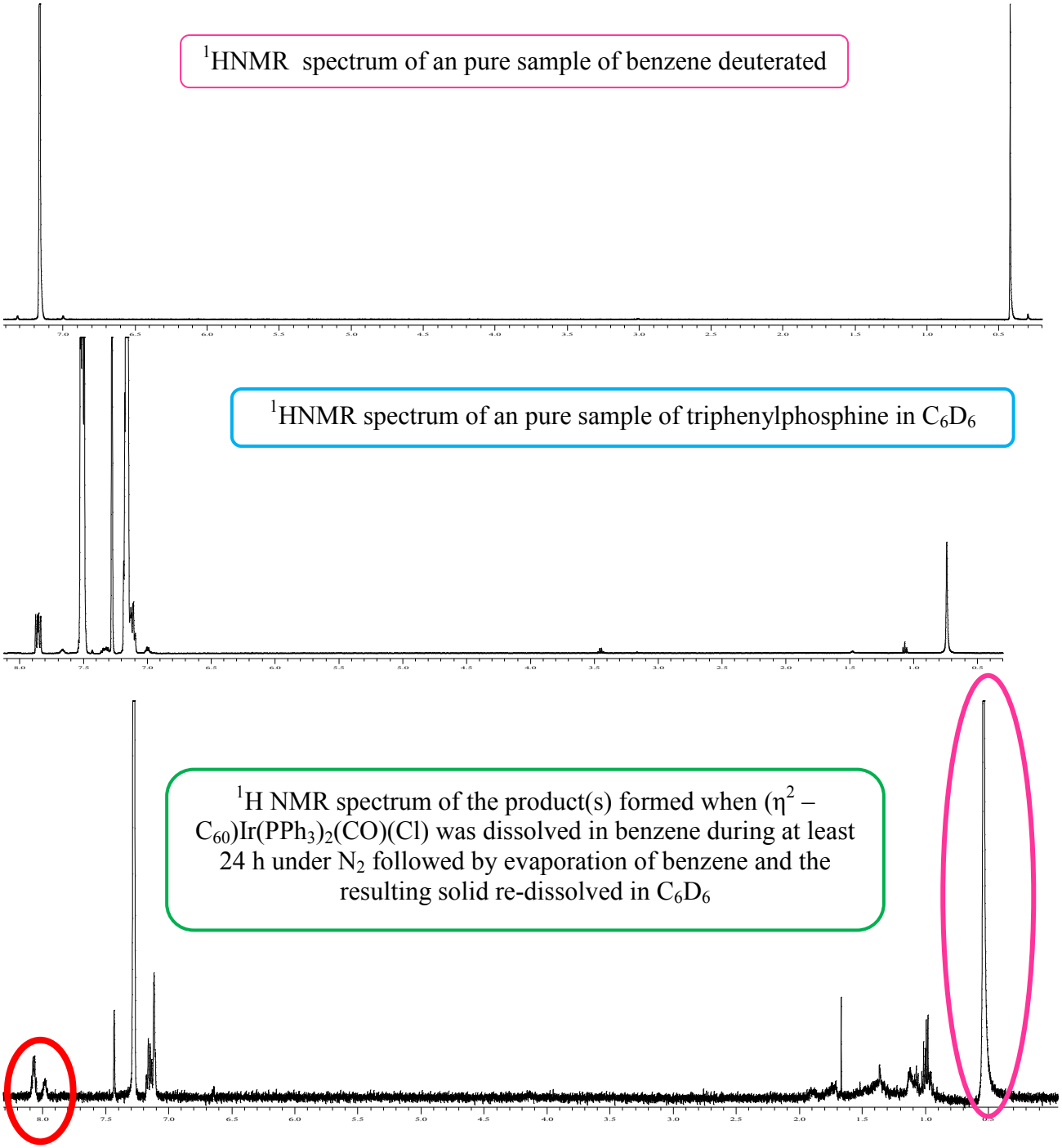

Figure 3.25 ^{1}HNMR Spectrum of of: A. deutered benzene (C_6D_6), B. Standard of triphenyl phosphine and C. spectrum of the product(s) that was formed from (η^2 – C_{60})Ir(PPh_3)$_2$(CO)(Cl) that was dissolved in benzene during at least 24 h under N_2 followed by evaporation of benzene and the resulting solid dissolved in C_6D_6show two new signal at 0.55 ppm and 8.10 ppm. The circulated area is the region of interest.

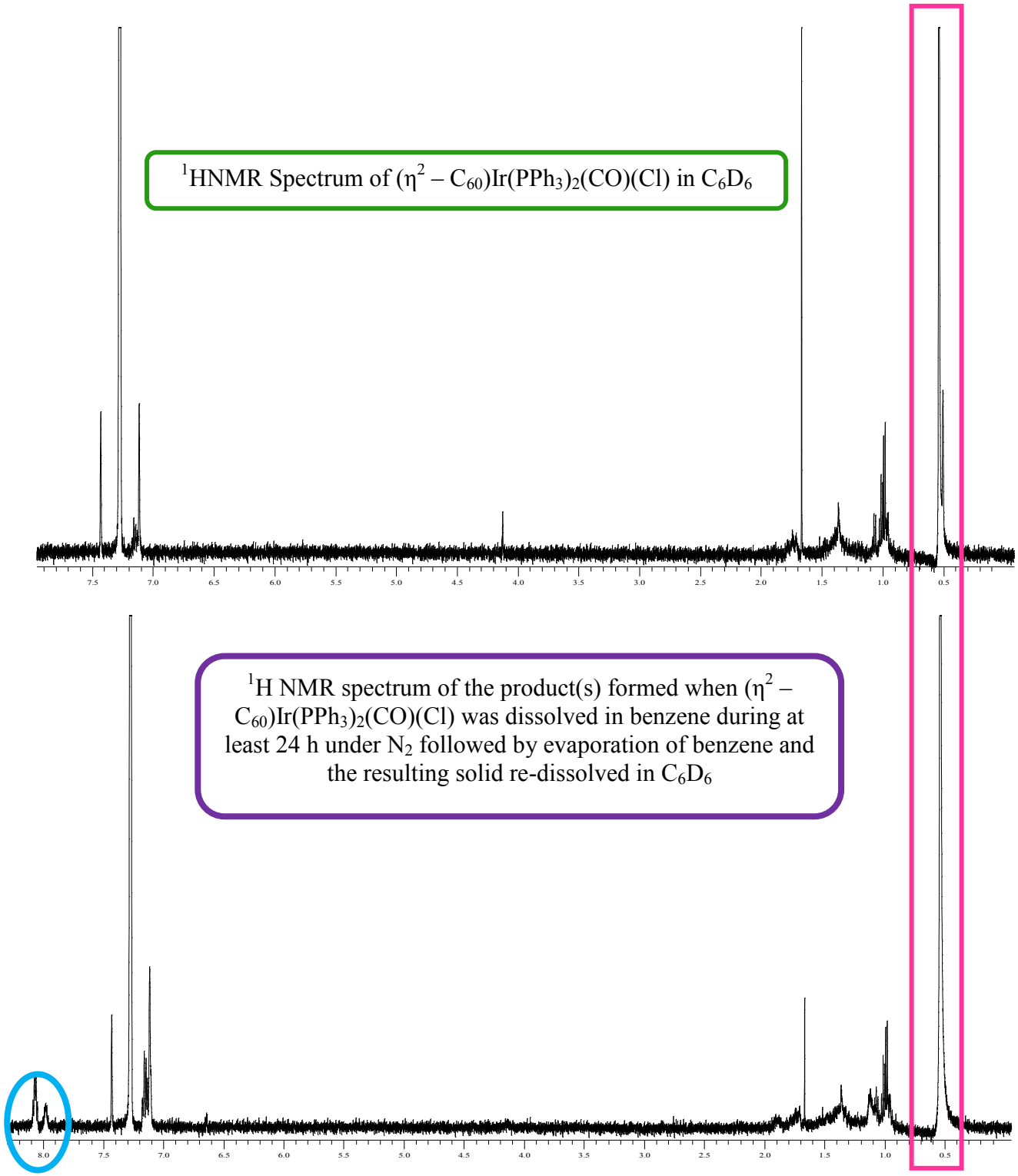

Figure 3.26 ^{1}H NMR Spectrum of: A (η^2 – C_6H_6)Ir(PPh_3)$_2$(CO)(Cl show one new signal at 0.55 ppm and B. spectrum of the product(s) that was formed from (η^2 – C_{60})Ir(PPh_3)$_2$(CO)(Cl) that was dissolved in benzene during at least 24 h under N_2 followed by evaporation of benzene and the resulting solid dissolved in C_6D_6 shows two new signals at 0.55ppm and 8.10ppm. The circulated area is the region of interest.

3.2.4.8 Products identification and reaction's progresses of Ir (CO)(PPh_3)$_2$Cl in benzene using ^{1}H NMR spectroscopy

In order to clarify the reactions that might be occurring related to the slow segment of the biphasic plot, we monitored the reactions progress by ^{1}H NMR spectroscopy. A solution was prepared containing 50/50 (C_6D_6)/C_6H_6 with approximately 1.0 mg of Ir(CO)(PPh_3)$_2$Cl. One hundred NMR measurements were obtained every five minutes for each spectrum. The ^{1}HNMR spectrum of Ir(CO)(PPh_3)$_2$Cl in the mixed solvent (C_6D_6 and C_6H_6) shows one signal at 7.85 ppm which intensity increases with time, (figure 3.27 y 3.28).

In order to distinguish whether this signal belongs to triphenylphosphine dissociated from the parent complex or to intermediate species or to benzene, spectrum of Ir(CO(PPh_3)$_2$Cl in deuterated benzene(C_6D_6) was obtained. It cannot be rule out that the signal at 7.85 ppm that was attributed to coordinated benzene does not belongs to residual benzene in the ampoule of deuterated benzene (figure 3.29).

A.

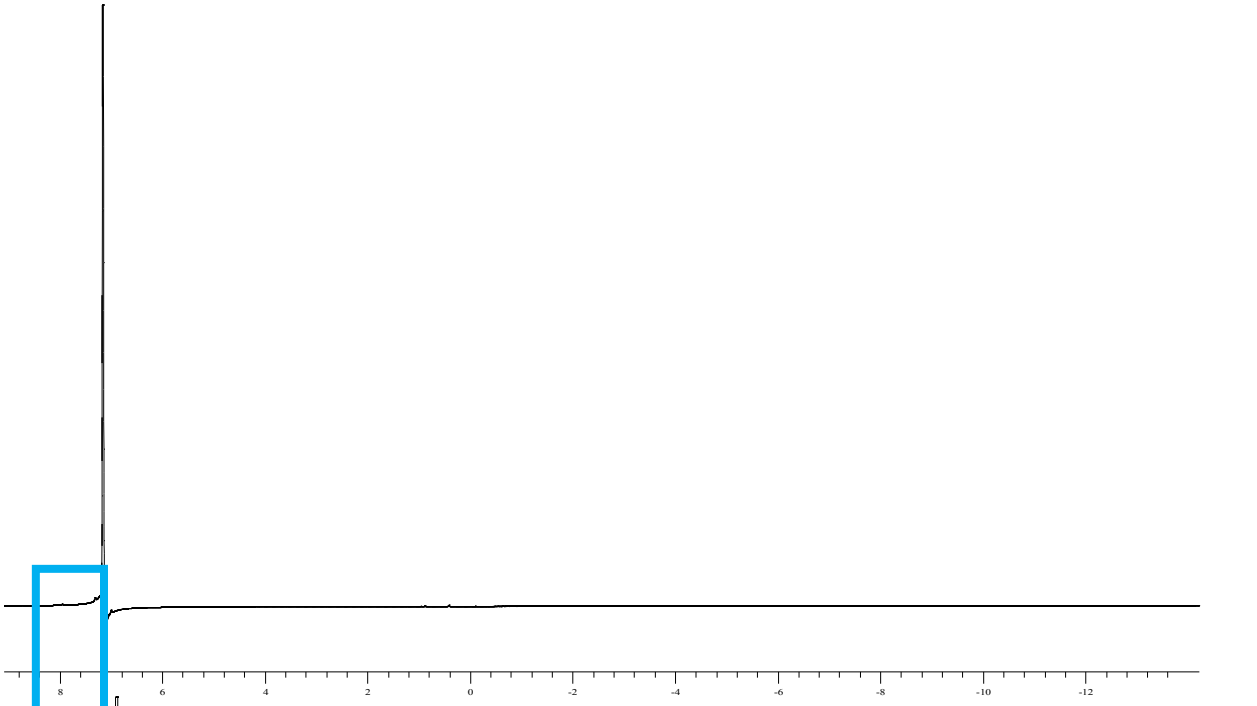

B.

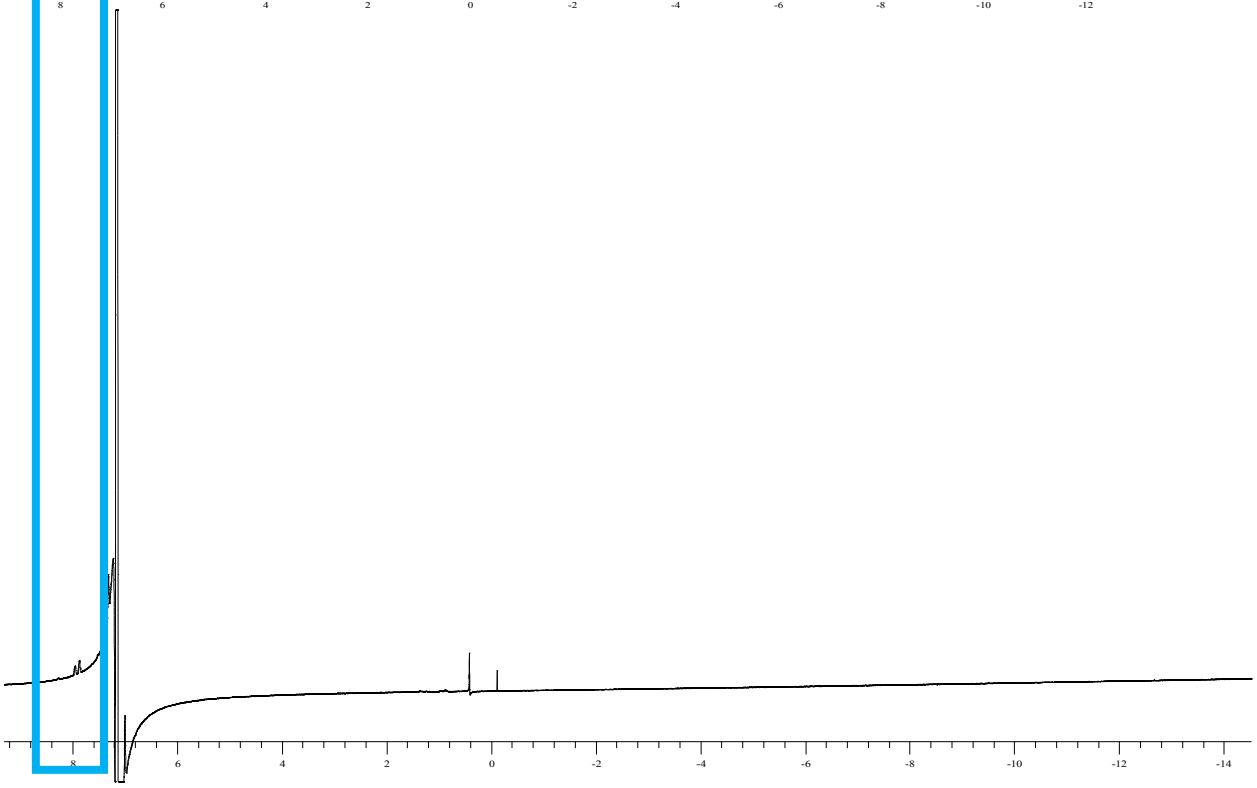

Figure 3.27 ***^{1}H NMR spectrum of $Ir(PPh_3)_2(CO)(Cl)$ complex in mixed of solvent of benzene(C_6H_6) and benzene deuterated(C_6D_6). This spectrum was show a signal at 7.85 ppm which increases in intensity with time. Spectrum A, corresponding to the first experiment and Spectrum B, corresponding to the last experiment. One hundred NMR measurements were obtained every five minutes for each spectrum. The circulated area is the signal of interest.***

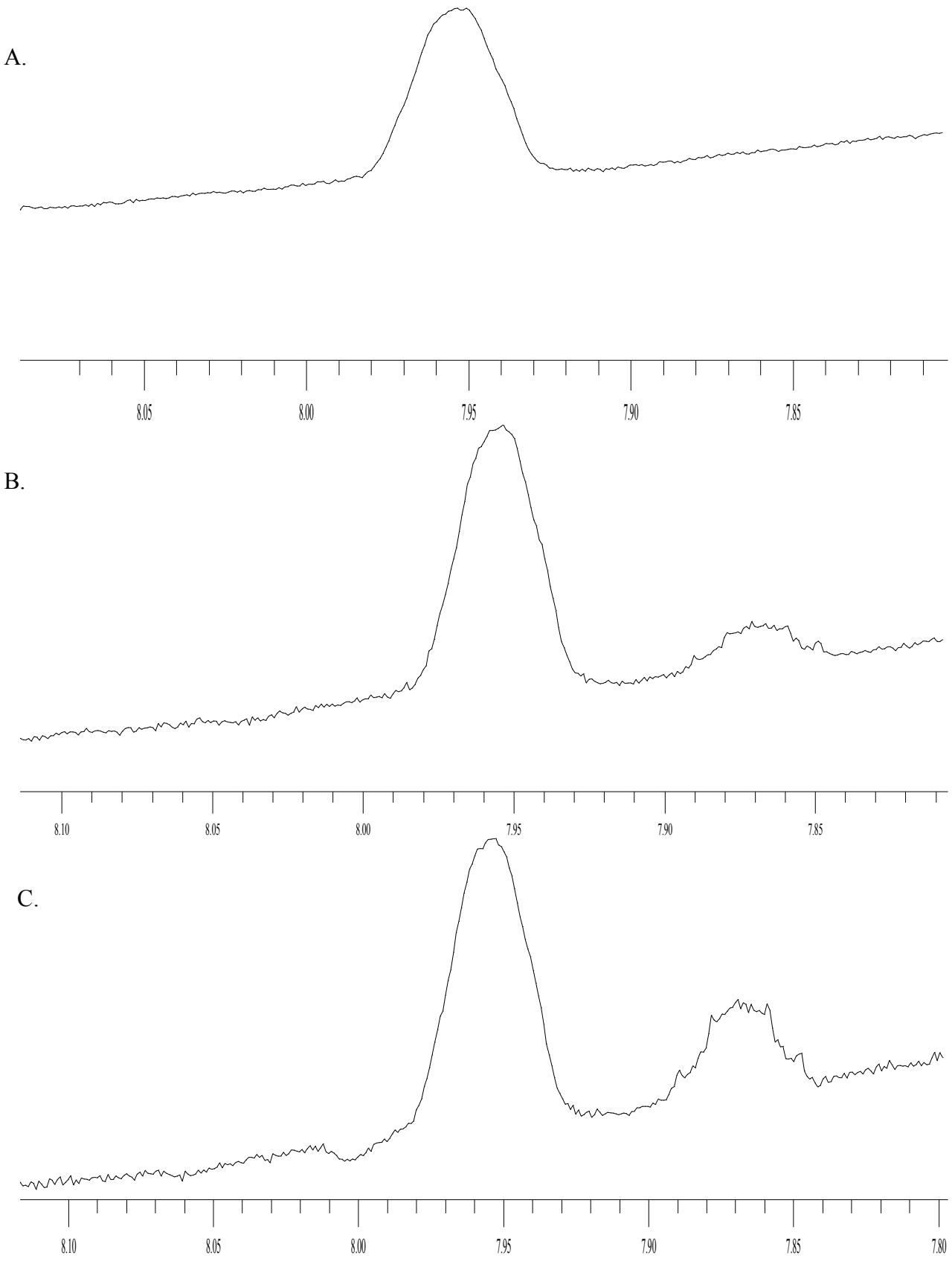
A.
8.05
8.00
7.95
7.90
7.85
B.
8.10
8.05
8.00
7.95
7.90
7.85
C.
8.10
8.05
8.00
7.95
7.90
7.85
7.80

D.

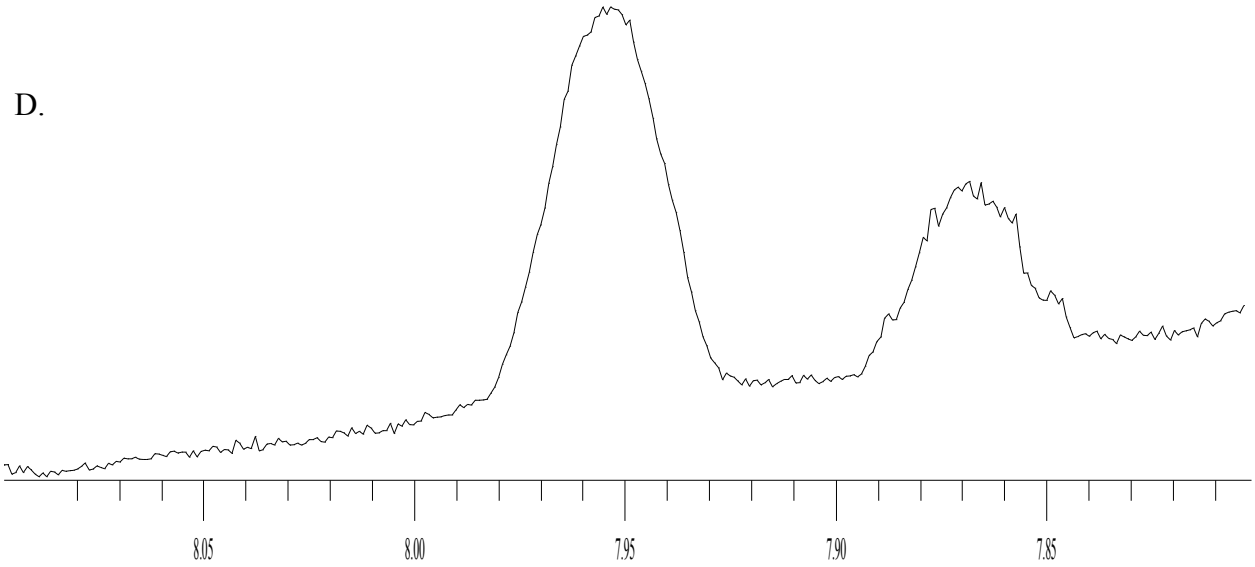
8.05
8.00
7.95
7.90
7.85

E.

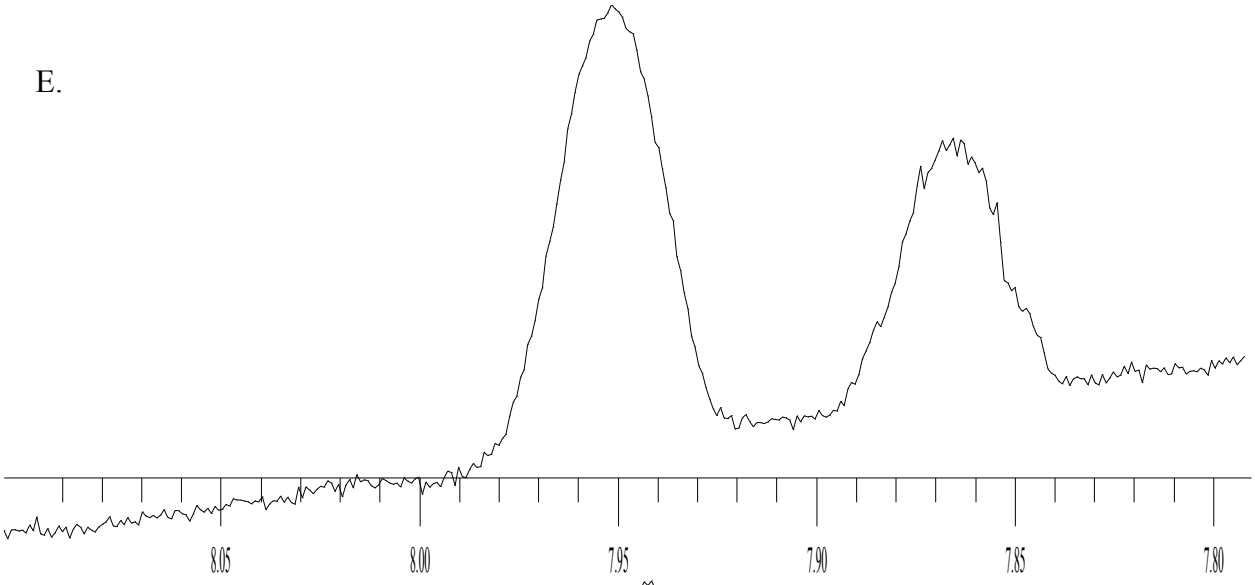
8.05
8.00
7.95
7.90
7.85
7.80

F.

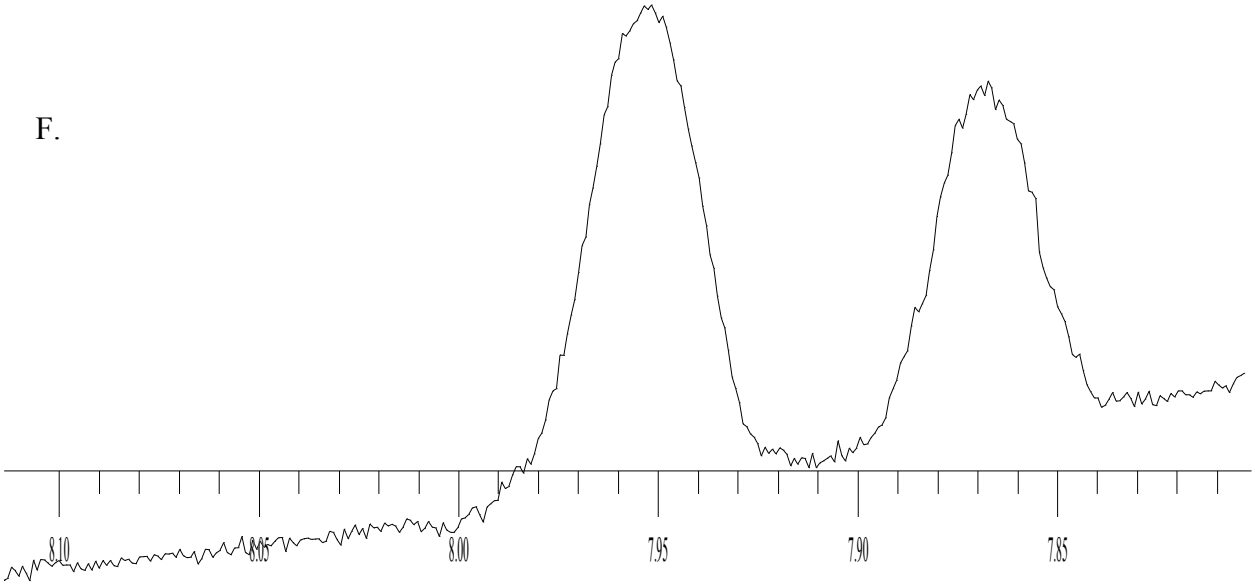
8.10
8.05
8.00
7.95
7.90
7.85

G.

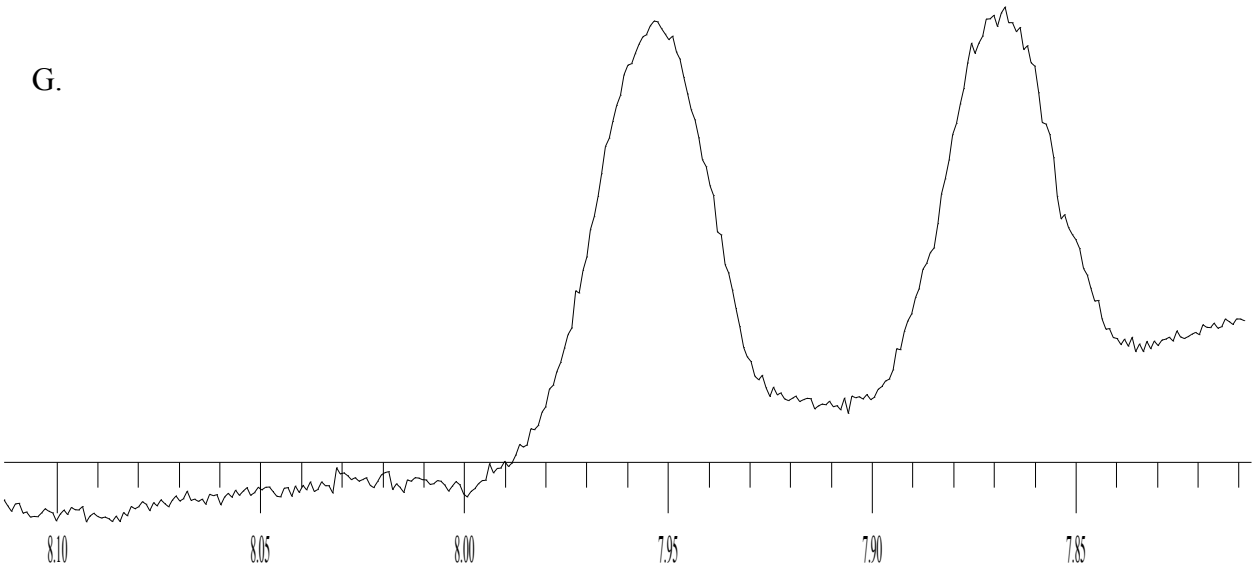
8.10
8.05
8.00
7.95
7.90
7.85

H.

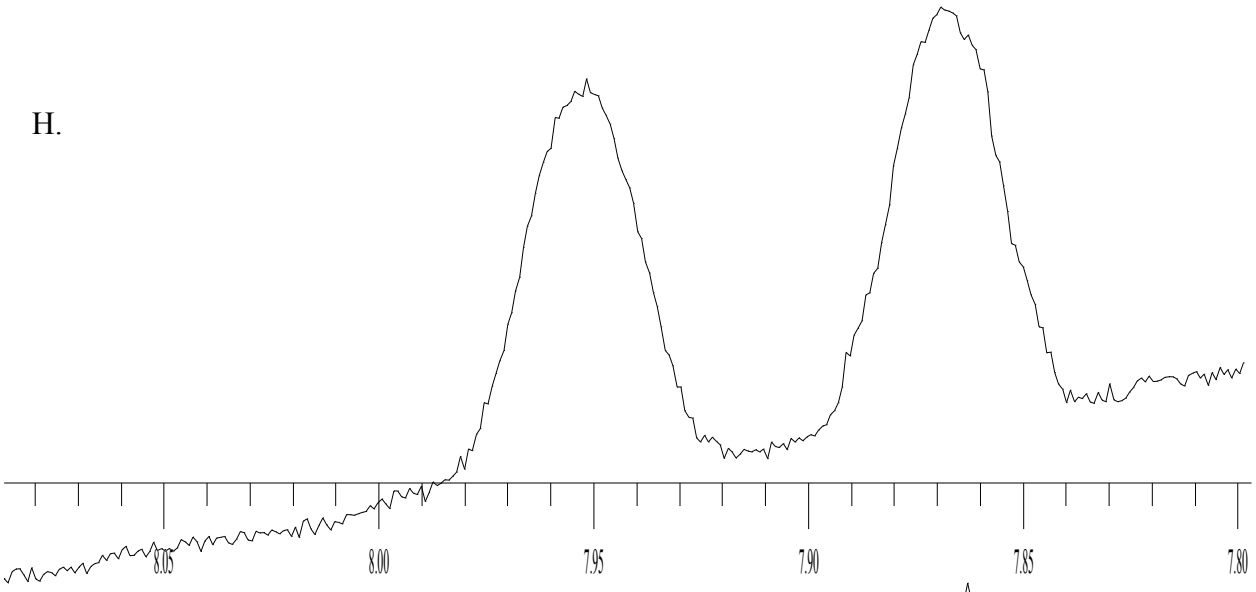
8.05
8.00
7.95
7.90
7.85
7.80

I.

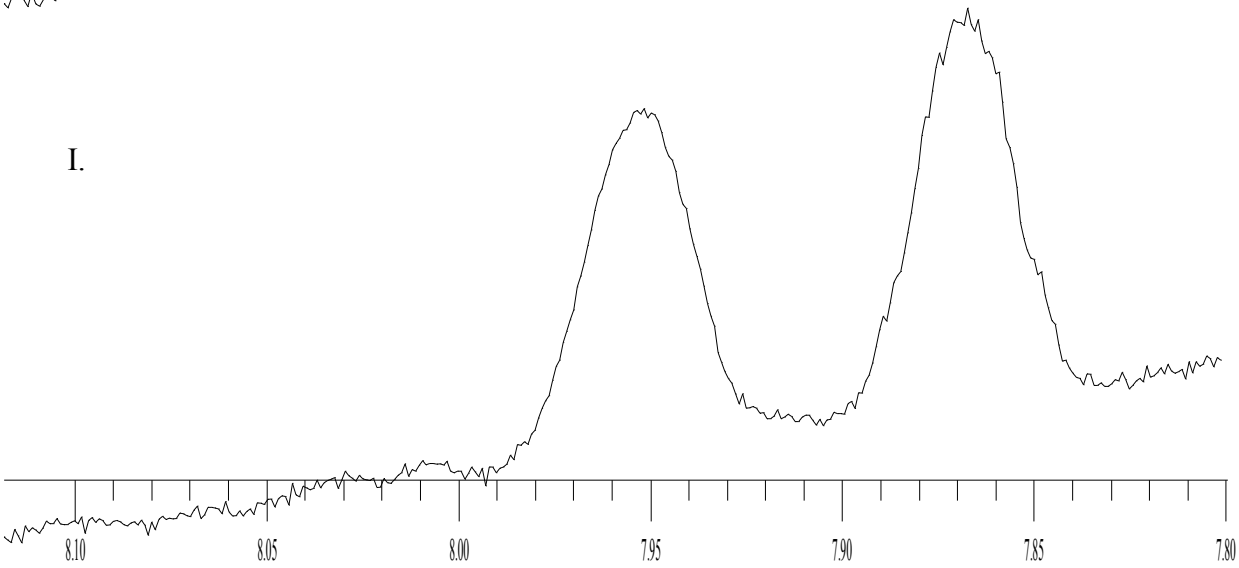
8.10
8.05
8.00
7.95
7.90
7.85
7.80

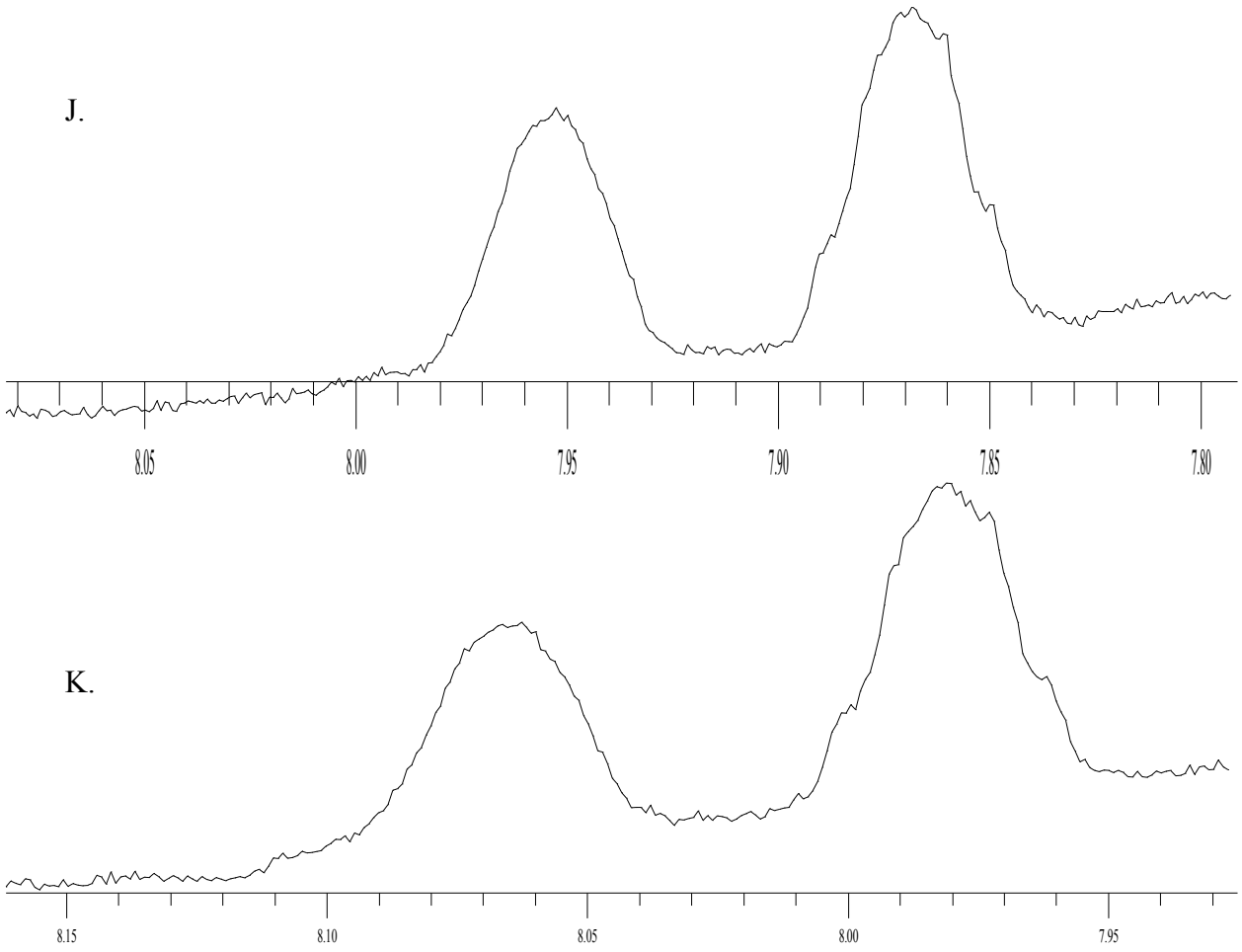

Figure 3.28 ^{1}H NMR Spectrum of $Ir(PPh_3)_2(CO)(Cl)$ complex dissolved in a mixture of solvents Benzene (C_6H_6) /deuterated (C_6D_6) and triphenylphosphine. This spectrum shows a signal at 7.85 ppm which intensity increases with time. Spectra a – J area enhaced of the 8.15 – 7.90 ppm region. Spectrum A is the first experiment, B is 10 experiment, C is the 20 experiment, D is 30 experiment, E is 40 experiment, F is 50 experiment, G is 60 experiment, H is 70 experiment, I is 80 experiment, J is 90 experiment and K is 100 experiment. One hundred NMR measurements were obtained every five minutes for each spectrum. The circulated area is signal of interest.

^{1}HNMR spectrum of an pure sample of benzene deuterated (C_6D_6)

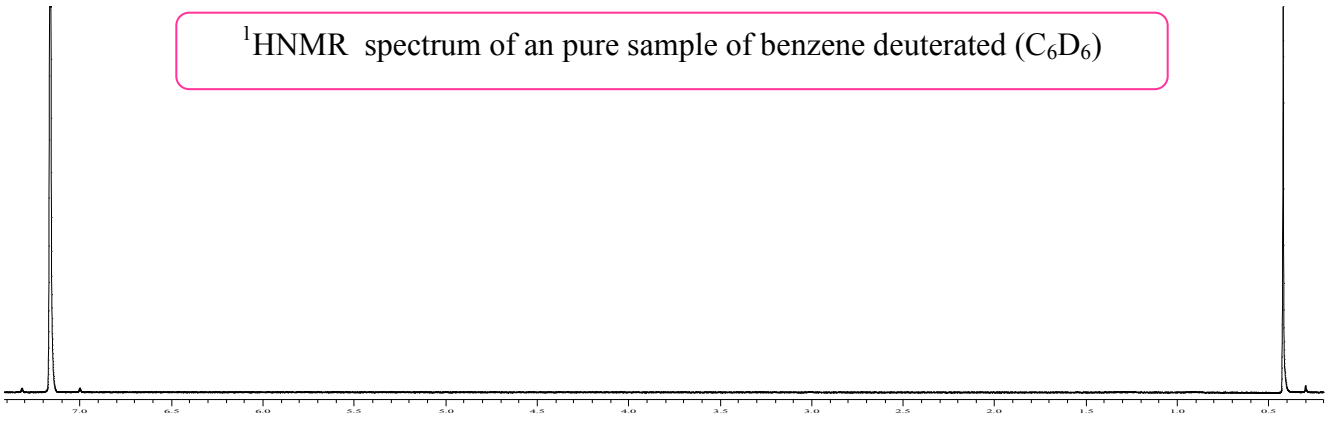

^{1}HNMR spectrum of an pure sample of triphenylphosphine in C_6D_6

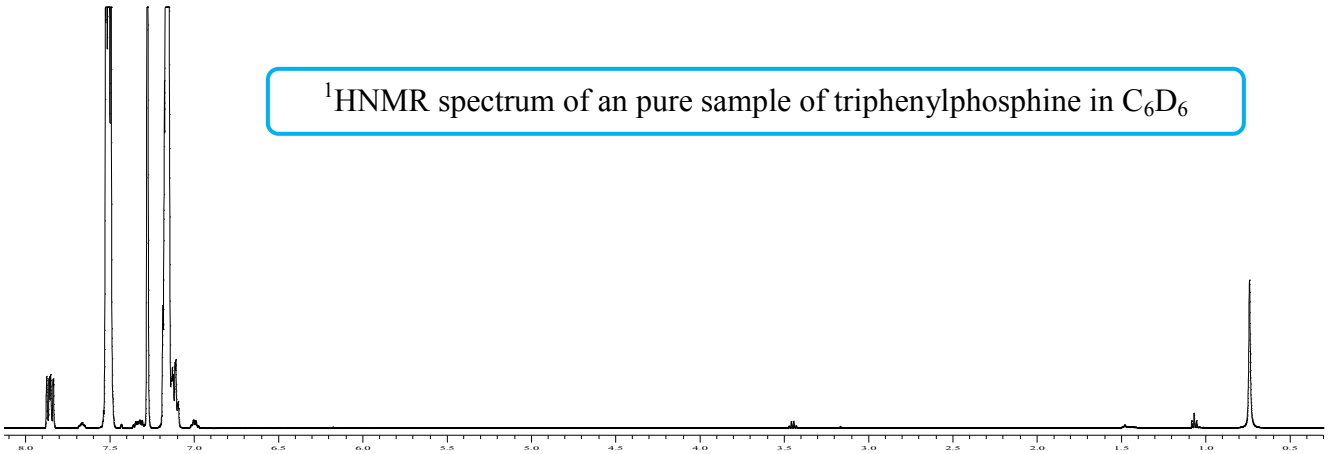

^{1}H NMR spectrum of $Ir(PPh_3)_2(CO)(Cl)$ in C_6D_6

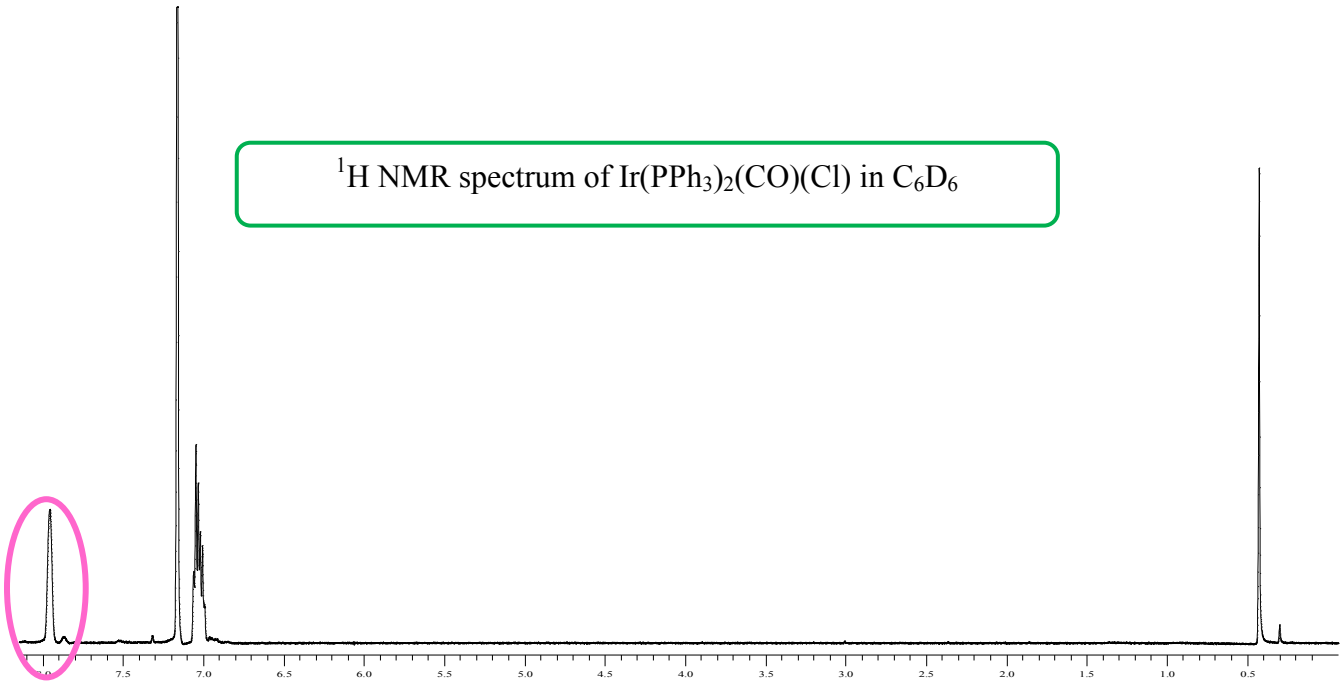

Figure 3.29 ^{1}H NMR Spectrum of $Ir(PPh_3)_2(CO)(Cl)$ in deuterated benzene(C_6D_6). This spectrum shows a signal at 7.85ppm. The circulated area is the signal of interest.

When the progress of the reaction was monitored by 1HNMR with a mixture of solvents, deuterated benzene (C_6D_6) and benzene (C_6H_6), a signal was observed at 7.85 ppm which increases with time, but the signal at 0.55 ppm, that was observed when no PPh_3 was added to the mixture, was not observed in this instance. For this reason a mixture of of 50:50 C_6H_6 : C_6D_6 with 1.0 mg of triphenylphosphine was prepared and Vaska's complex was dissolved in the resulting solution. The ^{1}HNMR spectrum of $Ir(CO)(PPh_3)_2Cl$ dissolved n the solvent mixture that contains C_6D_6, C_6H_6 and PPh_3 was different to the corresponding spectrum of the complex dissolved in C_6D_6/C_6H_6 mixture (no PPh3 added) in the sense that a new signal at 0.55 ppm was observed. This signal increased with time, (figure 3.30 and 3.31). Figure 3.30 shows the first experiment's (A) and the last experiment's (B) results, where the signal at 0.55 ppm in spectrum B has twice the intensity of the signal in spectrum A. Figure 3.31 shows the results for one hundred NMR measurements were obtained every five minutes for each spectrum, where it is observed that the signal's relative intensity at 0.55 ppm increased with time. These results suggest that parallel to triphenyl phosphine dissociation the formation of sigma complex between iridium and benzene may be forming.

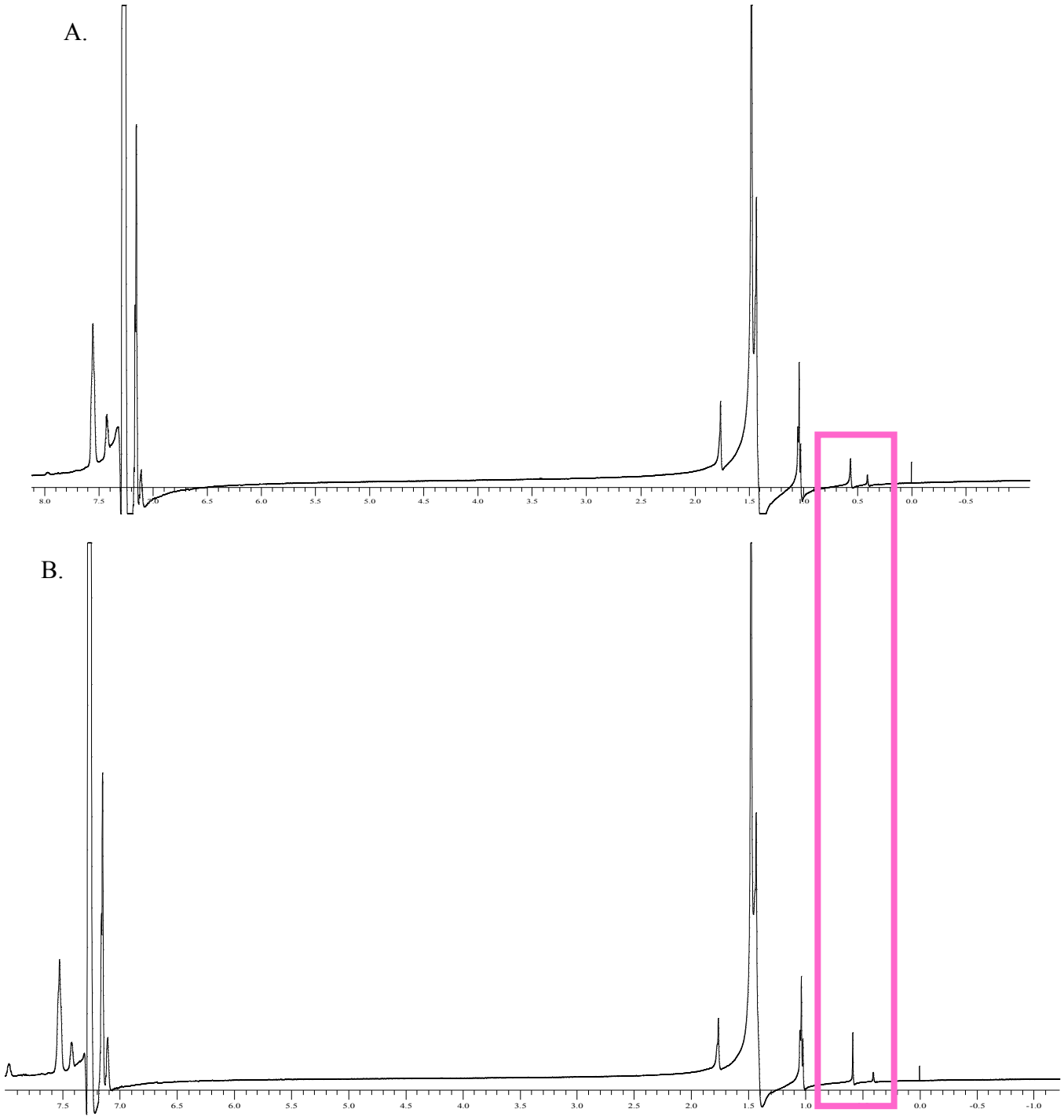

Figure 3.30 ***^{1}H NMR Spectrum of $Ir(PPh_3)_2(CO)(Cl)$ complex in mixed of solvent of benzene(C_6H_6), deuterated benzene (C_6D_6) and triphenylphosphine. This spectrum shows a signal at 0.55ppm with increases the intensity with the time. Spectrum A, corresponding to the first experiment and Spectrum B, corresponding to the last experiment. The circulated area is the signal of interest.***

A.

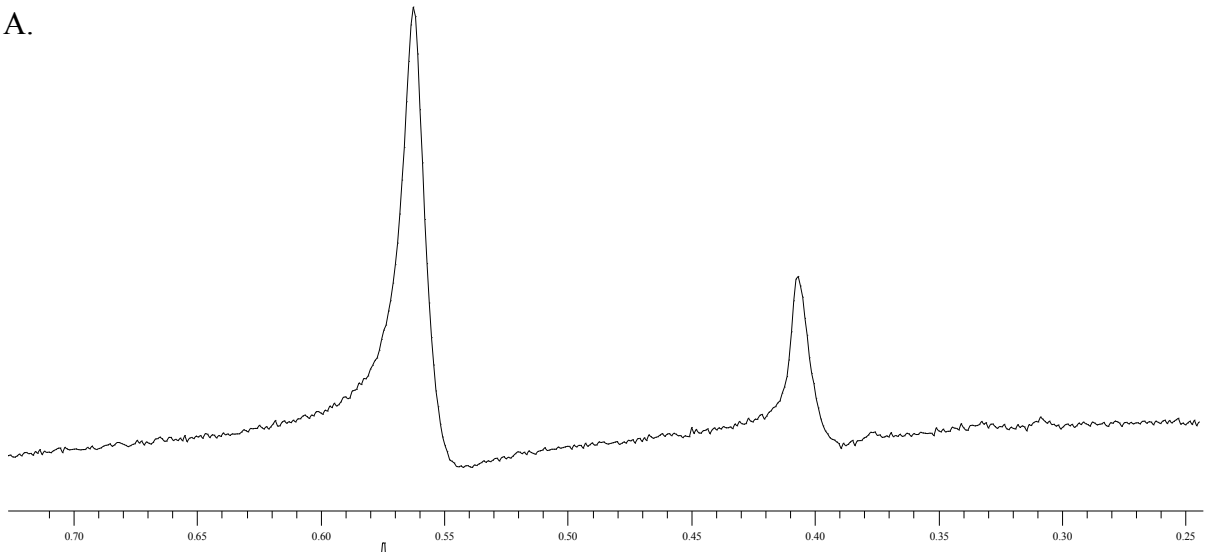
0.70
0.65
0.60
0.55
0.50
0.45
0.40
0.35
0.30
0.25

B.

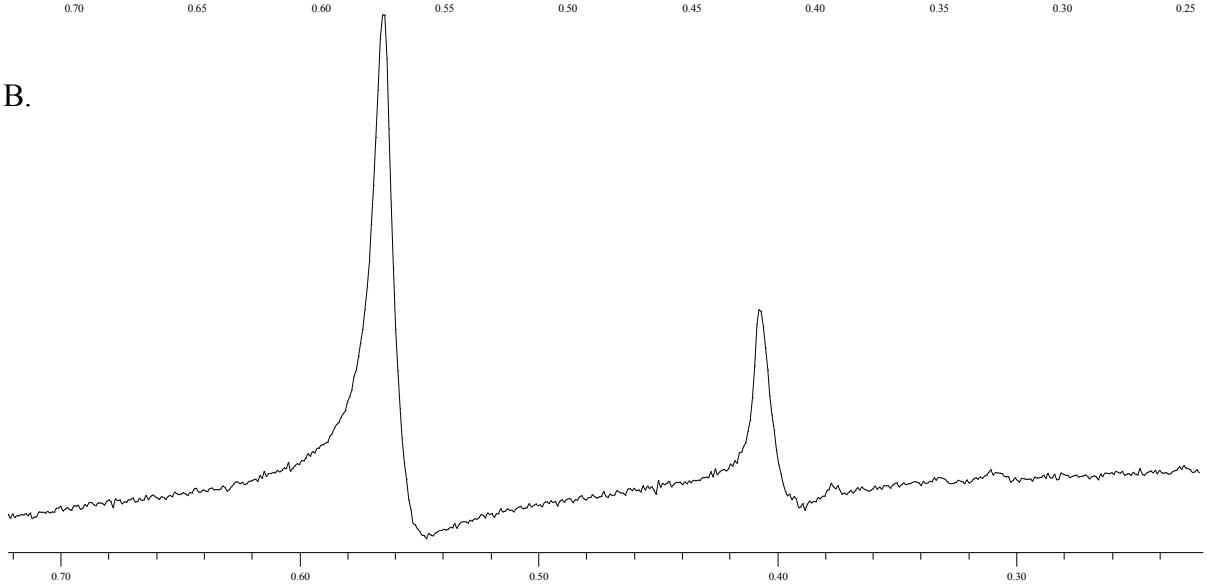
0.70
0.60
0.50
0.40
0.30

C.

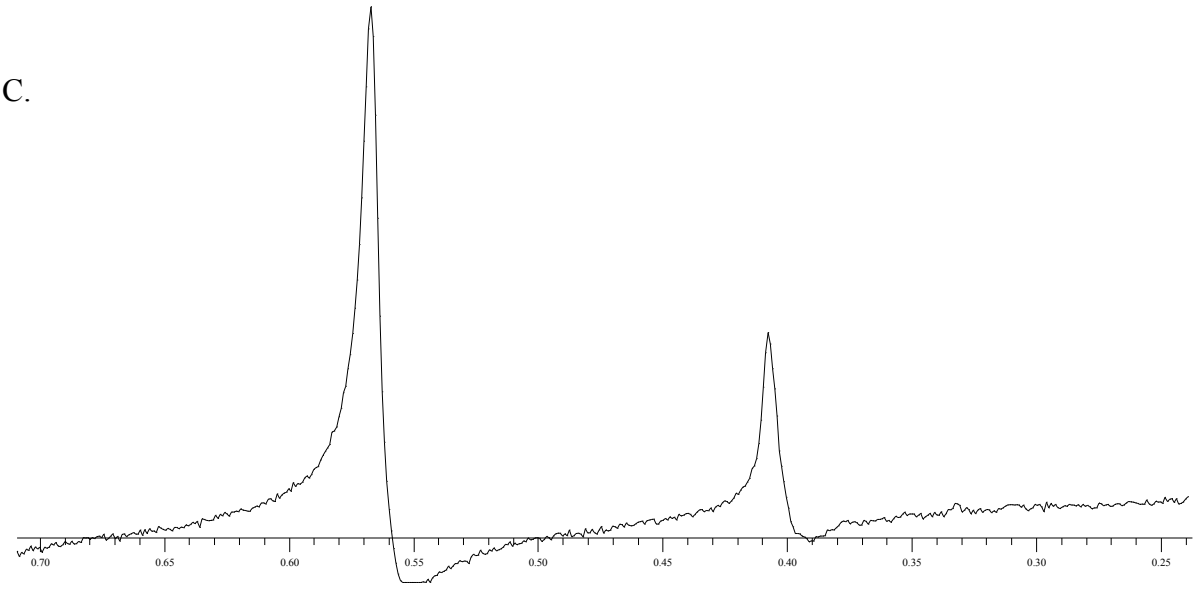
0.70
0.65
0.60
0.55
0.50
0.45
0.40
0.35
0.30
0.25

D.

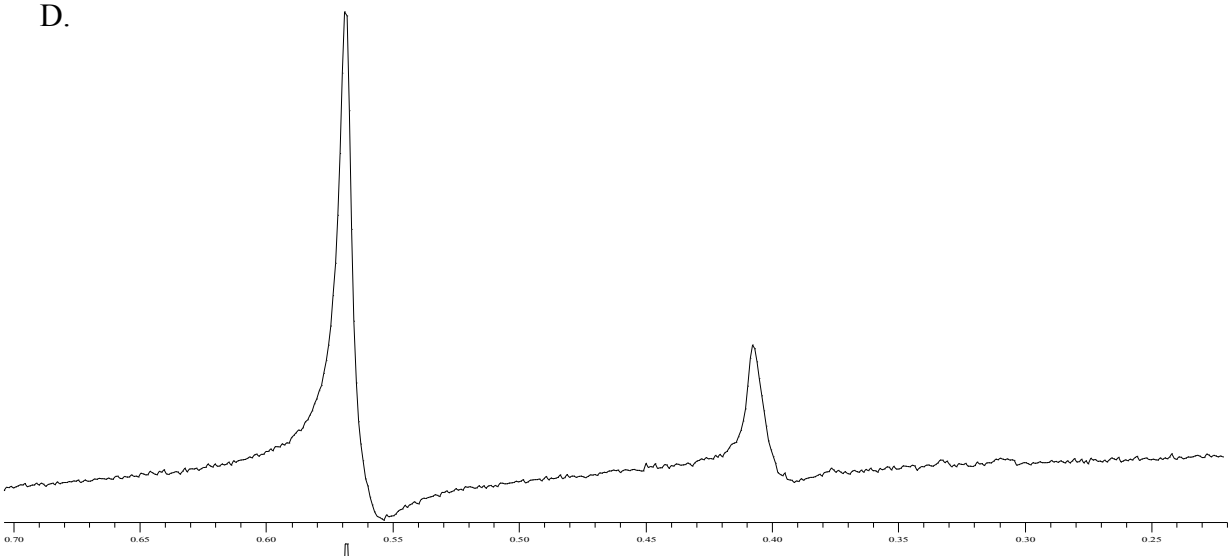
0.70
0.65
0.60
0.55
0.50
0.45
0.40
0.35
0.30
0.25

E.

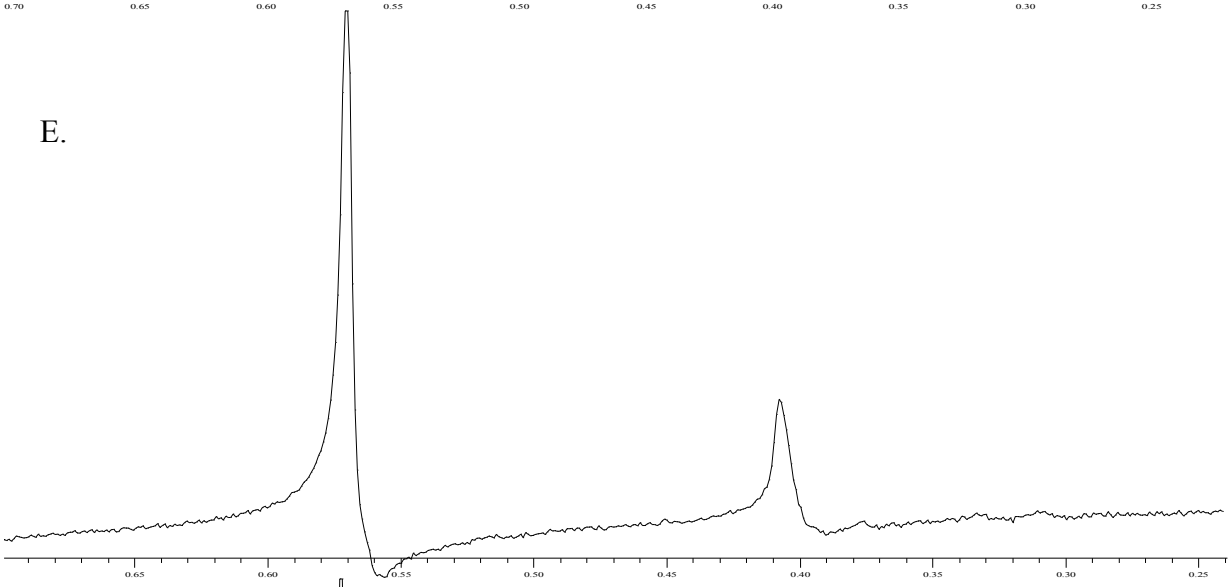
0.65
0.60
0.55
0.50
0.45
0.40
0.35
0.30
0.25

F.

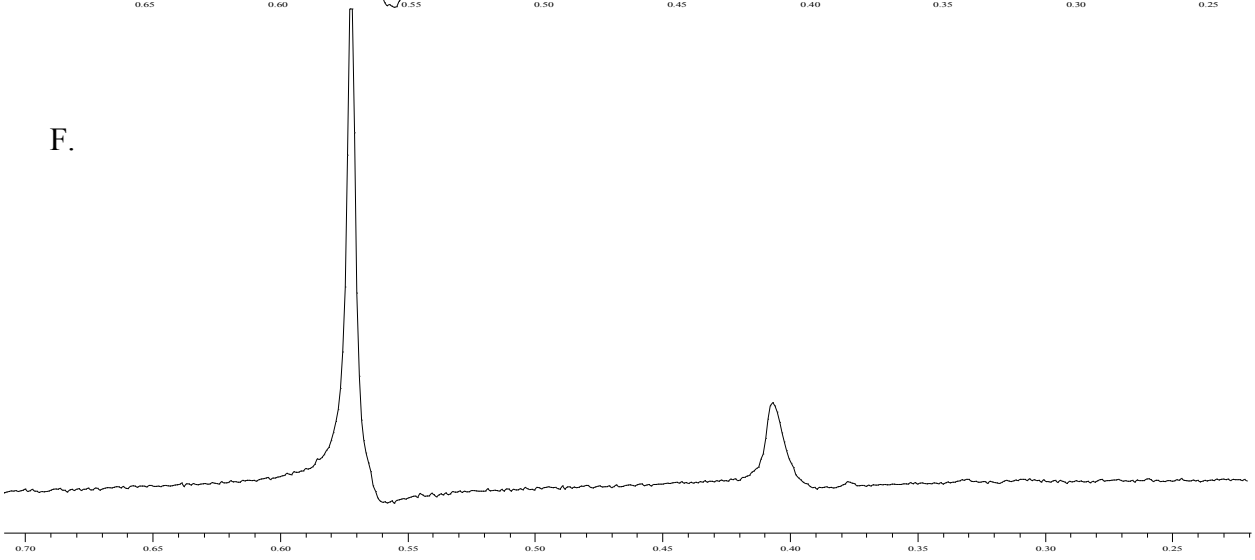
0.70
0.65
0.60
0.55
0.50
0.45
0.40
0.35
0.30
0.25

G.

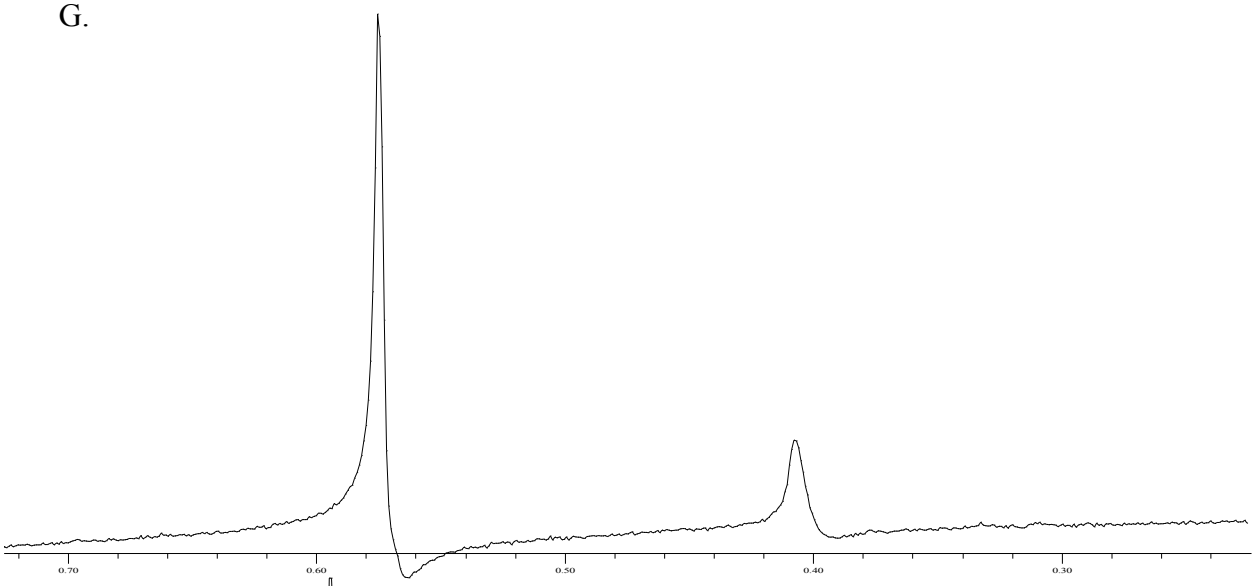
0.70
0.60
0.50
0.40
0.30

H.

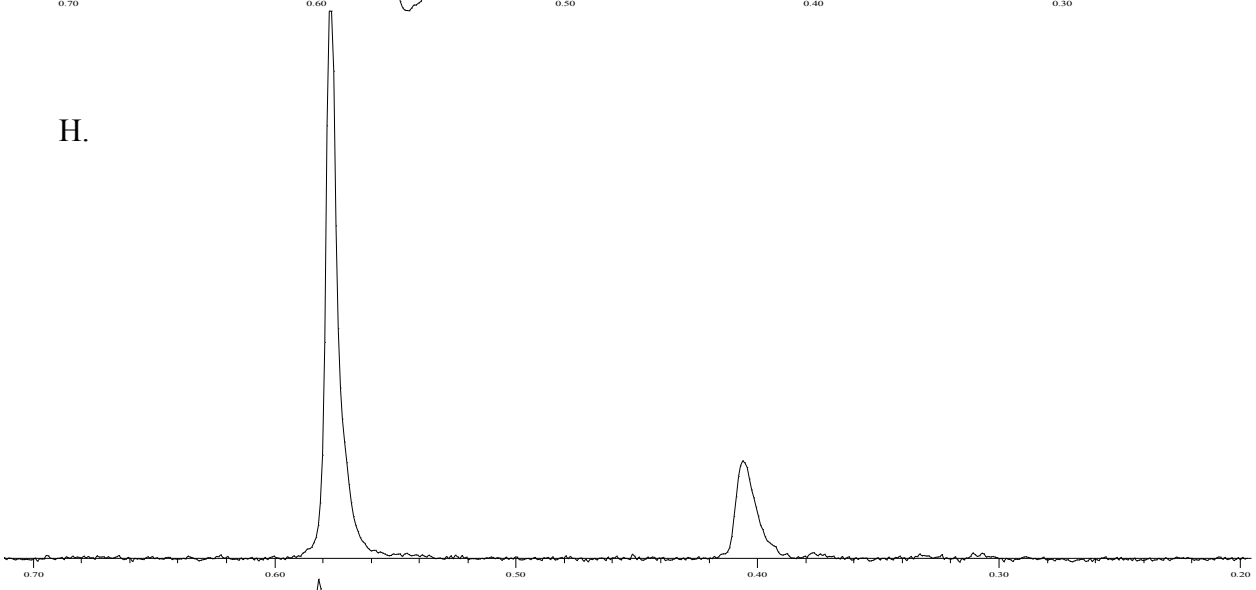
0.70
0.60
0.50
0.40
0.30
0.20

I.

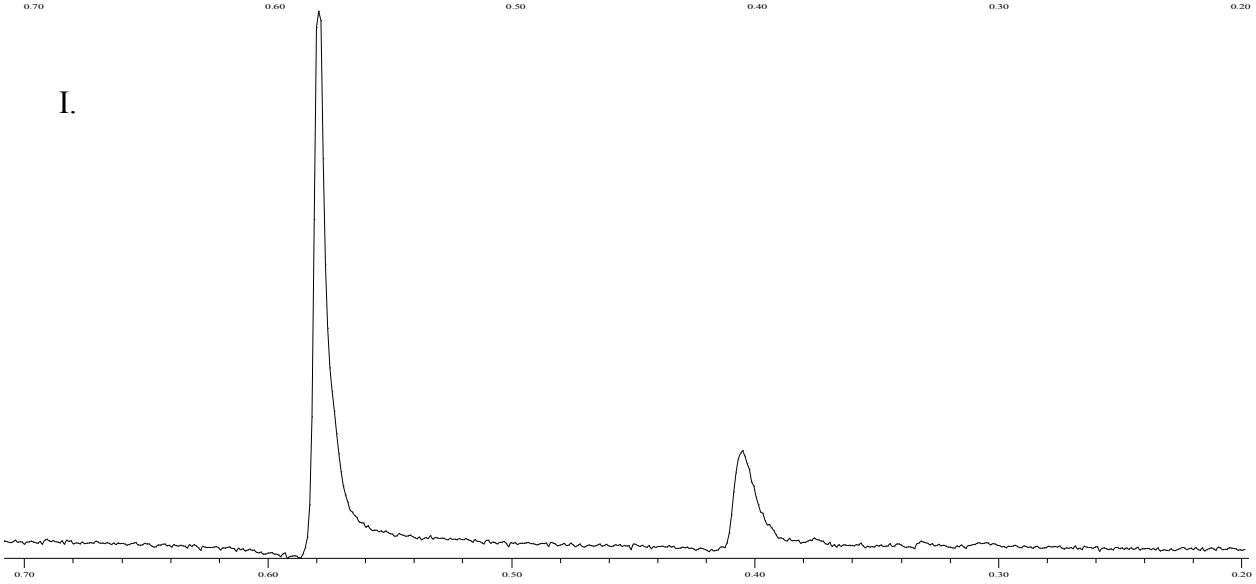
0.70
0.60
0.50
0.40
0.30
0.20

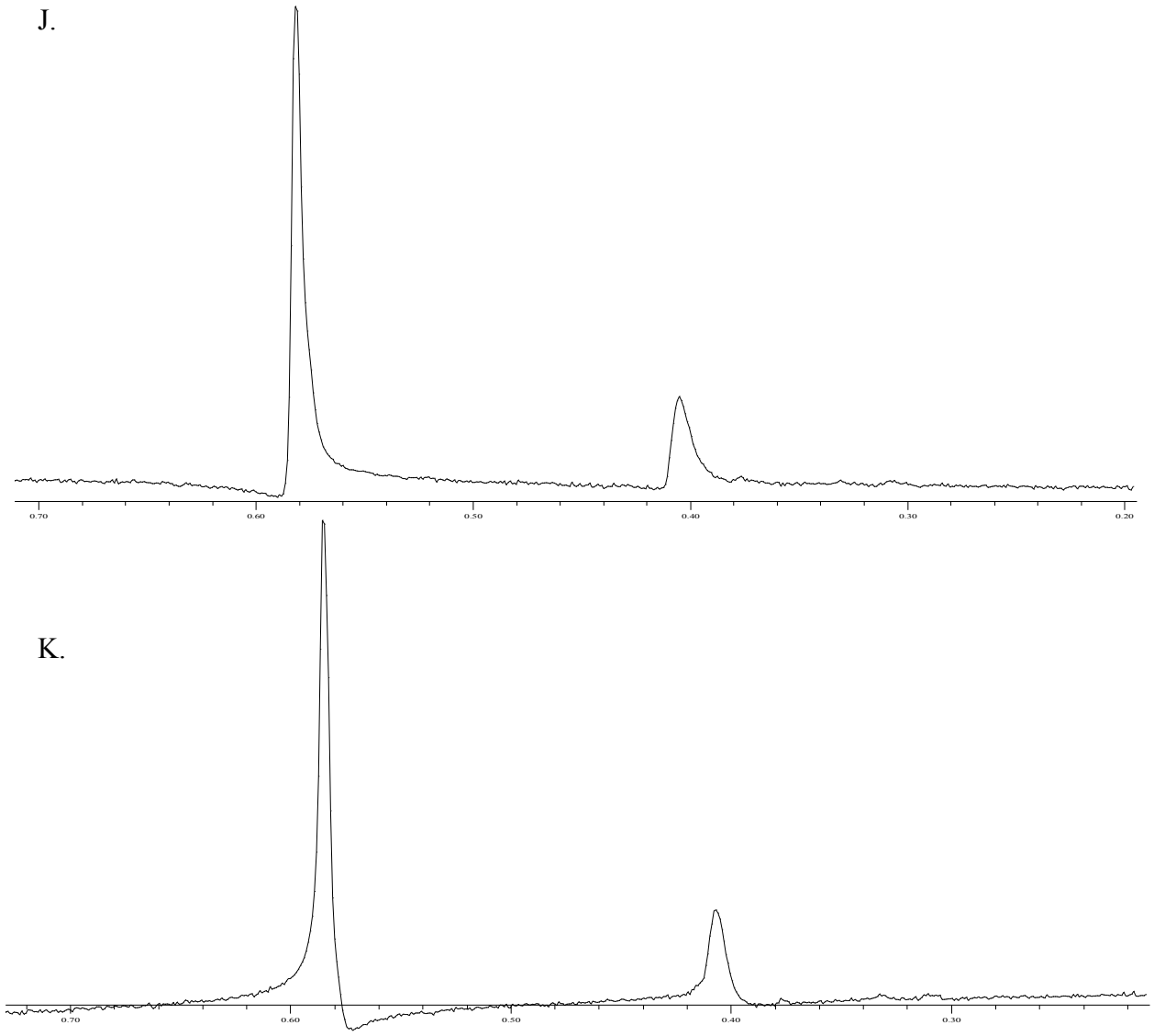

Figure 3.31 ^{1}H NMR spectrum of $Ir(PPh_3)_2(CO)(Cl)$ complex in mixed of solvent of benzene(C_6H_6), deuterated benzene(C_6D_6) and triphenylphosphine. This spectrum was show a signal at 0.55ppm with increases the intensity with the time. Spectra a – J are the close up in the region of 0.20 – 0.70 ppm, where we observed the signal at 0.55ppm grown with the time(s). Spectrum A is the first experiment, B is 10 experiment, C is the 20 experiment, D is 30 experiment, E is 40 experiment, F is 50 experiment, G is 60 experiment, H is 70 experiment, I is 80 experiment, J is 90 experiment and K is 100 experiment. The circulated area is the signal of interest.

3.3 Discussion

The rate of disappearance of $(\eta^2 - C_{60})Ir(CO)(Cl)(PPh_3)_2$ was followed by observing a decrease in the absorbance at 550 nm. The plots of absorbance vs. time(s) of the reactions studied under flooding conditions consist of two segments, where the fast segment depended of the nature and concentration of the solvent (figure 3.33). This evidence suggests that the solvent acts as an entering ligand that displaces C_{60} from $(\eta^2 - C_{60})Ir(CO)(Cl)(PPh_3)_2$. For the slow segment three parallel reactions; i) was attributed to parallel triphenylphosphine dissociation and ii) formation of a sigma-complex. Triphenylphosphine dissociation is supported by IR evidence while sigma complex formation is supported by NMR evidence. The signal at 0.55 ppm supports a Ir-H-C agostic bond while the nal at 7.85 ppm is attributed to Ir-coordinated benzene.

The reaction of $Ir(CO)(Cl)(PPh_3)_2$ with benzene was monitored in the ν(CO) region. Immediately after mixing (0 s), three bands at 1967cm^{-1}, 1953 cm^{-1} and 1810 cm^{-1} with two shoulders at 1821 cm^{-1} and 1802 cm^{-1} appeared. Twenty four hours after mixing, three bands were observed at 2005 cm^{-1}, 1964 cm^{-1} and 1818 cm^{-1}. In an effort to identify the nature and source of each band, Vaska's complex was dissolved in a solution containing benzene, and triphenyl phosphine and the IR spectrum measured. In this experiment two bands were observed immediately after mixing: one at 1964 cm^{-1} and the other with a negative absorbance at 1816 cm^{-1}. Twenty four hours after mixing, two positive absorbance bands were observed at 2005 cm^{-1}, 1964 cm^{-1} and one negative absorbance band at 1816 cm^{-1}. The evidence suggests that the band of 1964 cm^{-1} is attributable to the final product were triphenylphosphine undergoes dissociation from $(\eta^2\text{-}C_6H_6)Ir(CO)(Cl)(PPh_3)$ The band at 2005 cm^{-1} is attributed to the Ir (+3) sigma complex, $(\eta^2\text{-}C_6H_5)Ir(CO)(H)(Cl)(PPh_3)_2$, shown in figure 3.32.

The NMR spectrum of a solution containing Vaska's complex and benzene showed a signal at 7.85 ppm which intensity increased with time. This evidence suggests that a phenyl group enters the coordination sphere of the complex, while the triphenylphosphine is released.

The band at 2005 cm^{-1} is attributed to the sigma complex shown in figure 3.34, since this band's intensity increased in the presence of a large excess of of triphenylphosphine in solution. The interpretation is that the excess of triphenylphosphine inhibits the release of triphenyl phosphine from the complex. In effort to identify the bands, a solution consisting of triphenylphosphine and benzene was prepared. Two positive absorption bands were observed at 1951cm^{-1} and 1804 $cm^{-1,}$ which were assigned to triphenyl phosphine and two negative absorption bands were also observed at 1962 cm^{-1} and 1817 cm^{-1} which were ascribed to benzene. Furthermore, in a triphenylphosphine excess, the bands at 1953 cm^{-1} and 1804 cm^{-1} are not present in the IR spectrum. However, without excess of triphenylphosphine these bands are observed at approximately 300 – 400 seconds after mixing. Also in this product iridium increases its oxidative state from +1 to +3 as evidenced by the band at 2005 cm^{-1}. In addition, when the triphenylphosphine solution with benzene and Vaska's complex was prepared for NMR spectroscopy analysis, the signal observed at 0.55 ppm increased with time. The increase in this signal intensity suggests that an agostic bond is present in the reaction product [34].

The role of the solvent on the ligand exchange reactions of metal carbonyl complexes have been reported extensively [35-36]. Aromatic solvents such benzene, may interact with the substrate and intermediate species through an olefinic linkage [35-36]. The coordinated solvent undergoes isomerization to attain the most stable mode of coordination [35-36]. First coordinates via an agostic C-H-Ir in a "ring – edge" mode, then it alignes itself with iridium in a "ring center" position, finally its goes to a olefin coordination [35-36]. The activation parameters may

provide an estimate about the Ir – C_{60} bond dissociation enthalpy depending on the degree of solvent intervention in the transition state [35-36].

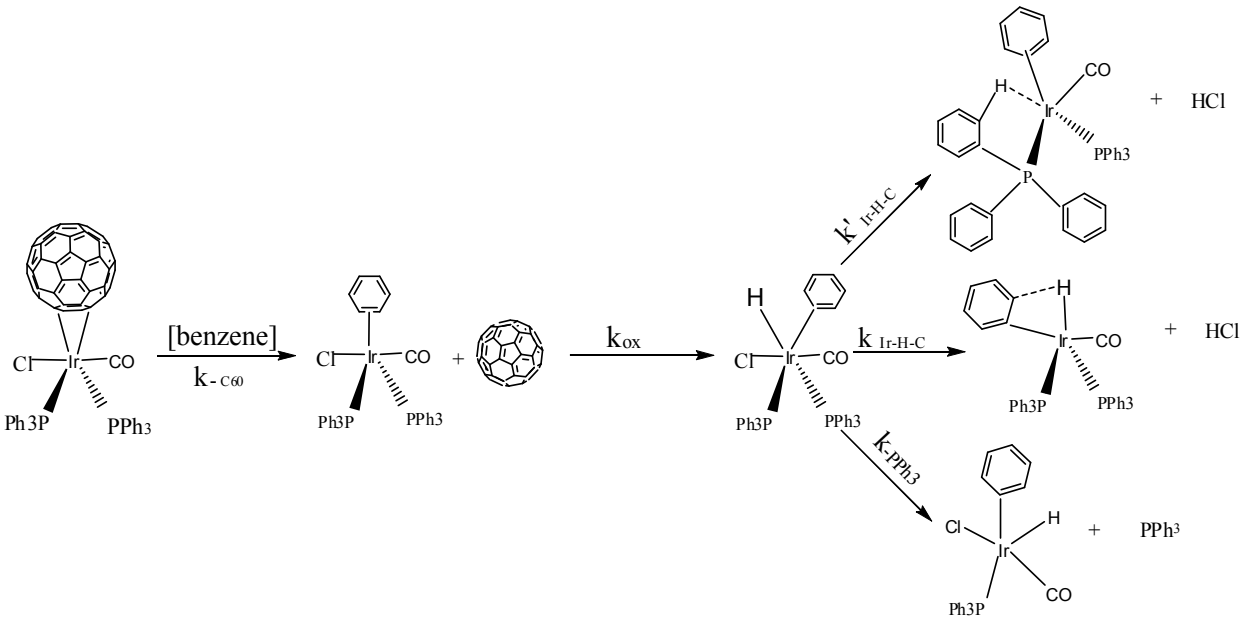

Figure 3.32 Proposed mechanisms C_{60} is displacement of the (η^2 – C_{60})Ir(CO)(Cl)(PPh_3)$_2$, then solvent enters in the metal coordination sphere form (η^2-C_6H_6)Ir(CO)(PPh_3)$_2$Cl. For the slow segment two parallel reaction; i) was attributed to parallel triphenyl phosphine dissociation and ii) formation of a sigma-complex.

The rate law derived from the fast segment is obtained by using the steady state approximation with the intermediate specie (η^2- C_6H_6) Ir(CO)(Cl)(PPh_3)$_2$. Now k_{obs} is shown in equation 3.8:

$$k_{obs} = k_{-C60,benzene}\,[\text{Benzene}] \qquad 3.3$$

$$k_{-C60,\,benzene} = \frac{k_{obs}}{[\text{Benzene}]} \qquad 3.4$$

Temperature (±.1 K)	$k_{obs,\,fast}$ (s^{-1})	$k_{obs,\,slow}$ (s^{-1})
289.2	0.041(8)	0.00204(2)
291.3	0.016(1)	0.00188(2)
291.3	0.10(6)	0.00467(1)
291.3	0.15(2)	0.0053(1)
293.2	0.0122(3)	0.00253(3)
293.2	0.040(5)	0.0079(1)
293.2	0.032(1)	0.00383(3)
295.2	0.048(9)	0.00478(5)
295.2	0.050(5)	0.0105(2)
295.2	0.3(2)	0.3(3)
295.2	0.08(3)	0.00979(9)
295.2	0.10(6)	0.0109(2)
295.2	0.11(2)	0.0126(4)
298.2	0.08(1)	0.0123(3)
298.2	0.06(2)	0.0148(2)
298.2	0.2(1)	0.0189(3)
300.2	0.11(5)	0.0159(5)
300.2	0.07(1)	0.025(1)
300.2	0.1(1)	0.0171(8)
303.2	0.2(2)	0.037(1)
303.2	0.7(1)	0.034(6)

Table 3.1 Rate constant values of $k_{obs,fast}$ for benzene/C60 exchange on (η^2-C_{60})Ir(CO)(PPh_3)$_2$Cl at different temperature under flooding condition and $k_{obs,\,slow}$ for the slow segment three parallel reactions; i) was attributed to parallel triphenylphosphine dissociation and ii) formation of a sigma-complex at different temperature.

Temperature (±.1 K)	$k_{-C60,\ benzene}$ (s^{-1})	$k_{obs,\ slow}$ (s^{-1})
289.2	0.0036(7)	0.00204(2)
291.3	0.0014(1)	0.00188(2)
291.3	0.009(5)	0.00467(1)
291.3	0.013(2)	0.0053(1)
293.2	0.0011(4)	0.00253(3)
293.2	0.0035(5)	0.0079(1)
293.2	0.0028(1)	0.00383(3)
295.2	0.0042(9)	0.00478(5)
295.2	0.0044(5)	0.0105(2)
295.2	0.03(1)	0.3(3)
295.2	0.007(2)	0.00979(9)
295.2	0.009(5)	0.0109(2)
295.2	0.010(1)	0.0126(4)
298.2	0.0071(9)	0.0123(3)
298.2	0.005(1)	0.0148(2)
298.2	0.018(9)	0.0189(3)
300.2	0.009(4)	0.0159(5)
300.2	0.006(6)	0.025(1)
300.2	0.007(6)	0.0171(8)
303.2	0.01(1)	0.037(1)
303.2	0.062(8)	0.034(6)

Table 3.2 Rate true constant values $k_{-C60,\ fast}$ for benzene/C_{60} exchange on (η^2-C_{60})Ir(CO)(PPh_3)$_2$Cl at different temperature under flooding condition and $k_{obs,\ slow}$ for the slow segment three parallel reactions; i) was attributed to parallel triphenyl phosphine dissociation and ii) formation of a sigma-complex at different temperature.

Rate constant values related to both segments of the biphasic plots are solvent-dependent. Kinetics experiments in benzene were carried out at various temperatures to estimate activation parameters using the Eyring plot (Figure 3.33). True rate constant values and activation parameters are given in table 3.1- 3.2 and table 3.3, respectively.

The activation parameters were estimated using the Eyring plot. The Eyring plot is a theoretical construct based on the transition state theory, equation 3.5. The graph of $\ln(k_{obs}/T)$ vs. 1/T, supposed to be linear over a range of temperature, figure 8.

$$Ln\ \frac{k-c60}{T} = -\frac{\Delta H\ 1}{R\ T} + Ln\frac{k\ B}{h} + \frac{\Delta S}{R} \qquad 3.5$$

Then the values for $\Delta H^{\ddagger}_{\text{-C60/benzene}}$ are determinate from the slope of this plot, equation 3.6:

$$\Delta H^{\ddagger}_{\text{-C60/benzene}} = -\ m*R \qquad 3.6$$

Where R = 8.314 J/mol*K.

Values for $\Delta S^{\ddagger}_{\text{-C60/benzene}}$ is determinate from the intercept of the plot, equation 3.7:

$$\Delta S^{\ddagger}_{obs} = R\ [b - Ln(k_B/h)] \qquad 3.7$$

Where $k_B = 1.381x10^{-23}$ J/K and $h = 6.626x10^{-34}$ J/s

The estimated activation parameters suggest a dissociative displacement of C_{60} from (η^2 – C_{60})Ir(CO)(Cl)(PPh_3)$_2$, where the solvent enters the coordination sphere of the complex. For the fast segment the activation enthalpy ($\Delta H^{\ddagger}_{\text{-C60/benzene}}$) is 99(±4) kJ/mol and the activation entropy ($\Delta S^{\ddagger}_{\text{-C60/benzene}}$) is -51(±108) J/mol*K. While for the slow segment, the activation enthalpy ($\Delta H^{\ddagger}_{\text{slow segment}}$) is 143(±2) kJ/mol and the activation entropy ($\Delta S^{\ddagger}_{\text{slow segment}}$) is 201(±51) J/mol*K. Analysis of reactions products by IR and ^{1}H NMR suggest that k_{slow} is a related to a series of parallel reaction: *i*) triphenyl phosphine dissociation from the non-steady intermediate ii) formation of a sigma-complex ; figure 3.32.

	$\Delta H^{\neq}$ (kJ/mol)	$\Delta S^{\neq}$ (J/ mol K)
Fast segment (C_{60}/benzene)	99(±4)	-51 (±108)
	$\Delta H^{\neq}$ (kJ/mol)	$\Delta S^{\neq}$ (J/ mol K)
Slow segment	143(±2)	201(±51)

Table 3.3. Activation parameters for benzene/C_{60} exchange on (η^2-C_{60})Ir(CO)(PPh_3)$_2$C, at different temperature under flooding condition and for the slow segment that consist in i) Triphenyl phosphine dissociation, ii) C-H oxidative cleavage of Ir-coordinated solvent and iii) Formation Ir-H-C agostic bond formation (sigma complex).

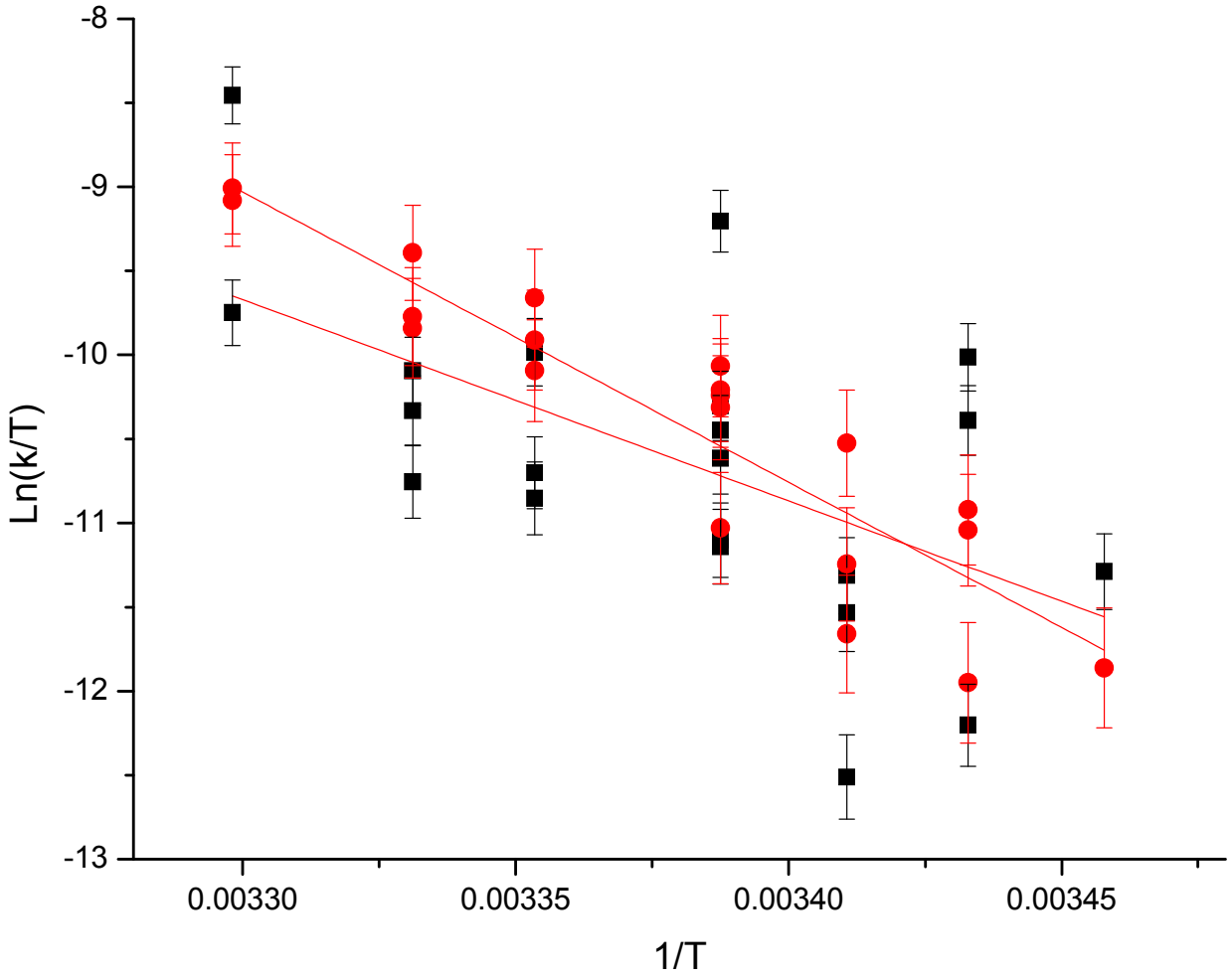

Figure 3.33

■ ***Eyring plot of Ln(K_{fast}/T) vs. 1/T for reaction of (η^2-C_{60})Ir(CO)(PPh_3)$_2$Cl with benzene. The $k_{\text{-}C60/benzene}$ values were obtained under flooding conditions where [Benzene]>> [η^2-C_{60})Ir(CO)(PPh_3)$_2$Cl]***

● ***Eyring plot of Ln(K_{slow}/T) vs. 1/T for reaction of (η^2-C_{60})Ir(CO)(PPh_3)$_2$Cl with benzene. The k_{slow} values were obtained under flooding conditions where [Benzene]>> [η^2-C_{60})Ir(CO)(PPh_3)$_2$Cl]***

3.4 Reactions in benzene/cyclohexane (two-solvent system)

Dissociation of C_{60} from (η^2-C_{60})Ir(CO)(PPh_3)$_2$Cl was monitored by UV-Vis in benzene and in benzene/cyclohexane mixtures. Kinetics experiments employing mixed solvents may provide information about selectivity related to solvent-Ir bond formation. The reactions were studied at various solvent compositions. The pseudo-first order rate constant values (k_{obs}) were determined using a non-linear curve fitting of the absorbance versus time plots as mentioned before. As in single solvents, the reactions of (η^2-C_{60})Ir(CO)(PPh_3)$_2$Cl in benzene/cyclohexane mixtures are biphasic (Figure 3.7), indicating a related to a series of parallel reactions as observed in single solvent systems. As before, the fast segment is correlated with solvent/C60 exchange, while he slow segment is assigned to the reaction described above, i.e., i) formation of a sigma-complex and ii)PPh_3 dissociation from the non-steady state intermediate (Figure 3.32)

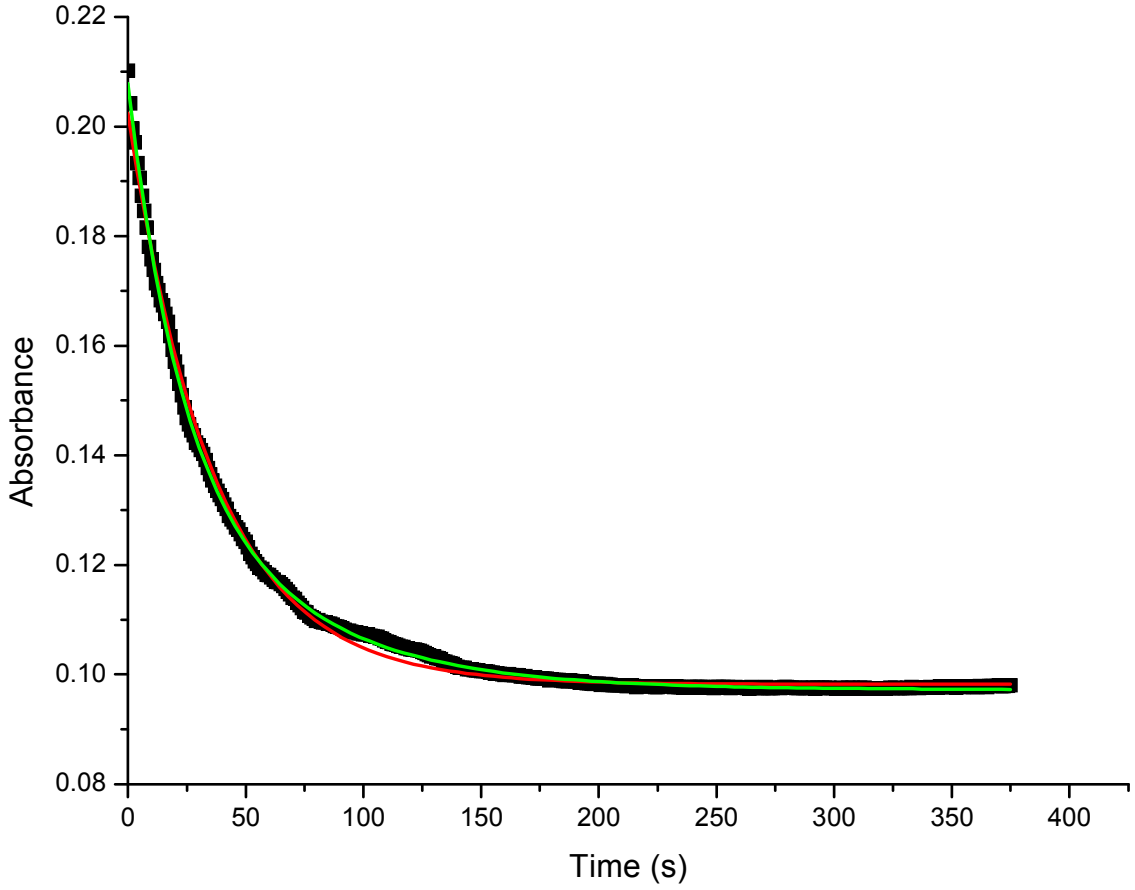

Figure 3.34 Plot of absorbance vs. time(s) at 550nm (Benzene/Cyclohexane)/C_{60} exchange on (η^2-C_{60})Ir(CO)(PPh_3)$_2$Cl at 295K. The continuous green trace corresponds toe absorbance values obtained from the function Absorbance = $0.095(1)e^{-(26.8\pm4)} + 0.034(1)e^{-(108\pm3)} + 0.0926(1)$. The continuous red trace corresponds to absorbance values obtained from the function Absorbance = $0.1042(4)e^{-0.0274(2)t} + 0.0982(8)$.[37]

[Benzene] = 5.07 M and [Cyclohexane] = 5.01 M

Rate constant values related to both segments of the biphasic plot are dependent on the solvent composition. The averages of k_{fast} and k_{slow} are show in table 4.

Temperature (±.1 K)	[Bz] (M)	[Cy] (M)	k_{fast} ($x10^{-2}$) (s^{-1})	k_{slow} ($x10^{-3}$) (s^{-1})
295.2	0.103	9.06	3.1 (4)	5.4 (4)
	0.543	8.71	5.1 (3)	6.9 (4)
	2.11	7.41	4.3 (2)	4.3 (2)
	3.27	6.47	5 (1)	5.0 (5)
	5.07	5.01	5.3 (1)	16 (1)
	7.08	3.72	3.4 (1)	10.9 (3)
	8.87	1.91	9.5 (4)	14.7 (3)
	10.32	0.83	11.0 (8)	20.7 (2)
300.5	0.105	9.09	5.5 (1)	6.8 (6)
	0.518	8.77	4.3 (1)	3.71 (6)
	2.13	7.44	4.42 (4)	4.1 (1)
	3.38	6.39	8.1 (6)	16. 1 (3)
	6.02	4.21	8.2 (1)	22.4 (2)
	8.48	2.18	9.5 (1)	25.3 (2)
	8.97	1.86	13 (1)	42 (1)

Table 3.4 Rate true constant values $k_{-C60,\,fast}$ for benzene/C_{60} exchange on (η^2-C_{60})Ir(CO)(PPh_3)$_2$Cl at different temperature in mixed of solvent (Bz/Cy) under flooding condition and $k_{obs,\,slow}$ for the three parallel reactions; i) was attributed to parallel triphenyl phosphine dissociation and ii) formation of a sigma-complex at different temperature.

Bz = Benzene* and Cy = Cyclohexane*

3.4.1 ***Discussion***

The rate of disappearance of $(\eta^2 - C_{60})Ir(CO)(Cl)(PPh_3)_2$ in mixed solvents (benzene/cyclohexane) was monitored observing a decrease in absorbance at 550nm. The reactions were studied under flooding conditions at different temperatures. The plots of absorbance vs. time(s) consist of two segments, (figure 3.34) where the both segment depended of the concentration of the both solvents, shown in figure 3.35 and 3.36. This evidence suggests that $(solvent_1/solvent_2)/C_{60}$ exchange of $(\eta^2\text{-}C_{60})Ir(CO)(Cl)(PPh_3)_2$ produces $(solvent_1)Ir(CO)(PPh_3)_2Cl$ and $(solvent_2)Ir(CO)(PPh_3)_2Cl$. Different from the observed outcome in one-solvent system, the slow segment depend of the chemical nature of both solvents as shown in figures 3.35 and 3.36. This observation indicates an equilibrium between the solvated species and other catalitically-significant reactions namely triphenylphosphine dissociation and formation of a sigma-complex (figure 3.37).

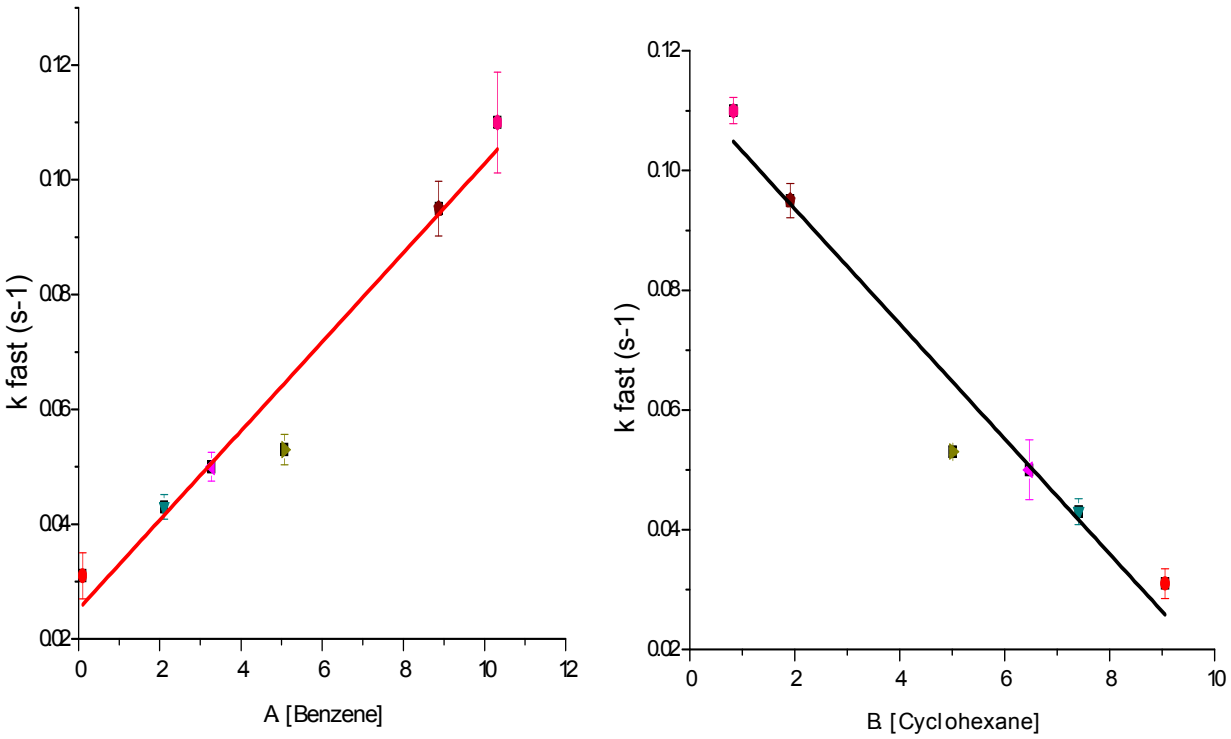

Figure 3.35 Plots of A) $k_{obs,\ fast}$ vs. [Benzene] and B) $k_{obs,\ fast}$ vs. [Cyclohexane] at 300.5K for dissociation on fullerene of coordinative sphere of $(\eta^2 - C_{60})Ir(CO)(Cl)(PPh_3)_2$ in mixed of solvent [Benzene]/[Cyclohexane]

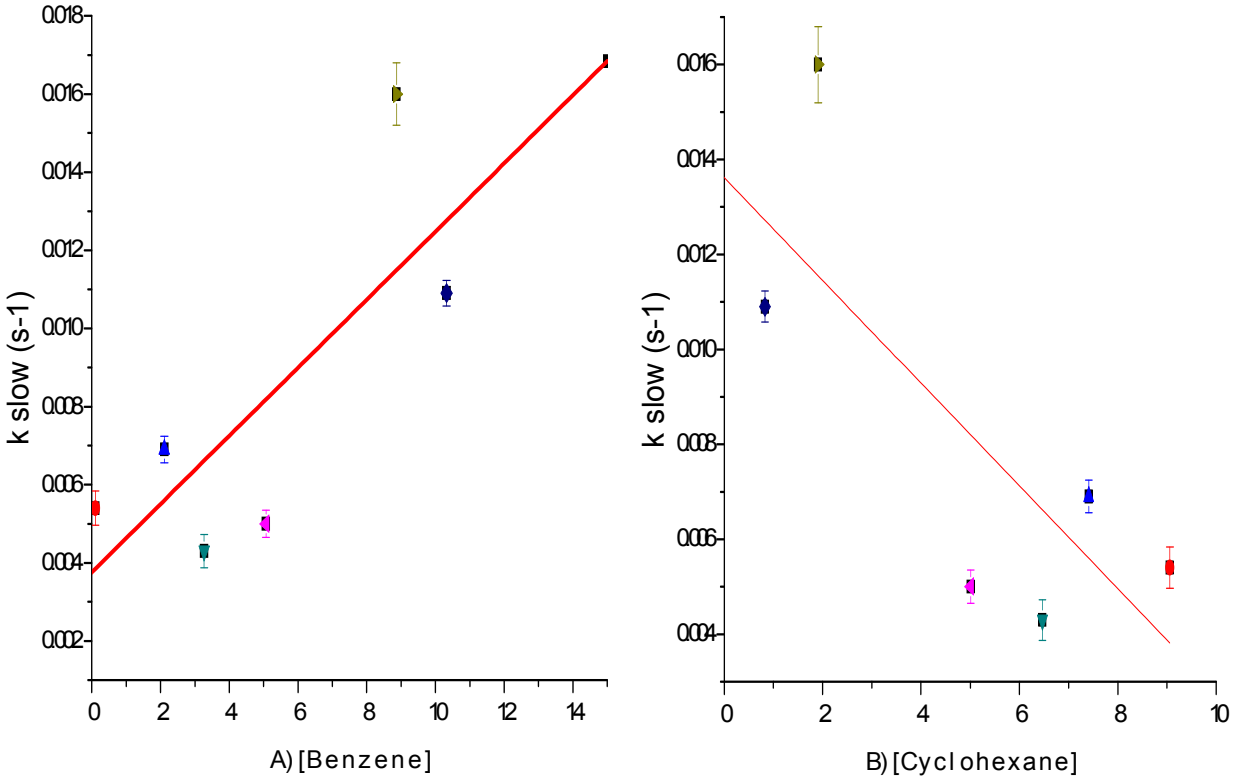

Figure 3.36 Plots of A) $k_{obs,\ slow}$ vs. [Benzene] and B) $k_{obs,\ slow}$ vs. [Cyclohexane] at 300.5K for dissociation on fullerene of coordinative sphere of $(\eta^2 - C_{60})Ir(CO)(Cl)(PPh_3)_2$ in mixed of solvent [Benzene]/[Cyclohexane]

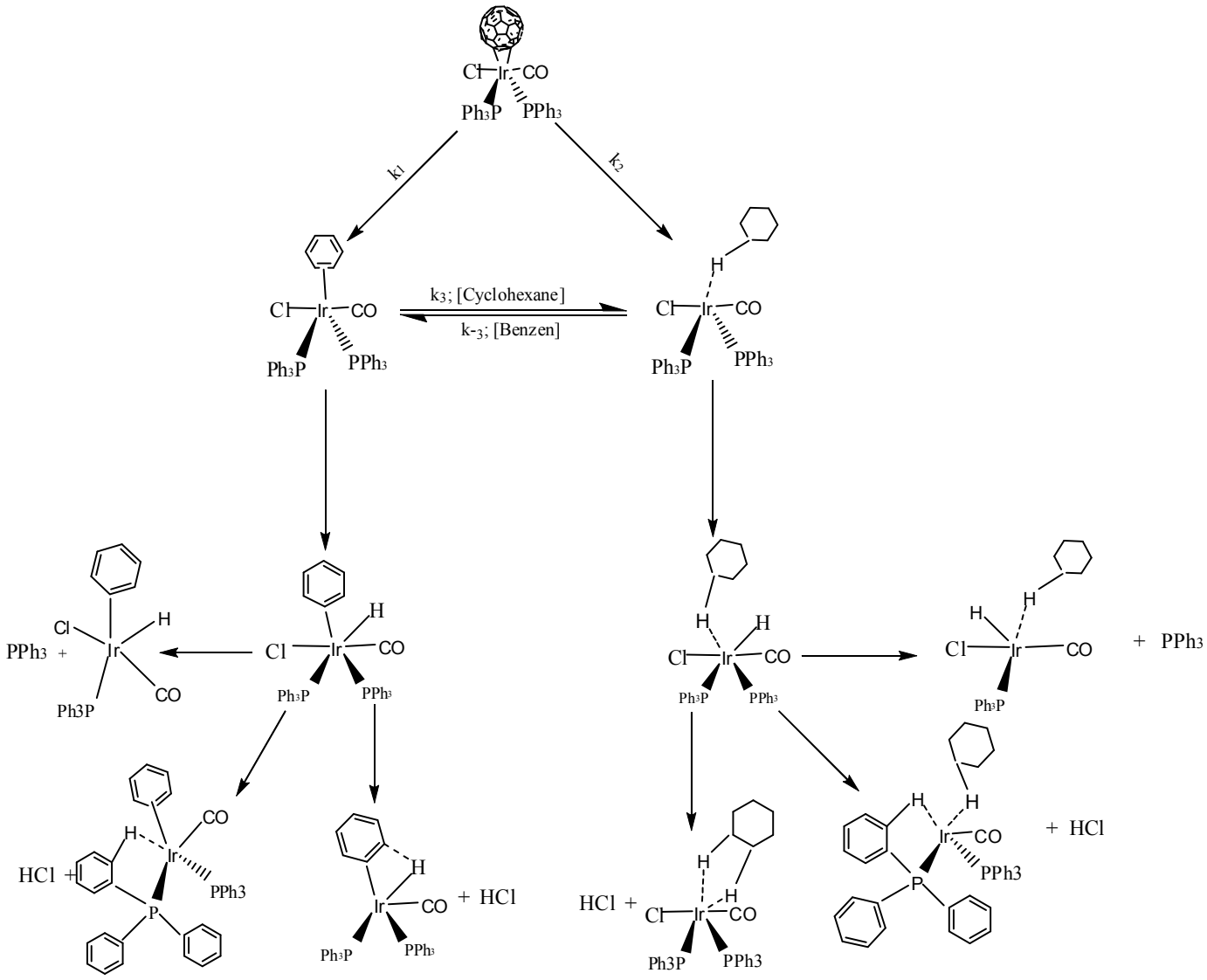

Figure 3.37 Proposed mechanisms for fullerene displacement from (η^2-C_{60})Ir(CO)(Cl)(PPh_3)$_2$ in mixed of solvent (Benzene/Cyclohexane), then the solvent enter in the coordinative sphere of the complex. Finally we have two parallel reactions, i) triphenyl phosphine dissociation and ii) formation of sigma complex.

The rate law derived from the mechanism is obtained by using the steady state approximation. Now k_{obs} is shown in equation 3.9:

$$k_{obs,\ fast} = k_{Bz}[\text{Benzene}] + k_{Cy}[\text{Cyclohexane}] \qquad 3.9$$

Plots of k_{obs} vs. [benzene] are linear (Figure 3.35). Observation of this linear plot indicates that $dk_{obs}/d[\text{benzene}]$ is constant. then equation 3.9 can be expressed as,

$$k\ obs\ =\ [Bz]\ \frac{d(k\ obs)}{d\ [Cy]}\ +\ k\ cy\ [Cy]o \qquad 3.10$$

The mathematic significance of the slope is

$$\frac{d(k\ obs)}{d[Bz]} = k\ bz\ \frac{d[Bz]}{d[Bz]} + [Bz]\frac{d(kbz)}{d[Bz]} + kcy\ \frac{d[Cy]}{d[Bz]} + [Cy]\ \frac{d(k\ cy)}{d\ [Bz]} \qquad 3.11$$

Then:

$$\frac{d\ (kobs)}{d\ [Bz]} =\ k\ bz\ + k\ bz\ \frac{d[Cy]}{d[Bz]} \qquad 3.12$$

Finally k_{obs} can be expressed as:

$$k\ obs\ =\ [Bz]\left\{ kbz\ +\ kcy\ \frac{d[Cy]}{d[Bz]}\right\} +\ k\ cy\ [Cy]0 \qquad 3.15$$

This equation has the form of y = mx +b.

Where:

y = k_{obs}

x = [Benzene]

m = $kbz + kcy\frac{d[Cy]}{d[Bz]}$

b = $kCy\ [Cy]0$

The graph of [Benzene] vs. [Cyclohexane] shown in figure 3.38 enables determination of the concentration of pure cyclohexane and $k_{fast,\ cyclohexane}$.

$$k\,cy = \frac{b}{[Cy]0} \qquad 3.16$$

The graph of k_{obs} vs. [Benzene] is shown in figure 3.35. Once the rate constant for C_{60} displacement from the (η^2-C_{60}) $Ir(PPh_3)_2(CO)Cl$ by cyclohexane is known, is substituted in the equation k_{Bz} for the first step.

$$k_{Bz} = m - k_{cy}\frac{d[Cy]}{d[Bz]} \qquad 3.17$$

Where:

M = slope of the plot k_{obs} vs. [Benzene]; figure 3.35
k_{cy} = is obtained of equation 3.16
$\frac{d[Cy]}{d[Bz]}$ = slope of the plot [Cyclohexane] vs. [Benzene]; figure 3.38

295.2	Benzene	
Fast segment	k_{fast} ($x10^{-3}$)	k_{slow} ($x10^{-3}$)
	5(2)	1.6(0.2)
Slow segment	Cyclohexane	
	k_{fast} ($x10^{-3}$)	k_{slow} ($x10^{-4}$)
	4 (1)	6(1)
300.5	Benzene	
Fast segment	k_{fast} ($x10^{-2}$)	k_{slow} ($x10^{-3}$)
	1(2)	3.5(0.6)
Slow segment	Cyclohexane	
	k_{fast} ($x10^{-3}$)	k_{slow} ($x10^{-4}$)
	5(1)	3(3)

Table 3.5 Rate constant values for mix of (benzene/cyclohexane)/C60 exchange on (η^2-C_{60})Ir(CO)(PPh_3)$_2$Cl at different temperature under flooding condition.

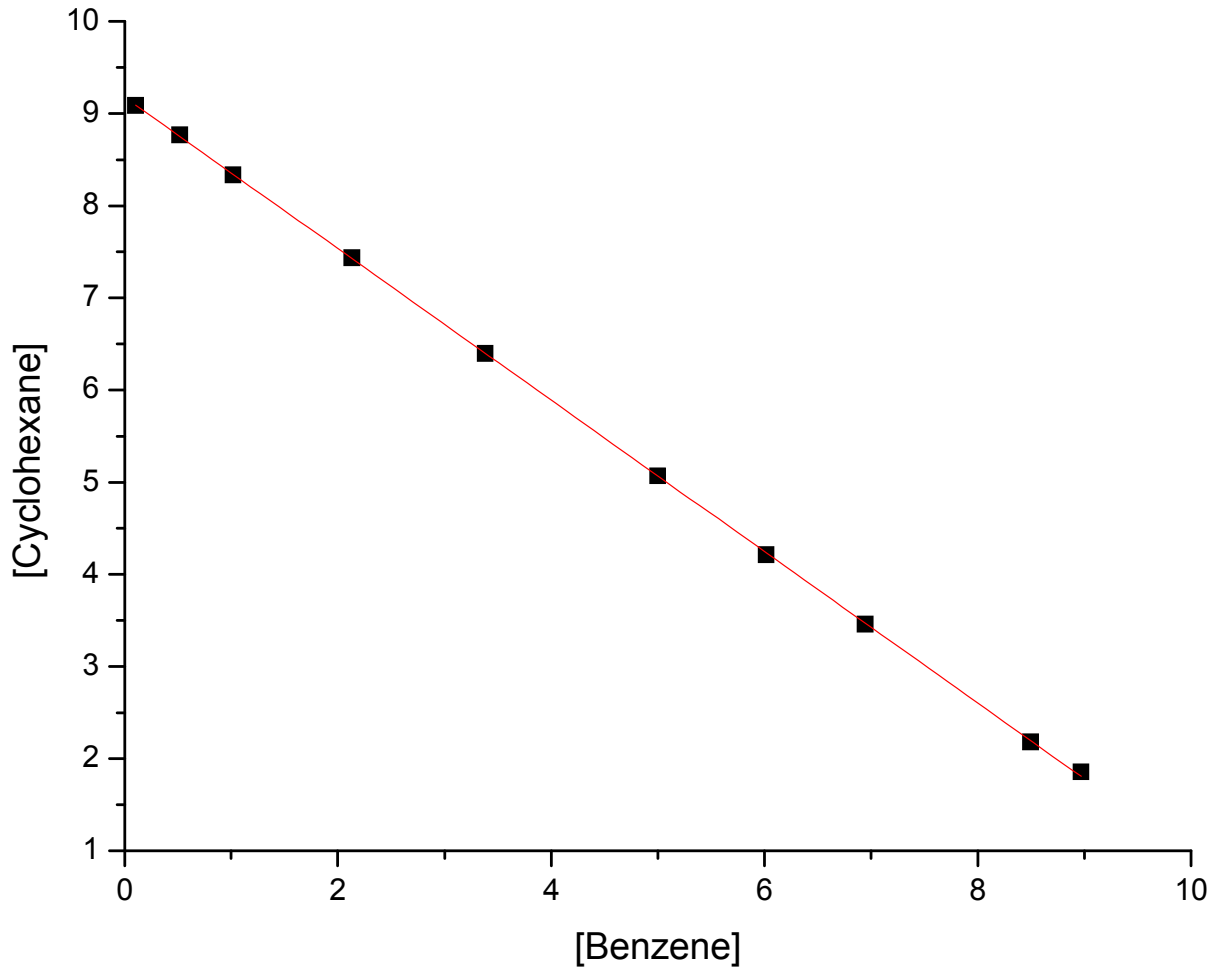

Figure 3.38 Plot of [Benzene] vs [Cyclohexane] at 300.5K for dissociation on fullerene of coordinative sphere of $(\eta^2 - C_{60})Ir(CO)(Cl)(PPh_3)_2$ in mixed of solvent [Benzene]/[Cyclohexane]

Chapter IV

Conclusion

Plots of absorbance vs. time for C_{60}/solvent exchange on $(\eta^2\text{-}C_{60})Ir(CO)(PPh_3)_2Cl$ and the subsequent reactions are decreasing and biexponential.. The fast segments were attributed to C_{60}/solvent exchange on $(\eta^2\text{-}C_{60})Ir(CO)(PPh_3)_2Cl$. The slow segments were assigned to: i) triphenyl phosphine dissociation, ii) C-H oxidative cleavage of Ir-coordinated solvent, and iii) Ir-H-C agostic bond formation (sigma complex). Values of $k_{fast,\ observed}$ and $k_{slow,\ observed}$ are independent of $[C_{60}]$ and dependentnof the solvent nature The fast and slow reactions were first order with respect to the molar concentration of $(\eta^2\text{-}C_{60})Ir(CO)(PPh_3)_2Cl$, and $(solvent)Ir(CO)(PPh_3)_2Cl$, respectively. The observed highly positive entropy of activation for C_{60}/solvent (benzene) ($\Delta S^{\ddagger}_{\text{-C60/benzene}} = -51(\pm 108)$ (J/K mol) suggest that benzene in the exchange is solvent-assisted in the sense that benzene and C_{60} become part of the same structure in the transition state. In this case the enthalpy of activation values reflects partitial C_{60}-Ir bond breaking and patial benzene-Ir bond formation. Values of $k_{obs,\ slow}$ are independent of the nature of solvent when reactions are conducted in one-solvent system. However, the corresponding values are $[solvent_1]$ and $[solvent_2]$ when reactions are conducted in binary solvent mixtures as reaction media. These observations indicate a series of parallel and consecutive reactions. Therefore the activations parameters estimated from the Eyring plot may lack physical meaning (if $k_{obs,\ slow}$ = summation of k_s) or cannot be attribute to a specific reaction step(s) with the information in this study. The qualitative description given in this work is based on NMR and IR spectroscopy.

Reactions in two solvent systems produce non – equilibrium mixtures of (solvent1)Ir(CO)(PPh_3)$_2$Cl and (solvent2)Ir(CO)(PPh_3)$_2$Cl. Like in one-solvent system, fast segments were attributed to C_{60}/solvent exchange on (η^2-C_{60})Ir(CO)(PPh_3)$_2$Cl. Similarly slow segments were assigned to: i) triphenyl phosphine dissociation, ii) C-H oxidative cleavage of Ir-coordinated solvent and iii) Formation Ir-H-C agostic bond formation (sigma complex).

Two possibilities can be envisioned for the sigma complex formation. In one benzene can form a four-member ring, whereas triphenyl phosphine can form five-member ring.

References

1. Bergman, R. Nature, **2007**, 446, 22, 391 - 393
2. Bernskoetter, W.; Schaurer, C.; Goldberg, K.; Brookhart, M. Science, **2009**, 326, 553 - 556
3. Senoff, C. Can J. Chem, 48, **1970**, 2444 - 2446
4. Balch, A.; Catalano, B.; Lee, J, Inorg. Chem.,1991, 30, 3958.
5. Vaska, L.; DiLuzio, J.W. J. Am. Chem. Soc., 1961, 83, 2784-2785.
6. Kadash, K.; Ruoff, R. Fullerenes. First edition, A John Wlley & Sons, Canada 2000.
7. Haddon, R; Palmer, R.; Kroto, H.; Sermon, P. Chem,. Phys.Ast, **1993**, 343, 53 - 62
8. Haddon, R. J. Phys Chem., **1987**, 91, 14, 3719 – 3720
9. Varma, C.; Zaanen, J.; Raghavachari, K. Science, 254, **1991,** 989 - 992
10. Igartúa-Nieves, E.; Ocasio-Delgado, Y.; Torres-Castillo, M.; Rivera-Betancourt, O.; Rivera-Pagán, J.; Rodriguez, D.; López, G.; Cortés-Figueroa, J., Dalton Trans., 2007 1293.
11. Igartúa-Nieves, E,;Ocasio-Delgado, Y.; Cortés-Figueroa, J., J. Coord. Chem. 2007, 60, 449.
12. Ocasio-Delgado, Y.;De Jesús-Segarra, J.; Cortés-Figueroa, J., J. Organomet. Chem, 2005, 690, 3366.
13. Rivera-Rivera, L.; Crespo-Román, G.; Acevedo-Acevedo, D.; Ocasio-Delgado, Y.; Cortés-Figueroa, J., Inorg. Chim. Acta, 2004, 357, 881.
14. Ocasio-Delgado, Y.; Rivera-Rivera, L.; Crespo-Roman, G.; Cortés-Figueroa, J., Inorg. Reac. Mech, 2003, 5, 13.

15. Rivera-Rivera, L.; Colón-Padilla, L.; Ocasio-Delgado, Y.; Martinez-Rivera, Y.; Mercado-Feliciano, S.; Ramos, C.; Cortes-Figueroa, J., Inorg. Reac. Mech, 2002, 4, 49.

16. Rivera, L.; Colón-Padilla, F.; Del Toro-Novalés, A.; Cortés-Figueroa, J., Coord. Chem, 2001, 54, 143.

17. Song, L.; Zhu, Y.; Hu, Q., Polyhedron, 1998, 17, 469.

18. Song, L.; Zhu, Y.; Hu, Q., Polyhedron 1997, 16, 2141.

19. Zanello, P. ; Laschi, F. ; Fontani, M. ; Song, L. ; Zhu, Y., J. Organomet. Chem. 2000, 7, 593–594.

20. Larsson, S.; Volosov, A.; Rosen, A., Chem. Phys. Lett., 1987, 137, 501.

21. Rosen, A.; Wastberg, B., J. Chem. Phys. 1989, 90, 2525.

22. Xie, Q.; Pérez-Cordero, E.; Echegoyen, L., J. Am Chem. Soc. 1992, 114, 3978.

23. Ohsawa, Y.; Saji, T., J. Chem. Soc. Chem. Commun. 1992 781.

24. Echegoyen, L. ; Echegoyen L. E. ; Acc. Chem. Res., 1998, 31, 593.

25. Dubois,D.; Jones, M. T.; Kadish, K. M., J. Am. Chem. Soc., 1992, 114, 6446.

26. F. Zhou, C. Jehoulet, A. J. Bard, J. Am. Chem.Soc, 1992,114, 11004.

27. Wang, N.; Wang, L.; Liu, W.; Ou, Y.; Li, W. Tetra Lett., 2001, 42, 7911 – 1913.

28. Capella Capella, Cynthia. Master theses, University of Puerto Rico at Mayaguez, 2008.

29. Igartua Nieves, Elvin. Master theses, University of Puerto Rico at Mayaguez, 2006.

30. Vincent, Alan. Molecular Symmetry and Group Theory : A Programmed Introduction to Chemical Applications, 2nd ed, John Wiley & Sons, England, 2001.

31. Espenson, James H. Chemical Kinetics and Reaction Mechanisms, 2nd ed, McGraw-Hill Science/Engineering/Math, Iowa, 2002.

32. Steinfeld, Jeffrey I., Francisco, Joseph S., Hase, William L. Chemical Kinetics and Dynamics, 2nd ed, 1998

33. Laidler, K. Chemical Kinetics, 3rd ed, Pearson Education Company, New York, 1987.

34. Aldeco, E.; Rosenthal, A.; Donnadieu, B.; Parameswaran, P.; Freenking, G.; Bertrand, G, Science, **2009**, 326, 556 – 559.

35. Ladogana, S.; Dobson, G. Smit, J. Inor Chim Ac, 271, **1998**, 105 - 111

36. Zhang, S.; Dobson, G.; Zang, V.; Bajaj, H.; Eldik, R. Inorg .Chem. **1990**, 29, 3477 – 3482.

37. Felix, T.; Cortes-Figueroa, J. J Chem Edu, **2010**, 87, 4, 426 – 428.

38. Bercaw, J.; Labingert, J. PNAS, **2007**, 104, 17, 6899 – 6900.

39. Chen, G.; Labingert, J.; Bercawt, J. PNAS, **2007**, 104, 17, 6915 – 6920.

40. Brookharta, M.; Green, M.; Parkinb, G. PNAS, **2007**, 104, 17, 6908 – 6914.